Estimation des niveaux marins extrêmes en utilisant de l'information régionale et historique

Laurie Saint Criq

Centre Eau, Terre et Environnement
École doctorale SIE

Estimation des niveaux marins extrêmes en utilisant de l'information régionale et historique

Laurie Saint Criq

Doctorat en sciences de l'eau de l'INRS
Doctorat de l'Université Gustave Eiffel

Jury

Président du jury	**Pr. André St-Hilaire**	INRS
Examinateur	**Dr. Jacob Stolle**	INRS
Rapportrice	**Pr. Liliane Bel**	AgroParisTech
Examinatrice	**Dr. Iwona Kuptel-Markiewicz**	IGF PAN
Co-encadrant de thèse	**Dr. Yasser Hamdi**	IRSN
Directeur de thèse	**Dr. Eric Gaume**	Université Gustave Eiffel
Co-directeur de thèse	**Pr. Taha Ouarda**	INRS

Remerciements

Je tiens tout d'abord à remercier mon encadrant de thèse Yasser Hamdi, et mes directeurs de thèse Éric Gaume et Taha Ouarda, de m'avoir suivie pendant ces trois années. Je les remercie pour leurs conseils, leur encadrement et leur temps. La complémentarité de leurs profils a été un atout pour la thèse.

Je tiens à remercier ensuite les membres du jury, André St Hilaire, Jacob Stolle, Liliane Bel et Iwona Kuptel-Markiewicz, pour le temps accordé à l'évaluation de ce manuscrit et pour leur présence à la soutenance.

Je remercie également les membres du comité de suivi, Déborah Idier et Michel Lang, pour leurs remarques précieuses ainsi que leur bienveillance.

Je remercie le BEHRIG pour le très bon accueil, et particulièrement Nathalie Giloy pour son expertise, ainsi que Lise Bardet pour son écoute et son efficacité.

Je remercie les personnes rencontrées à l'INRS, et particulièrement Patricia Munoz pour sa bienveillance.

Pour terminer, merci à ma famille et mes ami.e.s pour l'amour et le soutien inconditionnel.

Résumé

L'estimation des niveaux marins de l'aléa naturel submersion marine à prendre en compte pour la protection des centrales nucléaires constitue un enjeu de sûreté important pour l'IRSN. Pour estimer les niveaux marins de période de retour élevée, une analyse statistique locale peut être menée. Cependant, la faible qualité des données, due notamment à de courtes durées d'observation, a pour conséquence de fortes incertitudes d'estimation. L'information additionnelle, régionale et/ou historique, est utilisée en réponse à cette problématique. L'information régionale consiste à valoriser des données disponibles à des site proches du site de référence, et l'information historique consiste à valoriser des évènements observés avant le début des enregistrements au site de référence. Si l'exploitation de l'information additionnelle renforce les ajustement statistiques, elle pose aussi des difficultés méthodologiques.

Les niveaux marins extrêmes sont généralement estimés en ajustant une distribution statistique sur les surcotes de pleine mer météorologiques stochastiques, puis en faisant une convolution avec la distribution empirique des marées hautes astronomiques prédictibles. Les observations historiques sont des niveaux marins majeurs extraits des archives dont on peut estimer les surcotes de pleine mer associées. Si une surcote de pleine mer extrême coïncide avec une marée haute d'intensité faible ou modérée, elle n'engendre pas automatiquement un niveau marin extrême traçable dans les archives. L'exhaustivité des surcotes de pleine mer extrêmes historiques ne peut donc pas être garantie, cela peut conduire à des estimations biaisées. La problématique liée à l'information historique est donc sa possible non exhaustivité. L'information régionale se décompose généralement en deux étapes, la formation de régions homogènes et l'estimation régionale. Les problématiques qui en découlent sont donc de choisir une méthode pertinente pour former les régions et une méthode pertinente pour l'estimation régionale, et de prendre en compte les possibles dépendences entre les sites d'une région.

Des études ont déjà tenté de répondre aux problématiques associées à l'information régionale et historique, mais peuvent encore être améliorées. De plus, la combinaison de l'information régionale et historique n'a été que très peu traitée jusqu'à présent. La thèse vise donc à développer des méthodes afin de prendre en compte proprement de l'information régionale et/ou historique pour l'estimation des niveaux marins extrêmes. Les approches proposées sont illustrées sur les données de marégraphes européens localisés sur le littoral de l'océan Atlantique, de la Manche et de la Mer du Nord.

Mots clés : Evaluation des risques côtiers ; Niveaux marins extrêmes ; Surcotes de pleine mer ; Information historique ; Information régionale ; Théorie des valeurs extrêmes ; Analyse Bayésienne ; Océean Atlantique ; Manche ; Mer du Nord.

Abstract

Estimating the sea levels of the natural marine flooding hazard to be taken into account for the protection of nuclear power plants is an important safety issue for IRSN. To estimate sea levels corresponding to high return periods, a local statistical analysis can be conducted. However, the low quality of the data, due in particular to short observation periods, results in high estimation uncertainties. Additional information, regional and/or historical, is used in response to this problem. Regional information consists of evaluating data available at sites close to the reference site, and historical information consists of evaluating events observed before the beginning of recordings at the reference site. If the use of additional information strengthens the statistical adjustments, it also poses methodological difficulties.

Extreme sea levels are typically estimated by fitting a statistical distribution to stochastic meteorological skew surges, then doing a convolution with the empirical distribution of predictable astronomical high tides. The historical observations are major sea levels extracted from the archives from which the associated high tide surges can be estimated. If a skew surge coincides with a high tide of low or moderate intensity, then it does not automatically generate an extreme sea level traceable in the archives. The exhaustiveness of the historical extreme skew surges cannot be guaranteed, which can lead to biased estimates. The problem related to historical information is therefore its possible non-exhaustiveness. Regional information generally is composed of two steps, the formation of homogeneous regions and the regional estimation. The resulting issues are therefore to choose a relevant method to form the regions and a relevant method for the regional estimation, and to take into account the possible dependencies between the sites of a region.

A few studies have already attempted to respond to the problems associated with regional and historical information, but can be further improved. Moreover, the combination of regional and historical information has been treated very little up to now. The thesis therefore aims to develop methods to properly take into account regional and/or historical information for the estimation of extreme sea levels. The proposed approaches are illustrated on data from European tide gauges located on the coast of the Atlantic Ocean, the English Channel and the North Sea.

Keywords : Coastal risk assessment ; Extreme sea levels ; Skew surges ; Historical information ; Regional information ; Extreme value theory ; Bayesian analysis ; Atlantic Ocean ; English Channel ; North Sea.

Table des matières

Table des figures

Liste des tableaux

Chapitre 1

Introduction et objectifs

1.1 Mise en contexte

1.1.1 Contexte général

Chaque année, les inondations côtières touchent les populations du monde entier. Les dégâts peuvent être très importants et se traduisent en impacts sociaux, écologiques, matériels, économiques, ainsi qu'en pertes humaines. L'Europe de l'Ouest se souvient de la tempête de 1953 qui a fortement touché les Pays Bas, l'Angleterre, la France et la Belgique causant plus de 2000 morts (Gerritsen, 2005), ou plus récemment en 2010, de la tempête Xynthia qui a inondé plus de 50 000ha et causant la mort de 47 personnes en France (Kolen et al., 2013).

Le littoral doit donc être aménagé pour protéger la population, les ports, les industries... et ce, encore plus dans le contexte actuel de changement climatique. Les centrales nucléaires représentent un cas très particulier des infrastructures côtières à protéger.

Les inondations par submersion marine, aléas naturels hydro-météorologiques, intéressent particulièrement l'IRSN (Institut de Radioprotection et de Sûreté Nucléaire). Ce sont, en effet, l'une des agressions externes qui peuvent menacer la sûreté de certaines centrales nucléaires. Il y a 5 centrales nucléaires localisées sur le littoral Atlantique/Manche Français : Flamanville, Gravelines, Le Blayais, Paluel et Penly (voir Figure 1.1). La tempête Martin de 1999 a conduit à une inondation partielle du site de la centrale nucléaire du Blayais, entraînant la perte d'alimentation électrique et l'isolement physique du site.

Figure 1.1 – Carte des centrales nucléaires en France (Source : IRSN)

Les centrales nucléaires françaises doivent être conçues pour être préservées de l'aléa inondation par submersion marine suivant des politiques strictes qui ont été renforcées après l'incident du Blayais en France, la tempête Xynthia et l'accident majeur à la centrale de Fukushima au Japon en 2011, suite au séisme et au tsunami de Tohoku (voir Figure 1.2). La dernière réglementation en vigueur est le guide n°13 de l'ASN (Autorité de Sûreté Nucléaire) publié en 2013, qui préconise de protéger les centrales nucléaires d'un niveau marin équivalent à la somme conventionnelle du i) niveau maximal de la marée astronomique théorique, de ii) la borne supérieure de l'intervalle de confiance à 70% de la surcote millénale et de iii) l'évolution du niveau marin moyen extrapolée jusqu'au prochain examen de sûreté. Les analyses statistiques des niveaux marins et des surcotes extrêmes sont donc essentielles pour la sûreté des centrales nucléaires, mais aussi de manière plus générale pour l'aménagement du littoral.

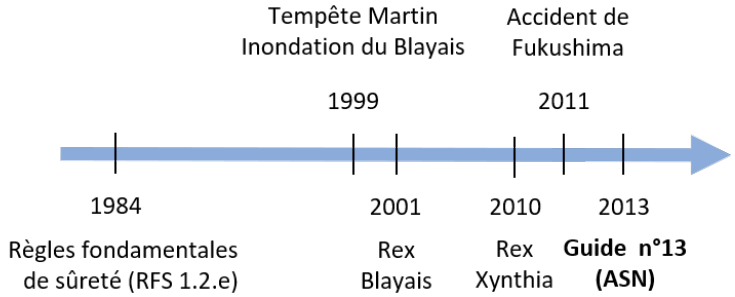

Figure 1.2 – Historique des réglementations

Les séries de données disponibles sont très souvent limitées et/ou pas assez informatives sur les extrêmes à cause notamment de courtes séries d'enregistrements et/ou des lacunes de mesures. Pour estimer une surcote avec une période de retour de 1000 ans, une analyse statistique locale basée sur des séries d'observations relativement courtes apparaît entachée de grandes

incertitudes. Il est cependent important d'avoir des estimations précises afin de mener une bonne gestion du littoral. Une façon d'enrichir les séries sur lesquelles les analyses statistiques sont conduites, consiste à intégrer de l'information additionnelle, c'est à dire, toute donnée supplémentaire qui n'a pas été enregistrée par le marégraphe au site d'intérêt. L'information additionnelle peut être de l'information historique (observations avant le début des enregistrements marégraphiques), de l'information régionale (données disponibles à d'autres sites proches du marégraphe de référence) ou même de l'information basée sur la connaissance et les avis d'experts. L'information additionnelle, et en particulier historique, permet aussi de relativiser une observation qui peut apparaître comme un "horsain" dans l'échantillon observé, en augmentant sa représentativité. Depuis quelques années, des études se concentrent sur l'intégration de l'information historique ou régionale dans l'analyse statistique des niveaux marins et des surcotes extrêmes, mais encore trop peu proposent de combiner ces deux types d'information additionnelle.

1.1.2 Objectifs

Généralement, pour estimer la distribution de probabilités des niveaux marins, on cherche à ajuster une distribution de probabilités sur les surcotes puis à faire une convolution avec la distribution empirique des marées astronomiques. La surcote, variable météorologique, est la différence entre le niveau marin observé (mesuré) et le niveau marin prédit (marée astronomique prédite) (voir Figure 1.3). On appelle données systématiques, les niveaux marins mesurées par des marégraphes à partir desquels, les marées astronomiques sont prédites et les surcotes déduites. L'information additionnelle (historique et/ou régionale) permet d'enrichir les échantillons systématiques, cependant son exploitation pose des difficultés.

Les données historiques sont des niveaux marins records décrits dans les archives et la presse de l'époque, ou dans des sources secondaires lorsque l'évènement est décrit des années après. La validation de ces données historiques est une étape nécessaire qui nécessite des compétences multiples. Les surcotes historiques associées à ces niveaux records historiques peuvent être déduites. Cependant, des surcotes extrêmes historiques peuvent passer inaperçues si, combinées à des marées astronomiques faibles ou modérées, elles n'engendrent pas de niveaux marins extrêmes, qui auraient pu marquer les mémoires et être répertoriés dans la presse locale de l'époque. On comprend ici la difficulté, voire l'impossibilité de garantir l'exhaustivité d'un inventaire de surcotes extrêmes historiques durant une période donnée. Pourtant, l'exhaustivité des séries historiques de variables supérieures à un seuil est indispensable pour une estimation statistique non biaisée (Gaume, 2018). Des publications tentent de répondre à cette problématique d'exhaustivité liée spécifiquement à la variable de surcote, au risque d'introduire de nouveaux biais dans l'analyse statistique (Hamdi et al., 2015 ; Hamdi et al., 2018 ; Bulteau et al., 2015 ; Frau et al., 2018). La première problématique de cette thèse est donc l'estimation d'une distribution statistique des surcotes en intégrant de l'information historique, tout en en garantissant l'exhaustivité afin de conserver une inférence statistique non biaisée.

D'un autre côté, l'intégration d'information régionale consiste à prendre en compte des données en plusieurs points de mesure d'une région, considérée comme statistiquement homogène, pour améliorer les estimations au site cible, pouvant être partiellement ou non jaugé. Dans le domaine maritime, les études régionales conduites jusqu'à présent sont très similaires et sont généralement basées sur la RFA (Regional Frequency Analysis), proposée originellement par Hosking et al. (1997) en hydrologie. Ces méthodes imposent des hypothèses assez contraignantes d'homogénéité statistique régionale, et nécessitent des adaptations en cas de dépendance spatiale des enregistrements entre les sites. Des travaux, comme Bernardara et al. (2011), Weiss (2014) et Hamdi et al. (2019), tentent de répondre à ces contraintes, mais méritent d'être approfondis. La deuxième problématique est donc d'intégrer proprement l'information régionale en améliorant les propositions précédemment publiées. C'est une question très large car, si jusqu'à présent une seule méthode a été utilisée dans le domaine maritime pour l'analyse régionale, il en existe une grande variété dans d'autre domaine tel que l'hydrologie. L'utilisation de variables physiographiques et météorologiques explicatives des caractéristiques statistiques locales des surcotes est également une piste de recherche prometteuse.

La troisième problématique est la combinaison de données régionales et historiques pour enrichir des séries locales dans les deux directions spatiale et temporelle. Il y a très peu de références, tout domaine confondu, abordant ce point, c'est donc un champ de recherche très ouvert.

Finalement, l'objectif général de cette thèse est d'améliorer les modèles statistiques d'estimation des surcotes extrêmes intégrant l'information historique et régionale de façon non biaisée. Cette approche doit aussi prendre en compte les incertitudes d'estimation et celles liées aux jeux de données (i.e. incertitudes liées à l'échantillonnage). La thèse doit donc répondre aux trois problématiques énoncées précédemment : 1) proposer une approche permettant de résoudre les biais d'intégration des informations sur les données historiques dans les analyses statistiques, 2) tester différentes approches pour l'analyse statistique régionale des surcotes et 3) combiner l'information historique et régionale pour en tirer le meilleur parti pour l'estimation statistique des surcotes.

1.2 Revue de littérature générale

Dans cette revue de littérature, on présente les variables affectant les niveaux marins, les méthodes d'estimations des événements extrêmes, d'abord sans information additionnelle, puis avec de l'information historique ou avec des approches régionales, et enfin la combinaison de l'information historique et régionale.

1.2.1 Les variables

1.2.1.1 Définitions

En l'absence de vagues, le niveau marin peut être interprété comme la combinaison de deux processus distincts : la marée astronomique liée à l'influence des forces gravitationnelles des

astres et la surcote causée par des phénomènes météorologiques (pression atmosphérique, vent). La marée astronomique est une variable déterministe prévisible alors que la surcote est une variable stochastique (aléatoire). Les marégraphes mesurent le niveau marin instantané. À partir de ces observations, la marée astronomique instantanée peut être prédite et une surcote instantanée peut ainsi être déduite : différence entre le niveau de mer astronomique théorique et le niveau de mer réellement observé. La surcote de pleine mer, pour un cycle de marée donné, est définie comme la différence entre le plus haut niveau marin observé et le plus haut niveau de la marée astronomique prédite (Vries et al., 1995), ces deux niveaux ne sont pas nécessairement concomitants (voir Figure 1.3). Dans les zones de marée semi-diurne, il y a en moyenne deux pleines mers et deux basses mers par jour et les niveaux marins extrêmes coïncident autour des moments de marée haute. La variable de surcote de pleine mer est alors privilégiée par rapport à la surcote instantanée dans ces zones. En effet, c'est un meilleur indicateur de l'impact météorologique sur les niveaux marins les plus importants (Arns et al., 2015 ; Batstone et al., 2013 ; Wahl et al., 2015). De plus, comme il n'y a que deux valeurs de surcotes de pleine mer par jour, il est plus facile de reconstruire les niveaux de pleine mer à l'aide d'une convolution avec les marées astronomiques de pleine mer, plutôt que de chercher à reconstruire les séries de niveaux marins à partir des surcotes instantanées.

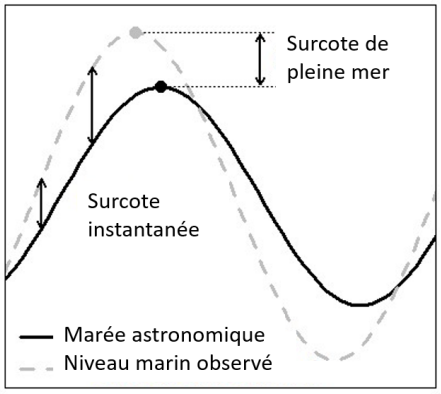

Figure 1.3 – Définition de la surcote de pleine mer

1.2.1.2 Intéraction marée - surcote

Dixon et al. (1999) proposent une méthode pour tester la dépendance entre la marée et la surcote horaires pour les surcotes importantes. Cette méthode consiste à diviser la gamme des marées en plusieurs classes de probabilité égale, le nombre de surcotes importantes devrait être le même pour chaque classe de marée s'il y a indépendance entre les deux composantes. À l'aide de cette méthode, Tomasin et al. (2008) montrent que les marées et surcotes horaires sont plus ou moins dépendantes selon les marégraphes dans la zone Manche Anglaise. Mazas et al. (2014) montrent qu'à Brest, les marées et les surcotes horaires sont dépendantes mais que cette dépendance s'estompe à marée haute. Dans la zone Est de la Manche Anglaise, les interactions entre les surcotes et les marées horaires sont expliquées par de faibles profondeurs d'eau et de forts courants de marée (Idier et al., 2012). Les surcotes y sont atténuées à marée haute et amplifiées à marée montante.

La dépendance entre la marée astronomique et la surcote instantanées semble importante. Qu'en est-il des interactions entre les surcotes de pleine mer et les marées astronomiques hautes ? D'après Kergadallan et al. (2014), elles sont non négligeables pour au moins la moitié des marégraphes sur le littoral Atlantique Français. À l'aide d'un test de Kendall et d'une visualisation graphique, Williams et al. (2016) ont démontré que n'importe quelle surcote de pleine mer peut coïncider avec n'importe quelle marée haute pour des marégraphes localisés en Angleterre, Irlande, Hollande et sur la côte Est des Etats-Unis. Ce résultat est nuancé avec un test plus complet, pour les 1% des niveaux marins les plus importants, la dépendance entre la surcote de pleine mer et la marée haute est non négligeable (Arns et al., 2020). Il faudrait idéalement tenir compte de cette dépendance pour reconstituer les niveaux marins à partir des surcotes de pleine mer. Cependant, par soucis de simplicité, il est courant de négliger cette dépendance, c'est le cas dans cette thèse.

1.2.1.3 Saisonalité

Les surcotes les plus importantes ont généralement lieu pendant l'hiver, alors que les marées astronomiques les plus importantes ont lieu autour des équinoxes dans les zones de marée semi-diurne. Cela a notamment été vérifié par Tomasin et al. (2008) en calculant la distribution mensuelle des marées astronomiques et des surcotes horaires au-dessus de leur quantiles 99.9% respectifs. La dépendance constatée plus haut entre les marées hautes astronomiques et les surcotes de pleine mer peut être une conséquence de la saisonnalité des deux phénomènes (Williams et al., 2016). Il peut être intéressant de tenir compte de la saisonnalité plutôt que de la dépendance des composantes du niveau marin.

1.2.2 Estimation des niveaux marins extrêmes

1.2.2.1 Théorie des valeurs extrêmes

Selon la théorie des valeurs extrêmes, la distribution d'un échantillon d'évènements maximums annuels tend asymptotiquement vers une distribution GEV (Generalized Extreme Value) et la distribution d'un échantillon POT (Peaks Over Threshold) d'évènements au-dessus d'un seuil $u \in R$ tend asymptotiquement vers une distribution GP (General Pareto) (Coles, 2001). Le nombre de dépassements du seuil u par an suit un processus de Poisson de paramètre λ (nombre moyen de dépassements du seuil u). Les fonctions de répartition de la distribution GEV et GP sont données respectivement par les Equations 1.1 et 1.2.

Equation 1.1 – Fonction de répartition de la distribution GEV

$$\forall x \in R,\ F(x) = \begin{cases} \exp\left\{-\left[1+\xi(\frac{x-u}{\sigma})\right]^{-\frac{1}{\xi}}\right\} & \text{si } \xi \neq 0, \\ \exp\left[-\exp(\frac{x-u}{\sigma})\right] & \text{si } \xi = 0. \end{cases}$$

où $u \in R$ **est le paramètre de position**
$\sigma > 0$ **est le paramètre d'échelle**
$\xi \in R$ **est le paramètre de forme**

Equation 1.2 – Fonction de répartition de la distribution GP

$$\forall x > u,\ F(x) = \begin{cases} 1 - \left[1 + \xi(\frac{x-u}{\sigma})\right]^{-\frac{1}{\xi}} & \text{si } \xi \neq 0, \\ 1 - \exp(\frac{x-u}{\sigma}) & \text{si } \xi = 0. \end{cases}$$

où $\sigma > 0$ **est le paramètre d'échelle**
$\xi \in R$ **est le paramètre de forme**

1.2.2.2 Inférence Bayésienne MCMC

La fonction de vraisemblance $L(X|\theta)$ décrit la probabilité de l'échantillon des données observées X en fonction des valeurs des paramètres θ d'une distribution de probabilité. L'analyse fréquentielle cherche à maximiser cette vraisemblance avec une méthode d'optimisation numérique afin d'obtenir un jeu de paramètres optimal. L'inférence Bayésienne, basée sur le théorème de Bayes (voir Equation 1.3), considère plutôt les paramètres comme des variables aléatoires (Gelman et al., 2014). Le résultat est alors une fonction de densité des paramètres de la loi $P(\theta|X)$ conditionnelle aux jeux de données X, à partir de laquelle on peut calculer un intervalle de crédibilité pour les quantiles de la distribution statistique. La largeur de ces intervalles de crédibilité reflètent le contenu informatif du jeu de données.

Equation 1.3 – Théorème de Bayes

$$P(\theta|X) = \frac{P(X|\theta)P(\theta)}{P(X)}$$

où $P(\theta)$ **est la distribution à priori des paramètres** θ
$P(X)$ **est la probabilité du jeu de données** X
$P(\theta|X)$ **est la probabilité conditionnelle de** θ **sachant** X
$P(X|\theta)$ **est la probabilité conditionnelle de** X **sachant** θ

S'il n'y a pas d'information à priori sur les valeurs des paramètres, il est courant de considérer $P(\theta) = 1$. L'algorithme MCMC (Monte Carlo Markov Chains), combinant les méthodes de marche aléatoire de Monte Carlo et les chaînes de Markov, est utilisé pour estimer la distribution à posteriori $P(\theta|X)$ des paramètres.

1.2.2.3 Méthodes directes

Pour estimer les niveaux marins extrêmes, il y a deux familles de méthodes : les méthodes directes et les méthodes indirectes. Les méthodes directes consistent à ajuster une distribution de probabilités sur les niveaux marins observés (Arns et al., 2013 ; Bulteau et al., 2015 ; Ben Daoued et al., 2020). Les méthodes directes ne permettent pas d'exploiter l'information de la marée astronomique (Tawn et al., 1989 ; Mazas et al., 2014) et ont tendance à sous-estimer les quantiles des niveaux marins correspondant à des périodes de retour élevées (Haigh et al., 2010 ; Andreewsky et al., 2014). Ainsi, les méthodes indirectes sont aujourd'hui privilégiées par la communauté scientifique. Les méthodes indirectes consistent à ajuster séparément une loi de probabilités des surcotes (ou surcotes de pleine mer) et des marées astronomiques,

puis de faire une convolution pour obtenir la distribution des niveaux marins. Les différentes méthodes indirectes proposées sont résumées ci-après.

1.2.2.4 Méthodes indirectes

Pugh et al. (1980) ont proposé la première méthode indirecte, appelée Joint Probability Method (JPM), basée sur la combinaison de la marée astronomique et de la surcote horaires. Ces deux composantes sont supposées indépendantes et la fonction f de densité de probabilité du niveau marin horaire est alors donnée par :

Equation 1.4

$$\forall z > 0,\ f(z) = \int_R f_T(z-x) f_S(x) dx$$

où f_T **est la fonction de densité de la marée astronomique horaire**
f_S **est la fonction de densité de la surcote horaire**

Pour calculer f, les échantillons horaires de la marée astronomique et de la surcote sont respectivement divisés en n_T et n_S intervalles, puis les intervalles sont recombinés pour reconstruire les niveaux marins :

Equation 1.5

$$\forall z > 0,\ f(z) = \sum_{i=1}^{n_T} \sum_{j=1}^{n_S} f_T(y_i) f_S(x_j) 1_{y_i + x_j = z}$$

La période de retour $T(x)$, en années, d'un niveau marin $z > 0$ est exprimée par :

Equation 1.6

$$T(z) = \frac{1}{1 - F(z)^N}$$

où $F(z) = \int_{-\infty}^{z} f(z)dz$ **est la fonction de répartition du niveau marin horaire**
$N = 24 \times 365.25 = 8766$ **est le nombre de niveaux marins horaires par an**

Cette méthode a deux limitations importantes. Premièrement, les observations horaires sont supposées indépendantes, ce qui n'est clairement pas le cas. Deuxièmement, la méthode sous-estime les niveaux marins extrêmes puisque le plus haut niveau marin qui peut être estimé est la somme de la plus haute marée astronomique observée et de la plus haute surcote observée.

La Revised Joint Probability Method (RJPM) proposée par Tawn et al. (1989) permet de répondre aux deux limitations de la JPM. La distribution de la surcote est divisée en deux parties : une distribution empirique (comme pour la JPM) pour les surcotes ordinaires et une distribution paramétrique GEV pour les surcotes extrêmes. Cela permet d'estimer des niveaux marins supérieurs à la somme de la plus haute marée astronomique observée et de

la plus haute surcote observée. La dépendance temporelle est prise en compte en modifiant la période de retour des niveaux marins z avec un indice extrémal $\theta(z) \in (0, 1]$ tel que $T(z) = 1/(1 - F(z)^{\theta(z)N})$. S'il y a parfaite indépendance entre les observations, $\theta(z) = 1$.

La Direct Joint Probability Method (DJPM) a été introduite pour traiter la dépendance entre la marée astronomique et la surcote horaires (Liu et al., 2010). La fonction de répartition du niveau marin z est alors la somme des probabilités des combinaisons de marée et de surcote résultantes d'un niveau marin inférieur ou égal à z :

Equation 1.7

$$\forall z > 0,\ F(z) = \sum_{i=1}^{n_T} \sum_{j=1}^{n_S} F(z_{i,j}) 1_{z_{i,j}=z}$$

où $F(z_{i,j})$ **est la probabilité jointe de la surcote** x_i **et de la marée astronomique** y_j **dont la somme est un niveau marin égal à** $Z_{i,j}$

Batstone et al. (2013) ont proposé une nouvelle version de la RJPD utilisant la variable de surcote de pleine mer au lieu de la surcote horaire. En effet, comme vu précédemment, la surcote de pleine mer est un meilleur indicateur de l'impact météorologique que la surcote horaire sur les niveaux marins extrêmes. De plus, il y a une valeur de surcote de pleine mer par cycle de marée (toutes les 12h et 36 minutes), donc les valeurs observées sont beaucoup moins corrélées que les surcotes horaires. Enfin, la dépendence entre la marée haute astronomique prédite et la surcote de pleine mer est plus faible qu'entre la marée astronomique et la surcote horaires (voir Section 1.2.1.2). Les surcotes de pleine mer ordinaires inférieures à un seuil u sont modélisées par la distribution empirique et les surcotes de pleine mer extrêmes supérieures à un seuil u sont modélisées par une distribution GP. La distribution des surcotes de pleine mer F_{SS} est alors donnée par :

Equation 1.8

$$F_{SS}(x) = \begin{cases} \tilde{F}_{SS}(x) & \text{si } x < u, \\ 1 - \left[1 - \tilde{F}_{SS}(u)\right] G_{SS}(x) & \text{if } x \geq u. \end{cases}$$

où $\tilde{F}_{SS}$ **est la distribution empirique des surcotes de pleine mer ordinaires**
G_{SS} **est la distribution de GP des surcotes de pleine mer extrêmes**

La fonction de répartition des niveaux marins est calculée à partir de la distribution jointe des surcotes de pleine mer et des marées astronomiques en découpant les marées astronomiques en M intervalles (voir Equation 1.9).

Equation 1.9

$$\forall x \in R,\ F_{SL} = \left[\prod_{t=T}^{M} F_{SS}(x - X_t)\right]^{1/M}$$

où X_t **est la marée haute astronomique prédite à l'intervalle** t
M **est le nombre d'intervalles de marées hautes astronomiques**

Cette dernière méthode a été largement adoptée par la communauté scientifique (Andreewsky et al., 2014 ; Mazas et al., 2014 ; Kergadallan et al., 2014 ; Hamdi et al., 2015 ; Hamdi et al., 2018 ; Frau et al., 2018).

1.2.3 Information historique

Les séries systématiques sont des séries enregistrées par des marégraphes, alors que les séries historiques sont composées d'observations ponctuelles de niveaux marins exceptionnels observés avant le début des enregistrements. Un évènement observé pendant une lacune de mesure peut aussi être considéré comme une donnée historique (Hamdi et al., 2015 ; Hamdi et al., 2019). La communauté scientifique s'accorde sur l'utilité de l'intégration de l'information historique notamment pour augmenter la taille de l'échantillon sur lequel les ajustements statistiques sont conduits et ainsi réduire les incertitudes d'estimation de la distribution statistique (Ouarda et al., 1998b ; Benito et al., 2004 ; Reis et al., 2005 ; Gaál et al., 2010 ; Payrastre et al., 2011 ; Hamdi et al., 2015). On va voir ci-dessous comment l'information historique peut être intégrée aux séries locales modélisées par les lois GEV ou GP.

1.2.3.1 Vraisemblance GEV

Soit X la série systématique des observations maximales annuelles pendant une période de w_s années. Y représente les observations historiques pendant une période de w_h années. La vraisemblance des données systématiques et historiques est donnée par l'Equation 1.10, et a été utilisée surtout en hydrologie (O'Connell et al., 2002 ; Naulet et al., 2005 ; Reis et al., 2005 ; Neppel et al., 2010 ; Gaál et al., 2010 ; Payrastre et al., 2011 ; Payrastre et al., 2013 ; Gaume, 2018), mais aussi dans le domaine maritime (Hamdi et al., 2015).

Equation 1.10

$$L(X, Y|\theta) = \prod_{t=1}^{w_s} f_\theta(x_t)\ .\ \prod_{i=1}^{h_1} f_\theta(y_i)\ .\ \prod_{j=1}^{h_2}\left[F_\theta(y_j^{up}) - F_\theta(y_j^{low})\right]\ .\ [1 - F_\theta(y_T)]^{h_3}\ .\ F_\theta(y_T)^{h_4}$$

où f_θ **est la fonction de densité de la GEV de paramètres** $\theta = (u, \sigma, \xi)$
F_θ **est la fonction de répartition de la GEV de paramètres** $\theta = (u, \sigma, \xi)$

Le jeu de données historiques peut contenir différents types d'information : i) h_1 années d'observations historiques supérieures à un seuil y_T connues précisément, ii) h_2 années d'observations historiques supérieures à y_T connues avec des incertitudes (intervalles), iii) h_3 années où le seuil y_T a été dépassé mais sans information supplémentaire sur les observations historiques et iv) h_4 années où le seuil y_T n'a pas été dépassé. La durée effective historique totale w_h est la somme des durées précitées : $w_h = h_1 + h_2 + h_3 + h_4$.

1.2.3.2 Vraisemblance GPD

Soit X la série systématique des observations au-dessus d'un seuil u pendant une période de w_s années. Y représente les observations historiques au-dessus d'un seuil u_H, avec $u_H > u$ pendant une période de w_h années. L'Equation 1.11 donne la vraisemblance de l'échantillon des données systématiques et historiques (Parent et al., 2003), et a été appliquée aux crues (Lumbroso et al., 2019), aux surcotes de pleine mer (Hamdi et al., 2015 ; Frau et al., 2018 ; Hamdi et al., 2018) et aux niveaux marins (Bulteau et al., 2015).

Equation 1.11

$$\begin{aligned} L(X, Y|\theta) =& P_\theta(N = n) \cdot \prod_{t=1}^{n} f_\theta(x_t) \cdot \\ & P_\theta(H = h) \cdot \prod_{i=1}^{h_1} \frac{f_\theta(y_i)}{1 - F_\theta(y_T)} \cdot \prod_{j=1}^{h_2} \frac{\left[F_\theta(y_j^{up}) - F_\theta(y_j^{low})\right]}{1 - F_\theta(y_T)} \end{aligned}$$

où f_θ **est la fonction de densité de la GP de paramètres** $\theta = (\lambda, \sigma, \xi)$
F_θ **est la fonction de répartition de la GP de paramètres** $\theta = (\lambda, \sigma, \xi)$
N **est le nombre de dépassements pendant la période systématique de** w_s **années et suit un processus de Poisson d'intensité** λw_s
H **est le nombre de dépassements pendant la période historique de** w_h **années et suit un processus de Poisson d'intensité** $\lambda w_h \, (1 - F_\theta(y_T))$

Le jeu de données historiques peut contenir différents types d'information : i) h_1 observations historiques supérieures à u_H connues précisément, ii) h_2 observations historiques supérieures à u_H connues avec des incertitudes (intervalles) et iii) h_3 observations historiques supérieures à u_H sans autre information disponible. Le nombre de dépassements pendant la période historique est de $h = h_1 + h_2 + h_3 + h_4$.

1.2.3.3 Durée effective historique

La durée effective historique associée aux données historiques (w_h dans les deux Sections précédentes) peut être définie comme le nombre d'années entre le premier évènement historique et le début des enregistrements systématiques. Une telle définition est cependant source de biais et conduit à sous-estimer la durée effective historique (Gaál et al., 2010 ; Strupczewski et al., 2014 ; Schendel et al., 2017 ; Gaume, 2018). En effet, les observations historiques ont

pu être retrouvées dans les archives car ce sont des évènements records et la plus ancienne observation historique est notamment généralement apparue exceptionnelle par rapport aux années qui l'ont précédée. Dans le cadre des maximums annuels, Strupczewski et al. (2014) proposent de doubler la longueur de la période historique, tandis que Schendel et al. (2017) proposent une correction plus modérée de la durée effective historique : $w_h + \frac{w_h+w_s-1}{k}$ où $k = h_1 + h_2 + h_3$ le nombre d'observations historiques ayant dépassé le seuil y_T. Cette dernière approche est plutôt retenue dans la suite de la thèse. Cette durée historique peut être complétée en ajoutant les périodes de lacunes de mesure pendant la période systématique (Bulteau et al., 2015 ; Hamdi et al., 2015 ; Hamdi, 2019).

1.2.3.4 Comment gérer la non exhaustivité de l'échantillon des surcotes historiques ?

En analyse côtière, les observations historiques sont des niveaux marins records, dont on peut estimer les surcotes de pleine mer associées. Cependant, certaines surcotes de pleine mer extrêmes peuvent passer inaperçues, si elles sont associées à des marées astronomiques faibles ou modérées et ne génèrent pas de niveaux marins extrêmes (Outten et al., 2020). Il est donc très difficile, voire impossible, de garantir l'exhaustivité de l'échantillon des surcotes de pleine mer extrêmes dépassant un seuil donné pendant la période historique considérée. On présente ci-après, un état des lieux des études qui tentent de répondre à cette problématique (Bulteau et al., 2015 ; Hamdi et al., 2015 ; Hamdi et al., 2018 ; Frau et al., 2018).

Par exemple, Bulteau et al. (2015) choisissent d'estimer les niveaux marins extrêmes avec une méthode directe en ajustant une distribution de GP sur un échantillon POT de niveaux marins systématiques avec des niveaux marins historiques. Cette méthodologie répond bien à la problématique d'exhaustivité car les niveaux marins historiques peuvent être supposés exhaustifs pendant la période historique au-dessus d'un seuil, à condition que ce seuil soit suffisamment élevé. Cependant, comme vu dans la Section 1.2.2.3, il est préférable de faire un ajustement statistique sur la surcote de pleine mer plutôt que sur le niveau marin, en utilisant une méthode indirecte (voir Section 1.2.2.4).

Contrairement à la proposition de Bulteau et al. (2015), les propositions de Hamdi et al. (2015) et Hamdi et al. (2018) et de Frau et al. (2018) pour intégrer de l'information historique sont basées sur l'estimation indirecte des niveaux marins extrêmes en ajustant une distribution de GP sur un échantillon POT de surcotes de pleine mer systématiques (ainsi qu'une distribution GEV sur un échantillon de maximums annuels pour Hamdi et al., 2015). Hamdi et al. (2015) font l'hypothèse d'exhaustivité des surcotes de pleine mer historiques au-dessus d'un seuil u_H pendant la période historique. Cette forte hypothèse pourrait entraîner une sous-estimation des quantiles liée à un sous-échantillonnage des surcotes de pleine mer historiques extrêmes. Dans Frau et al. (2018), la période historique est réduite en introduisant la notion de "durée crédible historique" d_{cr}^{hist}, basée sur l'hypothèse selon laquelle le nombre d'évènements au-dessus du seuil POT u par an est le même pendant la période systématique et historique (voir Equation 1.12). Ici, le seuil historique u_H est supposé égal au seuil systématique u (voir Section 1.2.3.2). Ainsi, cette méthode pourrait entraîner une

sur-estimation des quantiles, due à une sur-représentativité des surcotes de pleine historiques extrêmes pendant une courte période historique.

Equation 1.12

$$d_{cr}^{hist} = \frac{h}{\lambda}$$

où h **est le nombre de surcotes historiques supérieures au seuil** u
λ **est le nombre moyen de dépassements annuels**

1.2.4 Formation des régions

Le but de l'analyse régionale est de déduire des propriétés statistiques d'une variable locale à partir des observations disponibles sur d'autres sites. Elle est généralement composée de deux étapes : la formation de régions et l'estimation régionale. Cette partie donne un aperçu des méthodes disponibles pour former les régions à partir de séries de données enregistrées ou à partir de variables physiographiques et météorologiques.

1.2.4.1 Basée sur les séries de données

Récemment, une méthode a été mise en place, dans le domaine maritime, pour former les régions homogènes sur la base de considérations physiques (Weiss et al., 2014a ; Weiss, 2014). La procédure est basée sur un critère de propagation extrémal (des tempêtes) défini comme la probabilité que deux sites soient impactés par un même évènement extrême si un des deux sites est impacté. Deux observations extrêmes sont causées par la même tempête si elles ont eu lieu dans un intervalle de 24 heures et si les sites impactés sont séparés géographiquement par au plus η sites ($\eta = 14$ pour un échantillon de 67 marégraphes dans Weiss et al., 2013b). Les régions sont formées à partir de ce critère de propagation selon un algorithme de classification hiérarchique (voir *Classification ascendante hiérarchique* dans la Section 1.2.4.2). Cette méthode permet de former des régions homogènes fixes, mais si le site d'intérêt se situe à la limite de la région formée, il peut y avoir un effet de bord.

Pour répondre à cette limite, l'extremogramme empirique spatial a été introduit (Hamdi et al., 2016 ; Hamdi et al., 2019 ; Andreevsky et al., 2020) pour construire une région centrée autour d'un site cible. Dans cette méthode, le coefficient de dépendance extrémal est utilisé et est similaire au critère de propagation extrémal vu précédemment. C'est la probabilité qu'une observation à un site de la région est extrême sachant que dans un intervalle de 24 heures l'observation au site cible est extrême aussi. Un seuil de voisinage doit être choisi pour sélectionner les sites à inclure dans la région du site cible tel que le coefficient de dépendance extrémal des sites sélectionnés soit inférieur à ce seuil.

Ces deux méthodes permettent de former des régions physiquement homogènes, puis leur homogénéité statistique peut être vérifiée avec les mesures classiques de Hosking et al. (1997) (voir Section 1.2.4.3). La principale limite de ces méthodes est le fait qu'elles nécessitent des séries enregistrées suffisamment longues. Pour contourner cette problématique, d'autres

critères doivent être utilisés, par exemple, dans Sweet et al. (2020), le bassin Pacifique est divisé selon les processus physiques (marée dominante, cyclone tropical, extratropical, vague dominante, transition), puis selon la localisation des sites. Une des réponses à cette problématique peut aussi être le recours à des variables physiographiques et météorologiques.

1.2.4.2 Basée sur des caractéristiques physiographiques et météorologiques

Les méthodes suivantes permettent la formation de régions homogènes à partir des caractéristiques physiographiques et météorologiques des sites. Les régions formées peuvent être fixes avec la classification ascendante hiérarchique (HCA), ou centrée autour d'un site cible avec l'analyse canonique des corrélations (CCA) et la région d'influence (ROI).

Classification ascendante hiérarchique

L'HCA consiste à délimiter des régions homogènes fixes basées sur une mesure de similarités entre les sites. Comme vu précédemment, la mesure de similarités peut être basée sur les similarités des observations extrêmes entre les séries (Weiss et al., 2014a ; Weiss, 2014). Cette mesure de similarités peut aussi être basée sur les caractéristiques physiographiques et météorologiques locales (Burn, 1989). La première étape de l'HCA consiste à grouper les sites dans un arbre de classification binaire. Chaque site est initialement assigné à son propre cluster. De manière itérative, à chaque étape, les deux clusters les plus similaires sont joints en un nouveau jusqu'à ce qu'il n'y ait qu'un seul cluster global. Cette étape est souvent réalisée grâce à l'algorithme de Ward (Ward, 1963). Les résultats de l'HCA peuvent être représentés à l'aide d'un dendrogramme, aussi appelé diagramme en arbre. Le nombre de régions homogènes peut être défini arbitrairement ou déterminé en utilisant par exemple la règle de Mojena (Mojena, 1977).

Région d'influence

L'identification des sites à inclure dans la ROI d'un site cible est basée sur la similarité entre le site cible et les autres sites mesurée d'après leurs caractéristiques locales (Burn, 1990b). La distance euclidienne pondérée des caractéristiques physiographiques et météorologiques peut être utilisée comme mesure de similarité. Un site i doit être inclus dans la région d'influence du site cible t si $D_{it} \leq \theta_t$ où D_{it} est la distance entre le site i et t. La valeur du seuil θ_t doit être choisie de façon à ce qu'il y ait un bon compromis entre le nombre de sites dans la région et l'homogénéité entre les sites. Plus la valeur de θ_t est élevée, plus il y a de sites dans la région et moins l'homogénéité est forte, et inversement pour une faible valeur de θ_t.

Analyse canonique des corrélations

La CCA est une méthode de statistique descriptive multidimensionnelle dont l'objectif général est de déterminer une relation linéaire entre deux ensembles de données quantitatives observées sur les mêmes individus. Soient $P = \{P_1, P_2, ..., P_n\}$ les variables physiographiques et météorologiques et $Q = \{Q_1, Q_2, ..., Q_r\}$ les quantiles locaux de la variable d'intérêt, avec $n \leq r$. P et Q doivent être normalisés. Soient les combinaisons linéaires $V = a'P$ et $W = b'P$

et $C = \begin{pmatrix} C_{PP} & C_{QP} \\ C'_{PQ} & C_{QQ} \end{pmatrix}$ la matrice de covariance de P et Q. Le coefficient de corrélation entre W_i et V_i est donné par :

Equation 1.13

$$\rho = \frac{a'_i C b_i}{\sqrt{a'_i C_{PP} a_i b'_i C_{QQ} b_i}}$$

L'objectif de la CCA est de trouver des vecteurs a_i et b_i qui maximisent ρ sous la contrainte que V_i et W_i aient une variance égale à 1. Lorsque la première paire de variables canoniques (V_1, W_1) est obtenue, d'autres paires de variables canoniques peuvent alors être obtenues. Si p est le rang de la matrice C_{PQ}, $a*$ et $b*$ peuvent être identifiés tels que les coefficients de corrélation $\lambda_i = corr(V_i, W_i)$, $i = 1, ..., p$ soient maximisés. Il a été montré que les solutions $a*$ et $b*$ sont des vecteurs propres de $C_{PP}^{-1} C_{PQ} C_{QQ}^{-1} C'_{QP}$ et de $C_{QQ}^{-1} C'_{PQ} C_{PP}^{-1} C_{PQ}$ respectivement. V et W sont les variables canoniques et les λ_i sont les corrélations canoniques.

La CCA peut être utilisée pour la délimitation de régions homogènes autour d'un site cible (Ouarda et al., 2001). Au site cible, le score canonique v_0 est connu alors que le score canonique w_0 ne l'est pas, mais il peut être approximé par Λv_0 où $\Lambda = diag(\lambda_1, ..., \lambda_p)$. Les distances à la position moyenne dans l'espace canonique sont données par :

Equation 1.14

$$D^2 = (W - \Lambda v_0)'(I_p - \Lambda\Lambda)^{-1}(W - \Lambda v_0)$$

où I_p **est la matrice identité d'ordre** p

D^2 est la distance de Mahalanobis et suit une distribution du χ^2 avec p degrés de liberté. Les sites voisins peuvent donc être définis en excluant les réalisations w éloignées de la position moyenne Λv_0 du site cible (i.e. $D^2 > \chi^2_{\alpha,p}$, α est le niveau de confiance). Le choix de α peut être determiné avec une procédure de rééchantillonnage de type Jack-knife (Ouarda et al., 2001).

1.2.4.3 Homogénéité statistique

La méthode de l'indice (voir Section 1.2.5.1) pour l'estimation régionale nécessite que les régions formées soient statistiquement homogènes. Pour cela, la procédure développée par Hosking et al. (1997) est une référence. Elle repose sur l'hypothèse selon laquelle les rapports des L-moments devraient être identiques pour les sites d'une région statistiquement homogène. Soit $w_i = \left(t^i, t_3^i, t_4^i\right)$, le vecteur contenant les trois premiers rapports des L-moments calculés empiriquement au site i : t^i le L-CV, t_3^i le L-skewness et t_4^i le L-kurtosis.

La mesure de discordance locale de Wilks $D_{(i)}$ (voir Equation 1.15) permet d'identifier si un site est discordant à l'intérieur d'une région donnée. $D_{(i)}$ mesure si le site i est significativement

différent des autres sites de la région en fonction des rapport des L-moments w_i. Le site i peut être déclaré discordant, avec un niveau de risque 10%, si $D_{(i)} > 3$ pour les régions avec plus de 15 sites ($N > 15$).

Equation 1.15 – Mesure de discordance locale de Wilks

$$D_{(i)} = \frac{1}{3} (w_i - \bar{w})^T A^{-1} (w_i - \bar{w})$$

où $\bar{w} = \frac{1}{N} \sum_{i=1}^{N} w_i$

$A = \sum_{i=1}^{N} (w_i - \bar{w}) (w_i - \bar{w})^T$

Les mesures d'hétérogénéité régionale $H_{m=1,2,3}$ (voir Equation 1.16) permettent d'évaluer le niveau d'hétérogénéité (ou d'homogénéité) d'une région donnée en comparant les dispersions observées des L-moments aux dispersions attendues entre les sites dans une région statistiquement homogène. Ces dispersions ne sont pas connues pour une région théoriquement homogène mais peuvent être évaluées numériquement par des simulations de Monte Carlo avec tirages dans une distribution de Kappa à quatre paramètres ajustés sur les données observées. La distribution de Kappa est choisie pour sa flexibilité, elle est par exemple une forme générale de la GEV ou de la GP. La région peut être déclarée acceptablement homogène si $H_m < 1$, possiblement homogène si $1 \leq H_m \leq 2$ et définitivement hétérogène si $H_m > 2$.

Equation 1.16 – Mesures d'hétérogénéité régionale

$$H_m = \frac{V_m - E(V_m)}{\sigma(V_m)}, \ m \in \{1, 2, 3\}.$$

où V_m **sont les dispersions observées des L-moments**
$E(V_m)$ **et** $\sigma(V_m)$ **sont la moyenne et l'écart type des valeurs de** V_m **obtenues par simulations de Monte Carlo**

1.2.5 Estimation régionale

Une fois la région formée, plusieurs méthodes peuvent être employées pour l'estimation régionale, que ce soit à des sites jaugés (voir Section 1.2.5.1) ou à des sites non jaugés (voir Section 1.2.5.2).

1.2.5.1 Analyse fréquentielle régionale

La méthode RFA (Regional Frequency Analysis) repose sur l'hypothèse selon laquelle les sites appartenant à une région statistiquement homogène ont la même distribution régionale à un paramètre d'échelle près, l'indice local (Dalrymple, 1960 ; Hosking et al., 1997).

La communauté scientifique a largement adopté la RFA pour divers aléas naturels tels que les crues (Kjeldsen et al., 2002 ; Chebana et al., 2009 ; Gaume et al., 2010), les vagues (Mai Van et al., 2007 ; Weiss et al., 2014a ; Weiss et al., 2014b ; Lucas et al., 2017), les

précipitations (Kuswanto et al., 2021), la neige (Mo et al., 2022) ou les concentrations de solides en suspension en rivière (Tramblay et al., 2010). La RFA a aussi fait ses preuves dans le domaine maritime et a été appliquée aux surcotes (Mai Van et al., 2007), aux surcotes de pleine mer (Bardet et al., 2011 ; Bernardara et al., 2011 ; Weiss et al., 2012 ; Weiss et al., 2013b ; Weiss et al., 2013a ; Hamdi et al., 2019 ; Andreevsky et al., 2020) et aux niveaux marins (Van Gelder et al., 1998 ; Sweet et al., 2020).

Méthode de l'indice

La méthode de l'indice (Dalrymple, 1960) suppose que les observations des sites d'une région homogène ont la même distribution à un facteur d'échelle (indice) local près μ_i connu ou estimé. Cet indice local représente les spécificités locales d'un site. Une région homogène est composée de N sites et il y a n_i observations à chaque site i. Les séries locales standardisées par l'indice local $\tilde{x}_{ij} = x_{ij}/\mu_i,\ i = \{1, ..., N\},\ j = \{1, ..., n_i\}$ sont groupées dans un même échantillon et les paramètres de la distribution régionale θ_R sont estimés sur la base de cet échantillon enrichi par rapport à l'échantillon local. Le quantile x_T^i correspondant à une période de retour de T ans au site i est obtenu par le produit de l'indice local μ_i et du quantile régional estimé $\tilde{x}_T^R$ (voir Equation 1.17).

Equation 1.17

$$x_T^i = \mu_i \tilde{x}_T^R,\ i = \{1, ..., N\}\,.$$

La vraisemblance de l'échantillon régional $\tilde{X}$ est donnée par l'Equation 1.18 pour les séries de maximums annuels modélisés par une distribution GEV. Chaque série locale X_i, $i = \{1, ..., N\}$, suit une distribution GEV de paramètres $\theta_i = (u_i, \sigma_i, \xi_i)$.

Equation 1.18

$$L(\tilde{X}|\theta_R) = \prod_{i=1}^{N} \left[\prod_{j=1}^{n_i} f_{\theta_R}(\tilde{x}_{ij}) \right] = \prod_{i=1}^{N} \left[\prod_{j=1}^{n_i} f_{\theta_R}\left(\frac{x_{ij}}{\mu_i}\right) \right]$$

Distribution GP

La méthode de l'indice a été étendue aux séries POT modélisées par une distribution GP (Madsen et al., 1997 ; Ribatet et al., 2007). Chaque série locale X_i, $i = \{1, ..., N\}$, suit une distribution GP de paramètres $\theta_i = (\sigma_i, \xi_i)$.

L'échantillon régional $\tilde{X}$, composé des séries locales X_i normalisées par le seuil POT u_i, suit une distribution GP de paramètres $\theta_R = (\sigma, \xi)$. Le paramètre de forme ξ est supposé constant à l'intérieur de la région, alors que le paramètre d'échelle régional σ vérifie $\sigma = \sigma_i/u_i$, $i = \{1, ..., N\}$. Notons qu'on peut choisir un autre indice local que le seuil POT u_i, comme par exemple la surcote empirique annuelle locale (Bardet et al., 2011) ou la moyenne de

l'échantillon local des surcotes extrêmes (Bernardara et al., 2011 ; Weiss et al., 2013a). La vraisemblance de l'échantillon régional $\tilde{X}$ est donnée par :

Equation 1.19

$$L(\tilde{X}|\theta_R) = P_{\theta_R}(K = k) \; . \; \prod_{i=1}^{N} \left[\prod_{j=1}^{n_i} f_{\theta_R}(\tilde{x}_{ij}) \right] = P_{\theta_R}(K = k) \; . \; \prod_{i=1}^{N} \left[\prod_{j=1}^{n_i} f_{\theta_R}\left(\frac{x_{ij}}{u_i}\right) \right]$$

où K **est le nombre de dépassements dans l'échantillon régional et suit un processus de Poisson d'intensité** λr**,** r **est la durée effective régionale**

Problématiques

Les vraisemblances 1.18 et 1.19 nécessitent qu'il y ait indépendance entre les sites, autrement dit que les observations des séries locales soient indépendantes les unes des autres. La dépendance inter-sites n'introduit a priori pas de biais, mais augmente la variance d'estimation (Stedinger, 1983 ; Hosking et al., 1988). Afin de corriger les effets possibles des dépendances inter-sites, de nombreuses études (Bernardara et al., 2011 ; Weiss et al., 2013b ; Andreevsky et al., 2020 ; Sweet et al., 2020) choisissent de ne garder que l'observation maximale sur une fenêtre de temps, c'est à dire, lorsqu'une tempête touche plusieurs sites, la plus grande observation est conservée. Ce choix peut introduire un biais positif, certaines études préfèrent donc conserver toutes les valeurs (Bardet et al., 2011), dans ce cas, il faudrait en tenir compte dans le calcul de la période effective régionale.

La durée effective régionale peut être commodément définie comme la somme des durées locales mais devrait être réduite pour tenir compte des dépendances entre les sites d'une même région (Bardet et al. (2011)). Dans Weiss (2014) et Andreevsky et al. (2020), la durée effective régionale est estimée avec une fonction de dépendance régionale basée sur le critère de propagation extrémal défini comme la probabilité que deux sites soient impactés par un même évènement si un des deux sites est impacté (voir Section 1.2.4.1).

Dans le cas de l'échantillonnage POT, la possible variation du seuil d'un site à l'autre ajoute une source d'incertitude. Ce point est important à souligner, mais n'est pas un objet de recherche pour cette thèse.

1.2.5.2 Sites non jaugés

À notre connaissance, il n'existe pas dans la littérature d'analyses régionales menées sur les surcotes ou sur les niveaux marins incluant des variables physiographiques ou météorologiques pour l'estimation des quantiles à des sites non jaugés. Cependant, c'est une pratique courante en hydrologie (GREHYS, 1996a ; GREHYS, 1996b ; Ouarda, 2016 ; Rao et al., 2019).

Les deux principales méthodes d'estimation des quantiles aux sites non jaugés sont la régression linéaire multiple (MLR) et le modèle additif généralisé (GAM).

Régression linéaire multiple

La relation entre les variables $P = \{P_1, P_2, ..., P_n\}$ et $Q = \{Q_1, Q_2, ..., Q_r\}$ est décrite par le modèle suivant (Ouarda et al., 2000) :

Equation 1.20

$$Q = \beta_0 P_1^{\beta_1} P_2^{\beta_2} ... P_n^{\beta_n} \epsilon$$

où $\beta_0, \beta_1, ..., \beta_n$ **sont les paramètres du modèle**
ϵ **est le terme d'erreur supposé être normalement distribué**

Pour estimer les paramètres, l'Equation 1.20 est linéarisée avec une transformation logarithmique. Cependant, la transformation exponentielle de l'estimation introduit un biais (voir Equation 1.21) discuté dans Girard et al. (2004).

Equation 1.21

$$\mathbf{E}[Q] = \mathbf{E}[\exp(\log Q)] \neq \exp[\mathbf{E}(\log Q)]$$

Un tel modèle n'a jamais été utilisé avec des variables physiographiques ou maritimes pour l'analyse des surcotes ou des niveaux marins. Cependant, Hamdi et al. (2019) ont développé une approche basée sur la MLR pondérée pour compléter les séries mesurées aux pas de temps où les surcotes de pleine mer ont été manquées pendant des lacunes de mesures. Cela consiste en une relation entre les surcotes de pleine mer au site cible et celles aux sites voisins.

Modèle additif généralisé

Les modèles GAM, introduits par Hastie et al. (1986), sont plus flexibles que les modèles linéaires car ils relâchent la contrainte de relation linéaire entre des variables explicatives et la variable expliquée. Les modèles GAM sont une extension des modèles généralisés linéaires (GLM) qui sont eux-mêmes une généralisation de la MLR. Pour Y une variable expliquée et une matrice P dont les colonnes représentent r variables explicatives $P_1, P_2, ..., P_r$, le GLM est défini par :

Equation 1.22

$$g(Q) = \beta_0 + \sum_{j=1}^{r} \beta_j P_j + \epsilon$$

où g **est une fonction de lien**
$\beta_{j,j=0,...,r}$ **sont des paramètres inconnus**
ϵ **est le terme d'erreur**

Dans les modèles GAM, les relations linéaires sont remplacées par des fonctions lisses :

Equation 1.23

$$g(Q) = \beta_0 + \sum_{j=1}^{r} f_j(P_j) + \epsilon$$

où g **est une fonction de lien**
f_j **est une fonction lisse de** P_j

Les fonctions lisses sont représentées par des splines qui sont des fonctions polynomiales par morceaux reliées entre elles par un ensemble de points appelés nœuds. En général, une fonction lisse peut être définie par une combinaison linéaire de fonctions de base :

Equation 1.24

$$f_j(p) = \sum_{i=1}^{m_j} \beta_{ij} b_{ij}(x)$$

où b_{ij} **est la** i**-ème fonction de base de la** j**-ème variable explicative**
m_j **est le nombre de fonctions de base pour la** j**-ème variable explicative**
β_{ij} **sont des paramètres inconnus**

Pour éviter le sur-ajustement, l'estimateur $\hat{\beta}$ de β est obtenu en pénalisant la log-vraisemblance :

Equation 1.25

$$l_p(\beta) = l(\beta) - \frac{1}{2} \sum_{j=1}^{m} \lambda_j \beta^T S_j \beta$$

où $l_p(.)$ **est la fonction de la log-vraisemblance**
λ_j **est le paramètre de la** j**-ème fonction lisse** f_j
S_j **est une matrice connue**

1.2.5.3 Dans le cadre Bayésien

Grâce à sa flexibilité, le cadre Bayésien est particulièrement adapté à la combinaison de différents types d'informations en utilisant par exemple l'information à priori ou un modèle hierarchique.

Le prior

Une façon d'intégrer l'information régionale dans le cadre Bayésien est d'utiliser la distribution à priori (voir Equation 1.3). Par exemple, Seidou et al. (2006) proposent d'utiliser les observations locales et des distributions à priori obtenues avec un modèle de régression régionale log-linéaire sur un quantile et deux différences de quantiles $\tilde{\Delta}(q_T) = (\Delta(q_{T_1}), \Delta(q_{T_2}), \Delta(q_{T_3}))' = (q_{T_1}, q_{T_2} - q_{T_1}, q_{T_3} - q_{T_2})'$ tels que $\frac{1}{T_1} < \frac{1}{T_2} < \frac{1}{T_3}$. L'Equation 1.26 donne l'estimation régionale de $\tilde{\Delta}(q_T)$ qui suit une loi normale multivariée (MVN) en fonction de variables physiographiques et météorologiques. Le prior régional permet de stabiliser l'estimation du paramètre

de forme et d'améliorer les estimations des quantiles et des paramètres surtout pour les séries systématiques relativement courtes.

Equation 1.26

$$\log(\tilde{\Delta}q_T^R) = MVN(x\beta, \Sigma)$$

où $x = (1, A_1, ..., A_m)'$ **et** A_k **est la** k**-ième variable explicative au site d'intérêt**
β **est la matrice des coefficients de régression et est obtenue avec la méthode des moindres carrées ordinaires**
Σ **est la matrice de variance covariance**

Analyse hiérarchique Bayésienne

Une autre façon d'intégrer l'information régionale dans le cadre Bayésien est d'adopter l'analyse hiérarchique Bayésienne (HBA) introduite récemment et devenue très populaire pour l'estimation des évènements climatiques extrêmes tels que les précipitations (Cooley et al., 2007 ; Renard, 2011 ; Sharkey et al., 2019 ; Love et al., 2020), les débits (Reza Najafi et al., 2013 ; Lima et al., 2016) et les vagues (Clancy et al., 2016). Pour le moment, une seule étude s'est intéressée à l'application de l'HBA aux surcotes (Calafat et al., 2020). Les séries de maximas annuels de surcotes y sont modélisées par une distribution GEV et la dépendance inter-sites est capturée via un processus max-stable (Reich et al., 2012) pour interpoler les estimations (paramètres et quantiles) aux marégraphes non jaugés.

L'HBA est notamment populaire pour sa flexibilité à prendre en compte simultanément différents types d'informations ainsi que leurs incertitudes sans avoir à séparer le processus d'inférence en plusieurs étapes (Banerjee et al., 2015 ; Ahn et al., 2017). De plus, l'HBA relâche les contraintes imposées par la méthode de l'indice comme l'hypothèse d'homogénéité statistique. Il a été montré que l'HBA permet de réduire fortement les incertitudes, et plus particulièrement aux sites avec des séries courtes (Lima et al., 2016 ; Wu et al., 2019 ; Love et al., 2020).

L'HBA est un modèle hiérarchique basé sur au moins deux niveaux dans un cadre Bayésien et peut être décrit par l'Equation 1.27 (Shao, 2012). Le premier niveau de la hiérarchie $L(X|\theta)$ décrit la distribution conjointe à paramètres inconnus θ des observations X. Le deuxième niveau de la hiérarchie $L(\theta|\beta)$ décrit la variabilité spatiale des paramètres θ à l'aide d'un modèle de régression qui relie les valeurs des paramètres à des covariables décrivant les caractéristiques physiographiques et météorologiques du site. Le troisième niveau de la hiérarchie $p(\beta)$ est facultatif et décrit la distribution à priori des paramètres de régression β.

Equation 1.27

$$L(\theta, \beta|X) = L(X|\theta) \ . \ L(\theta|\beta) \ . \ p(\beta)$$

1.2.6 Combinaison des informations historique et régionale

La combinaison de l'information historique et régionale permet de réduire les incertitudes et d'améliorer les estimations par rapport à l'intégration d'un seul type d'information additionnelle (Merz et al., 2008a ; Merz et al., 2008b). Cependant, peu d'études ont exploré cette piste. La flexibilité du cadre Bayésien permet de prendre en compte facilement plusieurs types d'information additionnelle, ainsi que leurs incertitudes.

La méthode de l'indice (voir Section 1.2.5.1) consiste à incorporer dans l'analyse régionale les séries systématiques mesurées aux sites jaugés appartenant à une même région. L'approche de Gaume et al. (2010), Nguyen et al. (2013) et Nguyen et al. (2014) en est inspirée, mais consiste à incorporer, avec la série systématique X des observations maximales annuelles pendant une période de w_s années au site cible, des observations extrêmes historiques à des sites non jaugés appartenant à la même région que le site cible (voir Equation 1.28). Comme dans la méthode de l'indice, les observations locales sont normalisées par un indice local μ pour la série systématique X et $\mu_{k,k=\{1,..,K\}}$ pour les K observations extrêmes historiques Y. Aux sites non jaugés, l'index local $\mu_{k,k=\{1,..,K\}}$ est estimé avec un modèle de régression linéaire en fonction de la surface du bassin versant A : $\mu_k = cA_k^{\beta}$, c et β sont des paramètres à estimer. Dans Gaume et al. (2010), l'index local est estimé à priori afin de tenir compte de l'incertitude associée à l'estimation de l'indice. Dans Nguyen et al. (2013) et Nguyen et al. (2014), les paramètres de la distribution GEV et du modèle de régression linéaire (c et β) sont estimés conjointement. L'introduction des paramètres additionnels apparaît comme un facteur de stabilisation des estimations et non pas comme une source d'incertitudes additionnelles. De manière générale, les observations extrêmes historiques aux sites non jaugés sont informatives et permettent de réduire les incertitudes. La vraisemblance 1.28 peut être modifiée (voir Equation 1.29) pour intégrer dans l'analyse régionale, les observations extrêmes historiques aux sites jaugés (Nguyen et al., 2015 ; Halbert et al., 2016). Cette approche a été étendue aux échantillons POT dans le cadre multivarié par Sabourin et al. (2015).

Equation 1.28

$$L(X,Y|\theta) = \left[\prod_{j=1}^{w_s} f_\theta\left(\frac{x_j}{\mu}\right)\right] \cdot \left[\prod_{k=1}^{K} f_\theta\left(\frac{y_k}{\mu_k}\right) \cdot F_\theta\left(\frac{y_k}{\mu_k}\right)^{(h_k-1)}\right]$$

où h_k **est le nombre d'années où** y_k **est la plus grande valeur observée au site non jaugé** k
f_θ, F_θ **sont les fonctions de densité et de répartition de la distribution GEV**
θ **sont les paramètres de la distribution GEV pour Gaume et al. (2010)**
ainsi que c **et** β **pour Nguyen et al. (2013) et Nguyen et al. (2014)**
μ_k **est remplacé par** $\mu_k(\theta)$ **pour Nguyen et al. (2013) et Nguyen et al. (2014)**

Equation 1.29

$$L(X,Y|\theta) = \left[\prod_{i=1}^{N}\left[\prod_{j=1}^{n_i} f_\theta\left(\frac{x_{ij}}{\mu_i}\right)\right] \cdot \left[\prod_{k=1}^{K_i} f_\theta\left(\frac{y_{ik}}{\mu_i}\right) \cdot F_\theta\left(\frac{y_{ik}}{\mu_i}\right)^{(h_{ik}-1)}\right]\right]$$

où N **est le nombre de sites jaugés dans la région**

Viglione et al. (2013) utilisent le prior de l'inférence Bayésienne pour intégrer de l'information régionale aux données systématiques et historiques regroupées dans l'Equation 1.10. Ici, le prior régional est basé sur une relation entre la surface du bassin versant et les moments des crues annuelles maximales, mais on peut régionaliser les paramètres de la distribution au lieu des moments. Dans cette étude, l'analyse Bayésienne démontre que la combinaison de plusieurs sources d'information est très utile.

Finalement, dans le domaine maritime, seulement deux références combine l'information locale, régionale et historique (Frau et al., 2018 ; Hamdi et al., 2019). La première consiste à faire une analyse régionale en intégrant l'information historique aux sites où elle est disponible. Pour ce faire, les séries locales sont complétées par les données historiques, en définissant une nouvelle durée d'observation. Comme vu dans la Section 1.2.3.4, cette méthode pourrait largement surestimer les quantiles, elle n'est donc pas satisfaisante. La deuxième, à l'inverse, consiste à performer une analyse historique locale sur une série de surcotes de pleine mer dont les lacunes de mesure ont été complétées par de l'information régionale avec des régressions linéaires multiples (voir *Régression linéaire multiple* dans la Section 1.2.5.2). Cette approche est en deux étapes indépendantes et il est donc difficile de quantifier les incertitudes associées à chacune.

1.3 Structure de la thèse

Ce présent chapitre avait pour but d'introduire le contexte et les objectifs de la thèse ainsi que de présenter une revue de littérature générale du sujet. Les quatre prochains chapitres sont présentés sous la forme d'articles scientifiques. L'ensemble de ces derniers tentent d'apporter des réponses aux objectifs de la thèse.

Le chapitre 2 présente le premier article nommé "Extreme Sea Level Estimation Combining Systematic Observed Skew Surges and Historical Record Sea Levels". Ce papier a pour objectif de proposer une nouvelle méthode pour intégrer de l'information historique exhaustive dans l'analyse statistique des surcotes de pleine mer extrêmes. Il s'agit de combiner, dans une unique inférence Bayésienne, les surcotes de pleine mer mesurées pendant la période systématique et les niveaux marins extrêmes observés pendant la période historique. L'exhaustivité de l'information historique est basée sur le fait que les niveaux marins extrêmes historiques supérieurs à un seuil sont supposés tous connus, si ce seuil est suffisamment élevé. Ce qui en fait une hypothèse plus réaliste que de supposer l'exhaustivité des surcotes de pleine mer extrêmes historiques. L'aspect innovant de cette méthode est la combinaison de deux types

de variables. Pour cela, on doit faire l'hypothèse d'indépendance des marées hautes astronomiques et des surcotes de pleine mer. Les performances de cette méthode sont évaluées et comparées à celles d'autres méthodes à partir de simulations de Monte Carlo. Les estimations du maximum de vraisemblance et les intervalles de crédibilité Bayésiens obtenus avec la méthode proposée apparaissent non biaisés comparé aux autres méthodes existantes. De plus, l'intégration des niveaux marins extrêmes historiques permet de réduire les incertitudes. Finalement, la méthode est appliquée à quatre marégraphes français : Brest, Dunkerque, La Rochelle et Saint Nazaire.

Le premier article se veut relativement théorique. Alors, dans ce deuxième article, nous avons voulu rendre la méthode développée dans le premier plus accessible aux professionnel.le.s non spécialistes des statistiques tout en fournissant une sorte de guide pour l'utilisation des données historiques. De plus, ce deuxième article contient de nouveaux tests nécessaires pour challenger la méthode développée. Il est nommé "Extreme skew surge estimation combining systematic skew surges and historical record sea levels on the English Channel and North Sea coasts" et est présenté dans le chapitre 3. L'hypothèse d'indépendance des marées hautes astronomiques et des surcotes de pleine mer est toujours nécessaire ici. La vraisemblance a été mise à jour afin d'inclure le niveau d'incertitudes associé à l'information historique. Finalement, la méthode est illustrée avec de nouveaux marégraphes le long des côtes européennes : Aberdeen (GB), Calais (FR), Cherbourg (FR), Delfzijl (NL), Le Havre (FR), Newport (BE), Oostende (BE), Saint Malo (FR) et Vlissingen (NL). Ces deux premières études permettent respectivement de proposer et de consolider une méthode intégrant de l'information historique exhaustive dans l'analyse statistique des surcotes de pleine mer extrêmes. Cela constitue donc une réponse au premier objectif de la thèse.

On change maintenant de paradigme en s'intéressant à l'information régionale dans le troisième article nommé "Regional frequency analysis of extreme skew surges at ungauged locations" et présenté dans le chapitre 4. Ici, l'objectif est de tester l'applicabilité des approches régionales faisant intervenir des variables météorologiques et physiographiques pour l'analyse des surcotes de pleine mer à des sites non jaugés. Pour cela, un travail de recherche de variables physiographiques et météorologiques explicatives des surcotes de pleine mer a d'abord été effectué. Puis, ces variables ont été utilisées dans huit modèles régionaux. Chaque modèle est la combinaison d'une méthode pour la formation des régions et d'une méthode d'estimation régionale. Les modèles régionaux sont comparés entre eux, à travers une procédure de jack-knife, avec des critères classiques calculés pour les quantiles de période de retour 10, 50 et 100 ans. Les résultats montrent notamment qu'un modèle non linéaire est plus adapté qu'un modèle linéaire. De plus, les meilleures performances sont obtenues avec la formation de régions centrées autour d'un site cible à partir de la distance basée sur les caractéristiques physiographiques et météorologiques locales (ROI).

Le troisième article a été une étape nécessaire pour l'identification des variables physiographiques et météorologiques reliées aux surcotes de pleine mer. L'article 4 permet d'explorer le potentiel de ces variables pour combiner l'information locale et régionale afin de renforcer les estimations locales des distributions de surcotes de pleine mer. Cela est effectué avec

la méthode de l'indice combinée à des régions basées sur la similarité des variables physiographiques et météorologiques, et avec l'analyse Bayésienne hiérarchique. Puis, les données locales et régionales sont combinées aux niveaux marins extrêmes historiques locaux grâce à la méthode développée dans les deux premiers articles. Les résultats montrent que la méthode de l'indice tend à sous-estimer les incertitudes d'estimation. Alors que l'analyse Bayésienne hierarchique fournit des estimations précises, en particulier lorsque les deux types d'informations sont combinées. Ce quatrième article est nommé "Historical and regional information for extreme skew surge estimation" et est présenté dans le chapitre 5.

Le chapitre 6 constitue une discussion générale et une conclusion des travaux menés pendant cette thèse. Il s'agit de faire une synthèse des principaux éléments présentés dans les chapitres précédents et d'identifier les limites ainsi que les perspectives de cette recherche.

Chapitre 2

Article 1

Titre original : "Extreme Sea Level Estimation Combining Systematic Observed Skew Surges and Historical Record Sea Levels"

Titre en français : "Estimation des niveaux marins extrêmes en combinant les surcotes de pleine mer systématiques observées et les niveaux marins records historiques"

Laurie Saint Criq[1,2] (L.S.C.), Eric Gaume[3] (E.G.), Yasser Hamdi[1] (Y.H.), Taha B.M.J. Ouarda[2] (T.B.M.J.O.)

[1]Institut de Radioprotection et de Sûreté Nucléaire, Fontenay-aux-Roses, France

[2]Institut National de la Recherche Scientifique, Quebec City, QC, Canada

[3]Université Gustave Eiffel, Champs-sur-Marne, France

Cet article a été publié le 16 mars 2022 dans la revue "Water Resources Research", volume 58. Le doi est 10.1029/2021WR030873.

Ce doctorat étant en cotutelle France Canada, j'étais basée à l'IRSN en France pendant les 21 premiers mois, puis à l'INRS au Canada durant les 15 derniers mois. Yasser Hamdi (IRSN, France) a été plus investi dans mes recherches pendant la partie en France et Taha B.M.J. Ouarda (INRS, Canada) pendant la partie au Canada. Eric Gaume a suivi mes travaux de manière constante tout au long de la thèse.

Pour ce premier article, la conception a été pensée par L.S.C, E.G et Y.H, la méthodologie a été développée par L.S.C. et E.G., la partie programmation informatique incluant la préparation des données a été réalisée par L.S.C., les résultats ont été analysés par L.S.C., E.G., et Y.H., la première version de l'article a été préliminairement rédigée par L.S.C. et a été grandement corrigé par E.G., l'article a ensuite été révisé par Y.H. et T.B.M.J.O.. Ce travail a été encadré principalement par E.G. et Y.H.. Tous les auteur.e.s ont approuvé la version publiée de l'article.

Abstract

The estimation of sea levels corresponding to high return periods is crucial for coastal planning and for the design of coastal defenses. This paper deals with the use of historical observations, i.e. events that occurred before the beginning of the systematic tide gauge recordings, to improve the estimation of design sea levels. Most of the recent publications dealing with statistical analyses applied to sea levels suggest that astronomical high tide levels and skew surges should be analyzed and modelled separately. Historical samples generally consist of observed record sea levels. Some extreme historical skew surges can easily remain unnoticed if they occur at low or moderate astronomical high tides and do not generate extreme sea levels. The exhaustiveness of historical skew surge series, which is an essential criterion for an unbiased statistical inference, can therefore not be guaranteed. This study proposes a model combining, in a single Bayesian inference procedure, information of two different nature for the calibration of the statistical distribution of skew surges : measured skew surges for the systematic period and extreme sea levels for the historical period. A data-based comparison of the proposed model with previously published approaches is presented based on a large number of Monte Carlo simulations. The proposed model is applied to four locations on the French Atlantic and Channel coasts. Results indicate that the proposed model is more reliable and accurate than previously proposed methods that aim at the integration of historical records in coastal sea level or surge statistical analyses.

2.1 Introduction

Coastal defenses must be designed for very low probabilities of failure. Their design values, generally resulting from the statistical analyses of relatively short series of tide gauges, are particularly sensitive to inherent statistical estimation uncertainties. During the last decade, a number of coastal floods due to exceptional surges, resulted in significant damages, pointing to the importance of an appropriate design of coastal defense structures (Aelbrecht et al., 2004 ; Gerritsen, 2005 ; De Zolt et al., 2006 ; Kolen et al., 2013). It is now widely accepted that historical information even if partial and inaccurate, may significantly reduce statistical inference uncertainties, if properly processed (Ouarda et al., 1998b ; Benito et al., 2004 ; Reis et al., 2005 ; Gaál et al., 2010 ; Payrastre et al., 2011 ; Hamdi et al., 2015). This paper proposes some methodological improvements for the incorporation of historical information in coastal risk assessment studies.

The measured sea levels can be interpreted as the combination of two temporal signals : astronomical tides which can be predicted and residuals due to atmospheric and meteorological processes (see Figure 2.1). On average, 706 tidal cycles occur during a year. The maximum tidal sea level during a cycle can also be seen as the sum of the astronomical high tide and the skew surge - i.e. the difference between the observed maximum sea level and the predicted astronomical high tide (see Figure 2.1).

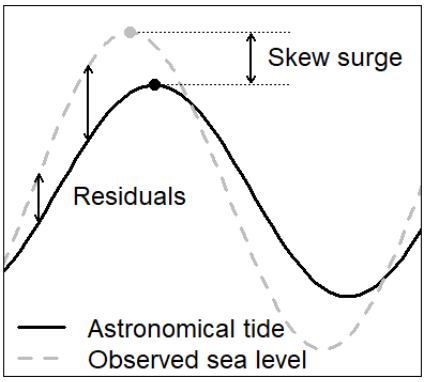

Figure 2.1 – Definition of residuals and skew surges

The common practice in extreme value statistics for coastal studies consists in fitting a theoretical statistical distribution to a sub-sample of the observed series. The sub-sample is generally a peaks over threshold (POT) sample of either maximum tidal sea levels (direct method) or skew surges or even maximum tidal residuals (indirect methods). The direct method, based directly on the analysis of maximum tidal water levels (Arns et al., 2013; Bulteau et al., 2015) does not exploit the available knowledge on the astronomical tidal component of the sea level (Tawn et al., 1989; Mazas et al., 2014). Moreover it seems to provide biased estimates of sea level quantiles corresponding to high return periods for locations with large tidal amplitudes (Haigh et al., 2010; Andreewsky et al., 2014). Indirect methods are therefore nowadays privileged. Indirect methods were first introduced based on the separate analysis of residuals and astronomical tides (Pugh et al., 1978; Pugh et al., 1980; Tawn et al., 1989; Tawn, 1992). They are nevertheless uneasy to implement, since the reconstruction of the maximum sea level statistical distribution implies a complex convolution between the astronomical tidal signal and the common and extreme residuals (Dixon et al., 1994; Dixon et al., 1999; Tomasin et al., 2008; Liu et al., 2010). Moreover, residuals and astronomical high tides may be dependent at some locations. Accounting for this dependence makes the approach even more challenging (Mazas et al., 2014). The indirect method, based on skew surges was introduced more recently in order to reduce the implementation complexity (Batstone et al., 2013; Kergadallan et al., 2014; Mazas et al., 2014; Hamdi et al., 2015). Note that the latter approach is used herein on a POT sample of skew surges X_{sys} larger than a threshold u.

Historical information, when available, is composed of a series of record sea levels Z_{hist} exceeding a threshold η_H. The corresponding historical skew surge series X_{hist} and the associated threshold u_H may be estimated for statistical inference combining systematic X_{sys} and historical X_{hist} skew surges. However, the exhaustiveness of the series of skew surges exceeding u_H during the historical period cannot be guaranteed. Indeed, some extreme historical skew surges may in fact remain unnoticed if they occur at low or moderate astronomical high tides

and do not generate extreme sea levels (Outten et al., 2020). The exhaustiveness of the historical POT series is an essential criterion for an unbiased statistical inference (Gaume, 2018). Some authors have proposed to proceed with the statistical inference including historical skew surges without considering their non-exhaustiveness (Hamdi et al., 2015). We suspect that the under-sampling of historical skew surges due to their non exhaustiveness could leads to some bias. Some others have proposed to adjust (i.e. reduce) the length of the historical period to account for the non-exhaustiveness (Frau et al., 2018). Reducing the historical duration leads to a possible over-representation of extreme skew surges in a very short duration and the introduction of some bias is suspected. None of these two approaches appears to be totally satisfactory. It is therefore proposed hereafter to keep the historical information in its original form and to combine, in the same inference procedure, two different types of information : systematic skew surges X_{sys} and historical record sea levels Z_{hist}. A likelihood based inference procedure is implemented. The main idea consists in replacing the analytical form of the sea level cumulative distribution function, which is unknown, by a numerical estimate in the likelihood formulation.

This paper presents the background of the proposed approach and its performances : accuracy of the estimated skew surge quantiles and of the corresponding Bayesian credibility intervals. These performances are evaluated through Monte Carlo experiments inspired by four real-life implementation case studies. The results are compared to those of several other inference methods : without the use of any historical information, when historical skew surges are exhaustively known, the method proposed by Hamdi et al. (2015), the method proposed by Frau et al. (2018) and a modification of this last method (Section 2.2.1). The proposed approach is then applied to the four observed data sets in order to evaluate its relevance and efficiency when implemented on real-life case studies.

The paper is structured as follows. The various tested methods and the statistical inference procedure are presented in Section 2.2. The evaluation methodology is explained in Section 2.3. The performances of the tested methods are compared in Section 2.3.3 and some reference methods as well as the proposed method are implemented on the observed data sets in Section 2.4. Section 2.5 is devoted to some discussion and conclusions.

2.2 Models and statistical inference procedure

2.2.1 The tested methods

The proposed method is compared to several methods including methods of reference (with only systematic data sets or in the case of perfect knowledge of historical skew surge series) and previously published methods integrating historical information (Hamdi et al., 2015 ; Frau et al., 2018). In total, six different methods are implemented and tested herein for the estimation of the 100-year skew surge quantile :

— **Method 1 :** The inference is only based on the series of systematic skew surges X_{sys} exceeding a threshold value u (see Section 2.2.2.1). This method with no historical information included is considered herein as the reference one.

— **Method 2 :** All historical skew surges exceeding the threshold u are known for the systematic and historical period. This is the ideal situation.
— **Method 3 :** The series of systematic skew surges X_{sys} exceeding u and historical record sea levels Z_{hist} exceeding a threshold value η_H are combined in a single likelihood formulation (see Section 2.2.2.3). This is the proposed method.
— **Method 4 :** The series of historical skew surges exceeding u_H, corresponding to the record sea levels exceeding η_H is supposed to be exhaustive. This method proposed by Hamdi et al. (2015) (see Section 2.2.2.2) will be called "naive", as the exhaustiveness of the historical skew surge series can never be guaranteed.
— **Method 5 :** The FAB method proposed by Frau et al. (2018) adjusts the duration of the historical observation period, assuming that the mean annual frequency of a skew surge exceeding the threshold value u is the same during the historical and the systematic periods (see Section 2.2.2.2).
— **Method 6 :** A modification of the FAB method accounting for the fact that the real skew surge sampling threshold u_H for the historical period may be much larger than u and that the mean annual frequency of exceedance should therefore be adjusted (see Section 2.2.2.2).

The likelihood formulations for all of these methods are provided in the next section.

2.2.2 Likelihood formulations

Let us denote $X_{sys} = \{x_{sys,1}, x_{sys,2}, ..., x_{sys,n}\}$ the POT series of n skew surges exceeding a threshold value u during the systematic observation period w_S (years). $Z_{hist} = \{z_{hist,1}, z_{hist,2}, ..., z_{hist,h_z}\}$ are the h_z record historical sea levels. It is assumed - ideally cross-checked with available archives - that the sample of record sea levels exceeding a threshold η_H is exhaustive over the considered historical period. η_H is often chosen equal to the minimum historical value : $\min(Z_{hist})$. Finally, $X_{hist} = \{x_{hist,1}, x_{hist,2}, ..., x_{hist,h_x}\}$ is the series of h_x historical skew surges, corresponding to the historical record levels and in the same time, exceeding the threshold u. Note that $h_x \leq h_z$. Let us also note θ the parameters of the skew surge statistical distribution to be estimated using the available observed data set.

Depending on whether the historical record sea levels or the historical skew surges are considered, the combined likelihood of the systematic and historical data sets may have two distinct formulations :

Equation 2.1

$$L(X_{sys}, X_{hist}|\theta) = L(X_{sys}|\theta) \ . \ L(X_{hist}|\theta)$$

Equation 2.2

$$L(X_{sys}, Z_{hist}|\theta) = L(X_{sys}|\theta) \ . \ L(Z_{hist}|\theta)$$

The likelihood terms $L(X_{sys}|\theta)$, $L(X_{hist}|\theta)$ and $L(Z_{hist}|\theta)$ are described in the next sections.

2.2.2.1 Likelihood of the systematic skew surge sample : $L(X_{sys}|\theta)$

The General Pareto (GP) distribution is usually selected as the statistical distribution of skew surges exceeding u. Indeed, according to the extreme value theory, it has been proven that a POT independent random sample converges to a GP distribution (Coles, 2001). The GP cumulative distribution function F_θ is given by :

Equation 2.3

$$\forall\ x > u,\ F_\theta(x) = \begin{cases} 1 - \left[1 + \xi\left(\frac{x-u}{\sigma}\right)\right]^{-\frac{1}{\xi}} & \text{if } \xi \neq 0, \\ 1 - \exp\left(-\frac{x-u}{\sigma}\right) & \text{if } \xi = 0. \end{cases}$$

where $\sigma > 0$ **is the scale parameter and** $\xi \in R$ **is the shape parameter**

The number of skew surges exceeding the threshold u per year is generally assumed to follow a Poisson process (Coles, 2001) with parameter λ (average number of skew surges exceeding the threshold u per year). The probability of observing n skew surges exceeding u during a systematic observation period of duration w_S years is then equal to :

Equation 2.4

$$P_\theta(N = n) = \frac{(\lambda w_s)^n}{n!}\ \exp\left(-\lambda w_S\right)$$

If the observed systematic skew surges $x_{sys,j=\{1,\dots,n\}}$ are considered independent and identically distributed, the likelihood of the systematic sample is given by Equation 2.5 where f_θ is the GP probability density function.

Equation 2.5

$$L(X_{sys}|\theta) = P_\theta(N = n)\ .\prod_{j=1}^{n} f_\theta(x_{sys,j})$$

The parameters to be estimated through the inference procedure are the scale and shape parameters of the GP distribution and the intensity of the Poisson process : $\theta = (\sigma, \xi, \lambda)$.

2.2.2.2 Likelihood of the historical skew surge sample : $L(X_{hist}|\theta)$

Considering the h_x historical skew surges exceeding a threshold value $u_H \geq u$ over a historical period of w_h years as independant and identically distributed, the likelihood of the historical skew surge sample is :

Equation 2.6

$$L(X_{hist}|\theta) = P_\theta(H_X = h_x) \cdot \prod_{j=1}^{h_x} \frac{f_\theta(x_{hist,j})}{1 - F_\theta(u_H)}$$

where $P_\theta(H_x = h_x)$ **is given by the Equation 2.7**

Equation 2.7

$$P_\theta(H_x = h_x) = \frac{[\lambda w_H (1 - F_\theta(u_H))]^{h_x}}{h_x!} \exp\left(-\lambda w_H \left[1 - F_\theta(u_H)\right]\right)$$

Methods 4, 5 and 6 differ by the estimation of the threshold value u_H and the considered effective duration of the historical period w'_H. The various proposed estimates and the final formulation of the likelihood $L(X_{hist}|\theta)$ are provided in Table 2.1.

Table 2.1 – Likelihoods of the historical skew surge samples for methods 4, 5 and 6

Method	u_H	w'_H	$L(X_{hist}\|\theta)$
4	$\min(X_{hist})$	w_H	$\frac{[\lambda w_H]^{h_x}}{h_x!} \exp\left(-\lambda w_H \left[1 - F_\theta(u_H)\right]\right) \prod_{j=1}^{h_x} f_\theta(x_{hist,j})$
5	u	$\frac{h_x}{\hat{\lambda}}$	$\frac{\left(h_x \lambda/\hat{\lambda}\right)^{h_x}}{h_x!} \exp\left(-h_x \frac{\lambda}{\hat{\lambda}}\right) \prod_{j=1}^{h_x} f_\theta(x_{hist,j})$
6	$\min(X_{hist})$	$\frac{h_x}{\hat{\lambda}\left[1 - F_{\hat{\theta}}(u_H)\right]}$	$\frac{R_\lambda(u_H)^{h_x}}{h_x!} \exp\left(-R_\lambda(u_H)\right) \prod_{j=1}^{h_x} \frac{f_\theta(x_{hist,j})}{1 - F_\theta(u_H)}$

$\hat{\theta}$ and $\hat{\lambda}$ represent the parameter set and the Poisson process intensity estimated with the maximum likelihood based on the systematic skew surges only and $R_\lambda(u_H) = h_x \frac{\lambda\left[1 - F_\theta(u_H)\right]}{\hat{\lambda}\left[1 - F_{\hat{\theta}}(u_H)\right]}$.

In the naive method (method 4), the threshold u_H is the minimum value of the historical skew surge sample $\min(X_{hist})$. But, due to the sampling approach based on record sea levels, there is a risk that this sample represents a partial and not the exhaustive record of all skew surges that have exceeded the threshold u_H during the historical period. A statistical inference based on the hypothesis of exhaustiveness and conducted on a partial sample will provide biased quantile values. To avoid this problem, the FAB method (method 5), proposes to introduce a corrected duration for the historical period w'_H. This duration is chosen to be perfectly consistent with the average number $\hat{\lambda}$ of skew surges exceeding the threshold per year and with the number of recorded historical skew surges h_x : $w'_H = h_x/\hat{\lambda}$. In the initial version of the FAB method (Frau et al., 2018), the historical sampling threshold was considered equal to the systematic threshold u. Since the minimum value of historical sampled skew surges appears often much larger than u, this *a priori* choice may be a source of significant biases

as will be illustrated hereafter. A modified version of the FAB method is therefore tested here (method 6), where the historical threshold is adapted to the available sample and the corrected duration w'_H is adjusted accordingly (see Table 2.1).

2.2.2.3 Likelihood of the historical sea level sample : $L(Z_{hist}|\theta)$

The likelihood formulation of the historical sea levels comprises (a) the probability associated to the $N - h_z$ ($N = 706 \times w_H$) maximum tidal levels that did not exceed the historical threshold η_H and (b) the probability associated to the h_z extreme historical maximum tidal levels that exceeded η_H during the historical period of duration of w_H years (Equation 2.8).

Equation 2.8

$$L(Z_{hist}|\theta) = \underbrace{\tilde{G}_\theta(\eta_H)^{N-h_z}}_{\text{(a)}} \cdot \underbrace{\left[1 - \tilde{G}_\theta(\eta_H)\right]^{h_z} \cdot \prod_{j=1}^{h_z} \frac{\tilde{g}_\theta(z_{hist,j})}{1 - \tilde{G}_\theta(\eta_H)}}_{\text{(b)}}$$

$\tilde{g}_\theta$, $\tilde{G}_\theta$ are respectively the probability density and cumulative distribution functions of maximum tidal levels which result from the combination of (1) the statistical distribution of the maximum astronomical tidal levels, (2) the statistical distribution of skew surges lower than the threshold u, and (3) the calibrated statistical distribution (f_θ, F_θ) of the skew surges exceeding u. The proposed numerical approximations of the functions $\tilde{g}_\theta$ and $\tilde{G}_\theta$ are presented in Section 7.1.

2.3 Test and evaluation methodology

The comparison of the different methods is based on samples generated through Monte Carlo simulations inspired by four real world case studies in order to verify the accuracy of the maximum likelihood (ML) estimates and the posterior credibility intervals.

2.3.1 Monte Carlo experiments

1000 synthetic series are randomly generated with characteristics corresponding to each of the four observed data sets : duration of the systematic and historical observation periods w_S and w_H, systematic and historical sampling thresholds u and η_H, parameters of the GP distribution and Poisson intensity for the skew surges exceeding u and empirical statistical distributions of the astronomical high tides and of the ordinary skew surges (lower than u) as well as the astronomical high tide/skew surge relation (see Sections 2.3.2 and 7.3).

Each synthetic sample is generated as follows :

- For the systematic period, n systematic skew surges X_{sys} are drawn from the Poisson process (intensity λw_S) and GP distribution.
- For the historical period, n_2 skew surges X_{hist} larger than u are drawn from the Poisson process (intensity λw_H) and GP distribution (series used for the implementation of

method 2) and complemented with $(w_H \times 706 - n_2)$ ordinary skew surges (lower than u), drawn from the empirical ordinary skew surge distribution. $w_H \times 706$ astronomical high tides are drawn from the empirical high tide distribution. Astronomical high tides and skew surges, assumed to be independent (see Section 7.3), are summed to generate $w_H \times 706$ maximum tidal levels. The subset of h_z sea levels Z_{hist} exceeding η_H is then extracted (series used for the implementation of method 3), as well as the corresponding subset of h_x skew surges larger than u for the implementation of methods 4 to 6.

2.3.2 Case study

Four tide gauges located on the French Atlantic and Channel coasts are used as examples for the configuration of the Monte Carlo experiment : Brest, Dunkerque, La Rochelle and Saint Nazaire. These tide gauges are selected because of the availability of historical information, but also because they cover a variety of situations : i) statistical distributions of the skew surges and tidal levels, ii) tide/surge ratio (Table 2.2), iii) tidal amplitude, iv) historical perception threshold level and number of documented historical events.

The hourly tide gauge data were retrieved from Shom, the French hydrographical and oceanographical service (data.shom.fr), harmonic analyis is applied on these data with the R package *TideHarmonics* (Stephenson, 2015), as well as a correction of sea level rise. Then, hourly astronomical tide levels were processed to extract the series of corresponding astronomical high tides and systematic skew surge series.

The threshold u for the POT sampling is selected according to the GP parameter stability criterion (Coles, 2001).

Table 2.2 – Characteristics of the systematic data set

Site	Period	w_S (years)	u (m)	n	Tide surge ratio*	$\hat{\sigma}$	$\hat{\xi}$	$\hat{\lambda}$
Brest	1953-2017	63.57	0.50	81	22.50	0.09	0.19	1.29
Dunkerque	1959-2016	47.75	0.74	58	15.58	0.14	0.34	1.23
La Rochelle	1941-2016	32.58	0.62	34	17.11	0.08	0.36	1.08
Saint Nazaire	1957-2014	47.56	0.66	53	15.45	0.11	0.12	1.14

$(\hat{\sigma}, \hat{\xi}, \hat{\lambda})$ are the selected values for the Monte Carlo simulations. *Ratio of the 98% astronomical high tide to the 98% skew surge quantile (Dixon et al., 1999).

Historical sea levels were extracted from Hamdi et al. (2018), Giloy et al. (2018) and Giloy et al. (2019) for Dunkerque (Table 7.2) and from Breilh et al. (2014) for La Rochelle (Table 7.3). At La Rochelle, the sampling threshold η_H had to be raised to ensure the exhaustiveness of the historical record levels and two reported record levels were ignored (see Table 7.3). In fact, the systematic observations started in 1846 and 1863 respectively at Brest and Saint Nazaire. The complete observed samples were split into systematic and historical samples for the sake of illustration. To test the proposed method, censored samples of historical record

sea levels were extracted at these two stations setting a threshold value of 8m at Brest and 7m at Saint Nazaire (Tables 7.1 and 7.4).

Table 2.3 – Characteristics of the historical data sets

Site	Period	w_H (years)	$\frac{h_x}{\hat{\lambda}}$ (years)	$\frac{h_x}{\hat{\lambda}[1-F_{\hat{\theta}}(u_H)]}$ (years)	η_H (m)	h_z	u_H (m)	h_x
Brest	1846-1952	120	2.33	13.72	8.02	10	0.69	3
Dunkerque	1720-1953	250	6.50	108.42	7.60	8	1.40	8
La Rochelle	1866-1940	80	3.70	13.31	7.15	4	1.00	4
Saint Nazaire	1863-1956	100	4.40	17.62	7.09	5	0.82	5

Table 2.3 presents the characteristics of the historical samples as well as the considered duration for the implementation of the various methods. As suggested by Schendel et al. (2017), the historical duration w_H is larger than the time laps between the first record and the start of the systematic period. The duration considered for the FAB method $h_x/\hat{\lambda}$ appears to be extremely reduced. For Dunkerque, the reported historical skew surges are extremely high if compared to the systematic data : 8 values exceeding $u_H = 1.40$m, when the largest measured value during the systematic period is 1.30m. Some inconsistencies between the historical and systematic data sets at Dunkerque may be suspected and will be discussed further in Section 2.4. The observed historical series are the result of a random drawing. The simulated historical series, based on the parameters calibrated on the observed series, may have slightly different characteristics on average, especially different numbers of record events (see Table 2.4).

2.3.3 Evaluation methods

The RStan package was used to conduct Bayesian MCMC (Monte Carlo Markov Chain) inferences based on the formulated likelihood with non-informative priors. The results of the inference procedure consist in the posterior densities for the calibrated parameters $\theta = (\sigma, \xi, \lambda)$ and of the corresponding skew surge quantiles, including the maximum likelihood estimates. The evaluation of the various tested methods (see Section 2.2.1) was conducted in two steps. The accuracy of the maximum likelihood estimator was first verified based on the 100-year quantile estimate (comparison between the quantile values $\hat{x}_{100}^{ML}$ and the real quantile value x_{100} for the 1000 generated series). The evaluation will be based on boxplots of the ratio $\hat{x}_{100}^{ML}/x_{100}$ and classical average performance estimation criteria : relative bias, relative standard deviation (RSD) and relative root mean square error (RRMSE).

In a second step, the average widths of the computed posterior credibility intervals for the 100-year quantile are compared and their reliability is evaluated based on the rank histogram diagnosis method (Bellier, 2018 ; Nguyen et al., 2014). For each of the 1000 inferences, the exceedance probability $P(\hat{x}_{100} < x_{100})$ of the real quantile value x_{100} is computed according to the estimated posterior density for the quantile. If the estimated posterior densities are

reliable, $P(\hat{x}_{100} < x_{100})$ should be uniformly distributed over $[0, 1]$ (Halbert et al., 2016 ; Gaume, 2018). Figure 2.2 illustrates how the rank histogram can be interpreted.

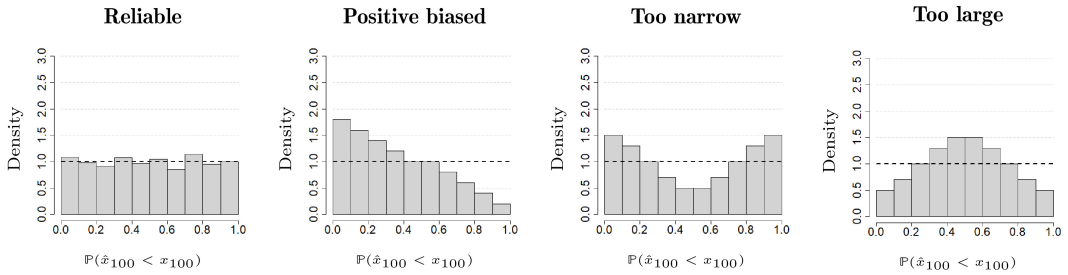

Figure 2.2 – Possible distributions of $P(\hat{x}_{100} < x_{100})$
Conclusions on the reliability of the posterior densities and corresponding credibility intervals.

2.3.4 Characteristics of the Monte Carlo simulations

Table 2.4 summarizes the characteristics of the 1000 simulated samples for each case study. It seems that the parameters of the Monte Carlo simulations, adjusted on the observed series, lead to generated series with contrasted characteristics like the number of sampled record sea levels or the sampling rate of the historical skew surges exceeding the threshold u. The selected threshold η_H at Brest leads to a large number of sampled historical sea levels. But due to a large tide/surge ratio, the corresponding samples of skew surges exceeding u represent only a small proportion of the total number of generated skew surge exceeding u for the historical period - on average less than 10%. Dunkerque and La Rochelle are considered intermediate cases where smaller average amounts of historical sea levels are sampled, but the skew surge sampling rate is higher due to a more favorable tide/surge ratio - i.e. due to a higher contribution of the skew surges to the record levels. Finally, Saint Nazaire appears to be an extreme case, where, due to a relatively high threshold value η_H, a limited number of record sea levels and skew surges are sampled. A high proportion of the generated historical samples at Saint Nazaire does not contain record sea levels exceeding η_H (33%) or skew surges exceeding u (45%).

Table 2.4 – Characteristics of the generated historical series

	Brest	Dunkerque	La Rochelle	Saint Nazaire
Generated historical sea levels				
Sampling threshold η_H (m)	8.02	7.60	7.15	7.09
Minimum generated value (m)	8.02	7.70	7.24	7.17
Average number of record values	22	7	3	1
Duration of the historical period (years)	120	250	80	100
Generated historical skew surges				
Sampling threshold u (m)	0.50	0.74	0.62	0.66
Minimum sampled value u_H (m)	0.55	1.63	0.90	0.93
Average number of skew surges $> u$	156	308	86	116
Average number of skew surges $> u_H$	26	18	24	28
Average number of sampled values $> u_H$	2	6	2	1
Average skew surge sampling rate (%)	7.63	33.33	8.33	3.57

2.3.5 Maximum likelihood estimates

The evaluation of the various tested inference procedures confirms some anticipated results, but also provides some satisfactions and surprises. The hypothesis of exhaustiveness for the sample of skew surges exceeding u_H during the historical period, on which the naive method (method 4) is based, is clearly not reached for the four test cases. The average skew surge sampling rates appear largely lower than 100% in Table 2.4. As a consequence, method 4 underestimates the 100-year skew surge quantile x_{100} (see Figures 2.3 and 2.4). Table 8.1 in the Supplementary Information provides the numeric values corresponding to Figure 2.4 for a more detailed analysis. The magnitude of the bias affecting the estimation of the parameter λ (i.e. average number of skew surges exceeding u per year) seems clearly dependent on the skew surge sampling rate for the historical period (see Figure 2.5 as well as 8.1, 8.2, 8.3 in the Supplementary Information). The estimation of the two parameters of the GP distribution is also biased since these parameters control the probability of exceedance of the threshold value u_H appearing in the likelihood formulation for the historical period in method 4 (see Table 2.1). The increase of the amount of information used for the inference in method 4 leads nevertheless to a significant decrease of the standard deviation of the x_{100} estimator, if compared to the method based on the systematic data only (method 1). Surprisingly, the balance between bias and reduced standard deviation appears positive for the naive method : for the four test cases, the RRMSE of the x_{100} estimator is significantly lower for the naive method than for the method based on the systematic data only (see Figure 2.4). This remains true, even for the Saint Nazaire case study, where a high proportion of historical generated series does not contain any recorded skew surges exceeding u. This issue will be addressed later.

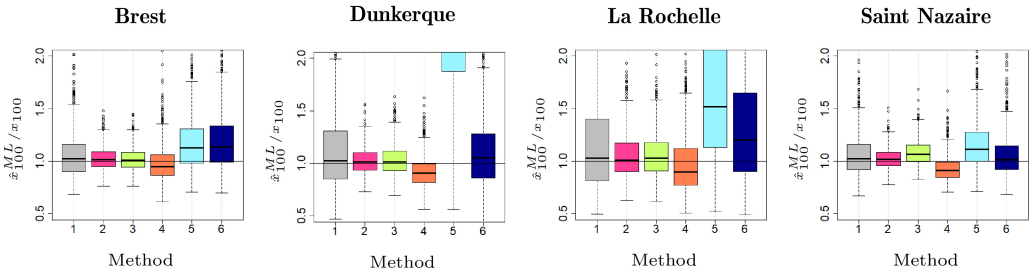

Figure 2.3 – Dispersion of the 100-year quantile estimated with the ML
The 100-year quantile obtained from simulations are divided by their real value.

The results also confirm the suspected biases introduced by the FAB method (method 5) and reveal other important anomalies. In fact, since an equivalent duration of the historical period is estimated, the information about the non-exceedances of the threshold u during the historical period, which is an important part of the historic information as shown by Payrastre et al. (2011), is not evaluated. The historical information is therefore only partly used and limited to the set of a few skew surges reported to have exceeded u, that complement the rich series of systematic skew surges. The possible added value of the historic data is hence extremely limited in the FAB method. Moreover, the sampling process for the historic and systematic surges are different : the sampling threshold is higher for the historic surges, especially for locations with low tide/surge ratios and highly skewed GP distributions (i.e. large ξ values). Merging the historic skew surges with the systematic sample without further adjustments introduces significant biases in the estimates of the parameters (σ, ξ) of the GP distribution (see Figure 2.5). As a conclusion, the FAB method cannot really contribute to reduce significantly the inference uncertainties and introduces some biases. Its implementation leads to an increase of the x_{100} estimation RRMSE if compared to the analyses of the sole systematic data (method 1). The proposed adjusted FAB method reduces partly the estimation biases but the effect on the estimation RSD remains limited if compared to method 1 (Figure 2.4). The principles of the FAB method appear as inefficient and statistically inconsistent. Its implementation leads to a deterioration in the inference results, if compared to the analyses of the systematic data only.

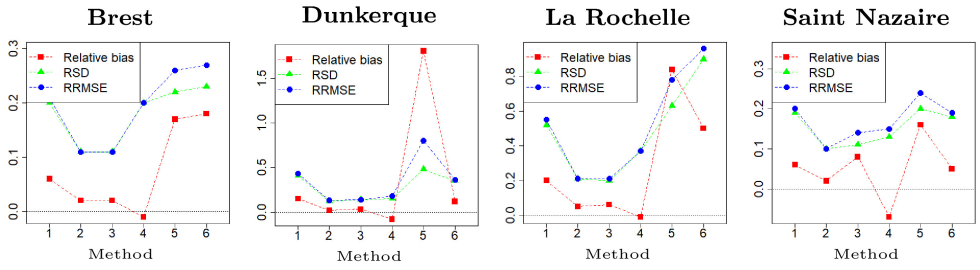

Figure 2.4 – Relative bias, RSD and RRMSE on the 100-year quantile estimated with the ML

In contrast, the proposed method (method 3) appears to perform almost as well as the ideal method (method 2). In details, the gain, if compared to method 1, seems to be mainly related to a more accurate estimation of the GP shape parameter ξ (Figures 2.5, 8.1, 8.1 and 8.1 in the Supplementary Information). These excellent performances may be surprising at first sight since many more historical events are evaluated in method 2 (about 80 to 300 additional historical skew surges) than in method 3 (1 to 22 record sea levels) (see Table 2.4). Moreover, the historical samples used in methods 2 and 3 are partly or totally dissociated - i.e. corresponding to different events (see Figure 7.1). The record sea levels included in the inference of method 3 do not necessarily involve the most extreme skew surges of the historical period. To understand this surprising result, it must be firstly considered that the high frequency of skew surges observed during the historical period does not provide significant additional information to the one contained in the systematic data set. The historical information is mainly encapsulated in the largest observed values, that will help constraining the skew surge distribution tail. Payrastre et al. (2011) have shown that when including historical information in a statistical inference procedure, the length of the documented historical period is a predominant factor : "accurate estimates of the values having exceeded the perception threshold are not necessarily needed when historical data is used in combination with systematic measurements ; provided that the theoretical return period of the perception threshold is sufficiently high, censored (only the values exceeding the threshold are known) or binomial censored (only the number of values having exceeded the threshold is known) historical data lead to similar inference results". This explains also why the results obtained with the proposed method for the Saint Nazaire case study, where a special case of binomial censored historic data set is frequently generated (no exceedance of the threshold η_H or in other words $h_z = 0$), are also satisfactory. It is worth noting that the maximum likelihood estimates of the GP parameters and quantiles appear slightly positively biased for all methods except method 4. This bias appears to be more pronounced when inference is conducted on a binomial censored sample (method 3 at Saint Nazaire). This appears to be a general feature for the ML estimates of the parameters of a GP distribution. Indeed, Hosking et al. (1987) indicated that the ML method leads to biased GP parameters estimates when the sample size is not large.

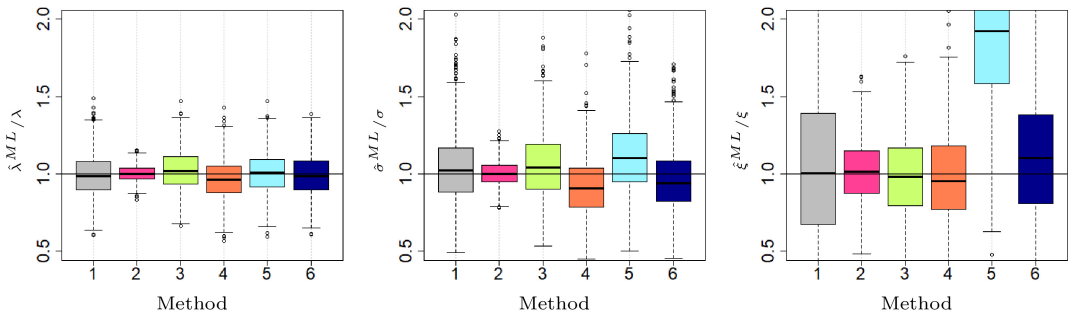

Figure 2.5 – Dispersion of the parameters estimated with the ML at Dunkerque

The parameters obtained from simulations at Dunkerque are divided by the real values.

The implemented Bayesian inference procedure generates not only best-estimates for the quantile values, but also credibility intervals and posterior distributions. The next Section compares this computed intervals for methods 1 to 4.

2.3.6 Posterior credibility intervals

The computed credibility intervals confirm the trends observed on the ML estimators. The added value of the historical information is confirmed by the reduced averaged widths of the posterior credibility intervals (Table 2.5). Without surprise, the widths of the posterior credibility intervals for the proposed method (method 3) are larger than those for the "ideal" method (method 2), but hence of similar magnitudes, confirming that the loss of historical information for proposed method if compared to the ideal case is limited, even for the Brest case study with a high tide/surge ratio. Some posterior intervals based on the naive method (method 4) may have lower widths than the intervals based on the proposed method -especially at Dunkerque, but the estimation bias related to method 4 should be considered (see next paragraph).

Table 2.5 – Average width of the posterior credibility interval

	Average width of posterior credibility interval for x_{100}			
Site	Method 1	Method 2	Method 3	Method 4
Brest	1.15	0.48	0.55	0.95
Dunkerque	6.05	1.10	1.31	1.05
La Rochelle	10.48	1.47	1.60	2.56
Saint Nazaire	1.37	0.46	0.67	0.52

The intervals are obtained for the 100-year quantile with the Bayesian MCMC procedure for methods 1, 2, 3 and 4.

Figure 2.6 shows the rank histograms of the 100-year skew surge quantiles for methods 1 to 4 and all of the case studies. The histograms confirm the conclusions drawn from the ML estimates. The naive method (method 4) has a clear tendency to underestimate the quantile value x_{100} for all case studies. A slight over-estimation tendency is detectable for methods 1 and 2, but the computed posterior distributions and the corresponding credibility intervals for x_{100} appear overall reliable. As far as the proposed method 3 is concerned, the over-estimation tendency is clearly marked for the Saint Nazaire case study. This suggests that the method should ideally be implemented on historical samples including some documented historical sea levels. The rank histograms also reveal that the estimated posterior credibility intervals based on method 3 are too large (the uncertainty affecting the estimated value is overrated) at stations with large tide/surge ratios : i.e. stations where the historical record sea level sample does not coincide with the historical record skew surges. This is visible on the histogram obtained for the Brest case study and to a lower extend for the La Rochelle case study. The outcome of the Bayesian-MCMC inference provides a pessimistic assessment of the accuracy of the estimated quantile values.

As a partial conclusion, the conducted tests indicate that the proposed method combining skew surges for the systematic period and sea levels for the historic period is reliable and provides inference results that are almost as accurate as those obtained through in the ideal situation with an inference based on systematic and historical skew surges (method 2). This is a satisfactory result, but it is important to keep in mind that these conclusions are valid provided that the underlying statistical model is valid : i.e. skew surges and astronomical high tides are independent and the distribution of the skew surges is a GP distribution. It is therefore interesting as a conclusion to evaluate how the proposed approach behaves when implemented on real-world data sets. The next Section presents and analyses the implementation of the method on the data sets available at the considered tide gauges.

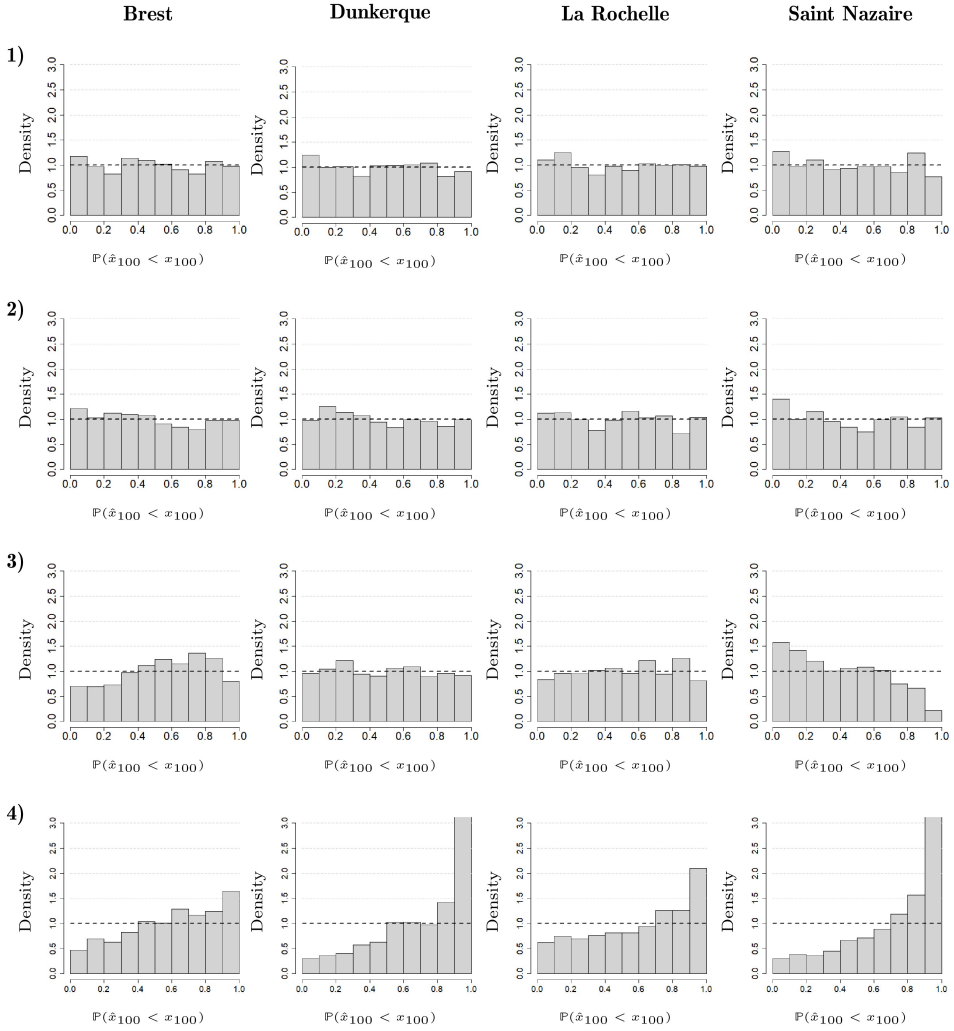

Figure 2.6 – Uniformity test

Distribution of $P(\hat{x}_{100} < x_{100})$ for the credibility intervals computed with the Bayesian MCMC procedure for methods 1, 2, 3 and 4.

2.4 Application of the proposed method to the observations

At Brest and Saint Nazaire, complete observed data sets of sea levels and estimated tides are available. It is hence possible to compare the results of method 3 with those of methods 1 and 2 at these two stations. At Dunkerque and La Rochelle, the historical data sets are composed of the observed record sea levels then, only methods 1 and 3 will be implemented. The hypothesis of independence between astronomical high tides and skew surges was tested and seems to be reasonably valid for all four stations (see Section 7.3).

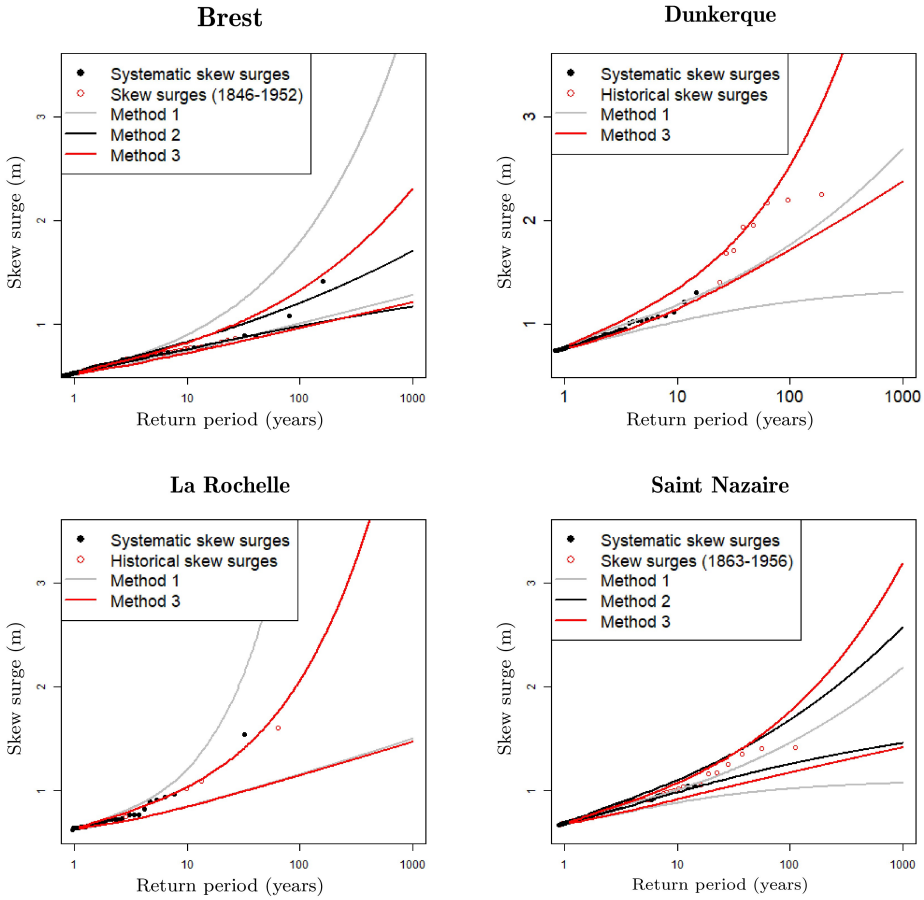

Figure 2.7 – 90% posterior skew surge credibility intervals

They are based on the systematic data (grey) and on the historic data with the proposed method (red) and in the ideal case (black). The empirical return periods of the historical records at Dunkerque and La Rochelle were corrected (reduced) according to the skew surge estimated sampling rates (see Table 2.4).

The implementation results of the methods at Brest and Saint Nazaire appear fully consistent with the conclusions previously drawn (Figure 2.7). The adjusted credibility intervals with the proposed method are very similar to those obtained with method 2, even if they are slightly larger. This is particularly striking for Brest where the historical sea levels do not represent the events with the largest skew surges. This confirms the consistency between the observations and the calibrated statistical model : GP distribution for the skew surges and independence between skew surges and astronomical high tides.

The inclusion of the historical information appears to have contrasted impacts between the case studies. For Brest and La Rochelle, the posterior credibility intervals accounting for the historical information are significantly reduced and totally coherent with the intervals based on the sole systematic data sets (Figure 2.7). This is the expected result which reveals an overall good consistency between (a) the systematic observations, (b) the historical data sets and (c) the calibrated statistical model. In the case of Saint Nazaire, the historical data do not help to reduce the estimation credibility intervals, but lead to a modification of the calibrated

statistical skew surge distribution. Note that this modification remains consistent with the systematic sample - i.e. the observations are contained in the revised posterior credibility intervals. This result may be explained by the peculiarities of the short systematic sample available at Saint Nazaire, which does not contain large skew surges - i.e. skew surges greater than 1m (Figure 2.7). Since the estimated uncertainties (i.e. widths of the posterior credibility intervals) are also related to the estimated variability of the skew surge distribution and especially to the magnitude of the parameter $\hat{\xi}$, the inclusion of the historical information at Saint Nazaire, leading to an increased $\hat{\xi}$ estimated values, does not result in a reduction of the inference estimation uncertainties. The case of Dunkerque is completely different : even if the length of the historical period is considered, the historical record levels and corresponding skew surges appear strongly inconsistent with the systematic data set. This inconsistency, revealed by the inference trials presented herein, remains to be explained.

As a conclusion, a final inference test was conducted to confirm the robustness of the proposed approach, even in cases where limited information about historical record sea levels is available and to verify if the conclusions drawn by Payrastre et al. (2011) based on historical river record discharges are also valid for historical record sea levels. For the considered case studies, the historical threshold η_H was selected such as there is no remaining documented record level exceeding the threshold (i.e. $h_Z = 0$, case 3* in Table 8.2 in the Supplementary Information). The resulting credibility intervals appear to be only moderately affected by this simplification of the historical information if compared to case 3. Even the knowledge that a given sea level has not been exceeded over a considered historical period (i.e. a given coastal defence structure has never been over-topped for instance) is a valuable information, that can efficiently processed with the new inference procedure presented herein. This opens new perspectives in coastal risk assessments.

2.5 Conclusions

A new statistical inference procedure is proposed and evaluated to properly integrate historical sea levels in coastal risk assessment studies. This procedure enables the combined analysis of data sets of different nature : skew surges for the recent period and sea levels for the historical period. It overcomes a major limitation in the previously proposed methods to include historical information in sea level frequency analyses. The key idea of this new method consists in replacing, in the likelihood formulation, the analytic expression of the probability density or cumulative distribution functions related to the historical sea level observations, by their numerical approximations (see Section 7.1). The related R source codes as well as the data files corresponding to the test cases are available at : doi.org/10.5281/zenodo.6260203. Based on the results presented herein, some major conclusions can be drawn.

1. The suggested numerical scheme for the estimation of the historical sea level likelihood as well as its incorporation in the statistical inference procedure are effective and reliable. This is particularly well illustrated by the comparison with the results of the "ideal" method (method 2).

2. Unlike the previously published approaches which appear to be biased, the proposed method allows for accurate and reliable estimates of the maximum likelihood quantiles, as well as of their posterior distributions in a Bayesian MCMC inference framework.
3. The proposed method is almost as accurate as the ideal method - i.e. method based on a perfect knowledge of the historical skew surges - even in places exhibiting high tide/surge ratios. This is valid if the hypotheses on which the calibrated statistical model is based, especially the independence between high tides and skew surges, are reasonably consistent with the observations. It seems to be the case at Brest.
4. This last conclusion may appear surprising, since the data set used in the "ideal" method contains apparently much more information on skew surges, but it is consistent with the conclusions of previous studies dealing with statistical inferences based on historical records (Payrastre et al., 2011). It seems that the length of the documented historical period is more decisive than the number or the accuracy of the documented record events.

The proposed approach could be further improved in several ways. First, even if moderate, some estimation biases remain present : over-estimated credibility intervals in cases with large tide/surge ratios and over-estimations in the case of binomial censored historical samples with no exceedance. It would be satisfying if the origin of these biases were understood and if they could be corrected. Moreover, the possible dependence between high tides and skew surges, as well as some seasonal features may be considered in the inference procedure, to increase its pertinence and application range. In fact, the largest skew surges often occur during winter storms while high tides are observed around the equinoxes (Tomasin et al., 2008).

The method could also be implemented on a larger number of case studies and results should be compared to those of previous assessments. The possible implementation of the method on samples with no documented record sea level exceeding the threshold seems to lead to satisfactory results (see the concluding paragraph of Section 2.4). This opens new perspectives, especially at sites where little or no historical records are available. Indeed, any coastal structure with known altitude that has not been submerged during a considered historical period, may provide valuable information for the statistical inference.

Finally, the method was developed for the analysis of coastal sea levels, but the same principles could certainly be adapted for the statistical analysis of other geophysical variables.

Nomenclature

X_{sys}	POT sample of systematic skew surges
u	threshold value for X_{sys}, $u \geq \min(X_{sys})$ (m)
n	length of X_{sys}
w_S	systematic duration (years)
Z_{hist}	historical record sea levels
η_H	threshold value for Z_{hist}, $\eta_H \geq \min(Z_{hist})$ (m)
h_z	length of Z_{hist}
X_{hist}	corresponding skew surges of Z_{hist} and exceeding u_H
u_H	threshold value for X_{hist}, $u_H \geq \min(X_{hist})$ and $u_H \geq u$ (m)
h_x	length of X_{hist}, $h_x \leq h_z$
w_H	historical duration (years)
λ	intensity of Poisson process, $\lambda > 0$
σ	scale parameter of the GP distribution, $\sigma > 0$
ξ	shape parameter of the GP distribution, $\xi \in R$
θ	parameters to estimate, $\theta = (\sigma, \xi, \lambda)$

List of abbreviations

GP	General Pareto
POT	Peaks Over Threshold
ML	Maximum Likelihood
MCMC	Monte Carlo Markov Chain
RSD	Relative Standard Deviation
RRMSE	Relative Root Mean Square Error

Chapitre 3

Article 2

Titre original : "Extreme skew surge estimation combining systematic skew surges and historical record sea levels on the English Channel and North Sea coasts"

Titre en français : "Estimation des surcotes de pleine mer extrêmes en combinant les surcotes de pleine mer systématiques et les niveaux marins records historiques sur les côtes de la Manche et de la Mer du Nord"

Laurie Saint Criq[1,2] (L.S.C.), Eric Gaume[3] (E.G.), Yasser Hamdi[1] (Y.H.), Taha B.M.J. Ouarda[2] (T.B.M.J.O.)

[1]Institut de Radioprotection et de Sûreté Nucléaire, Fontenay-aux-Roses, France

[2]Institut National de la Recherche Scientifique, Quebec City, QC, Canada

[3]Université Gustave Eiffel, Champs-sur-Marne, France

Cet article a été accepté le 8 septembre 2022 dans le numéro spécial "Flood risk and resilience in coastal zones and tropical islands" de la revue "Journal of Flood Risk Management".

Pour ce deuxième article, la conception a été pensée par L.S.C, E.G, Y.H et T.B.M.J.O., la méthodologie a été développée par L.S.C., E.G., Y.H et T.B.M.J.O., la partie programmation informatique incluant la préparation des données a été réalisée par L.S.C., les résultats ont été analysés par L.S.C., E.G., T.B.M.J.O., la première version de l'article a été préliminairement rédigée par L.S.C. qui a ensuite été révisée par E.G. et T.B.M.J.O.. Ce travail a été encadré par E.G., Y.H. et T.B.M.J.O.. Tous les auteur.e.s ont approuvé la version soumise (et acceptée) de l'article.

Dans le premier article, nous avons proposé une nouvelle méthode pour intégrer de l'information historique pour l'estimation des surcotes de pleine mer extrêmes qui répond à la problématique d'exhaustivité des données historiques. Cette méthode consiste à combiner, dans une unique inférence Bayésienne, les surcotes de pleine mer enregistrées pendant la période systématique et les niveaux marins records observés pendant la période historique. Cette nouvelle méthode pour intégrer de l'information historique apparaît fiable, non biaisée et pertinente. Les limites de cette méthode reposent sur les hypothèses posées, à savoir, l'indépendance entre les surcotes de pleine mer et les marées hautes et l'approximation numérique de la distribution des niveaux marins historiques. De plus, la méthode telle que développée dans l'article 1 ne permettait pas la prise en compte des incertitudes de l'information historique.

Dans le deuxième article, la méthode est challengée en l'appliquant à de nouveaux marégraphes localisés sur les côtes européennes pour vérifier notamment que les hypothèses posées n'ont pas d'influence significative sur les résultats. De plus, une extension de cette méthode est proposée pour prendre en compte les incertitudes des niveaux marins records historiques. Cela permet d'inclure des connaissances d'experts telles qu'un certain niveau n'a jamais été dépassé durant une période donnée. Ce point est très important pour les marégraphes où l'information historique n'est pas disponible car la collecte de données historiques est une tâche difficile et coûteuse.

Abstract

Coastal planning implies the estimation of extreme sea levels. As the distribution of astronomical high tides can be predicted, most recent publications suggest focusing on the estimation of extreme skew surges. Historical information, record sea levels observed before the beginning of systematic tide gauge recordings, can improve estimations. The corresponding skew surges can be estimated but are not necessarily exhaustive. Indeed, some historical extreme skew surges can remain unnoticed if they are combined with low or moderate tides, or for a variety of reasons. To deal with this exhaustiveness issue, a previous publication proposed an unbiased method for combining systematic period skew surges with historical period extreme sea levels. This method appeared more reliable than previously proposed approaches. The present study aims at presenting a broader evaluation of this method, based on its application to nine sites located on the English Channel and North Sea coasts. The method is also improved to consider several historical periods and various types of historical information. Results confirm the method to be reliable, useful and relevant. A number of recommendations is also formulated for the selection and use of historical information for sea level frequency analyses.

3.1 Introduction

Coastal planning needs to consider the risk of marine submersion especially in the present context of climate change. Then, estimating extreme sea levels, and especially extreme sea levels at high tide (maximum sea levels) which are the most dangerous, is essential for design purposes. Maximum sea levels can be defined as the combination of the predicted astronomical high tide and the skew surge. The astronomical high tide is a deterministic and predictable variable caused by gravitational forces. The skew surge is the difference between the observed maximum sea level and the predicted astronomical high tide during a tidal cycle and it is caused by atmospheric phenomena. The statistical distribution of maximum sea levels (or sea levels) is usually obtained after a convolution of the statistical distribution of predicted astronomical high tides (or predicted astronomical tides) and the statistical distribution of skew surges (or surges) which needs to be estimated (Batstone et al., 2013; Dixon et al., 1999; Liu et al., 2010; Mazas et al., 2014; Pugh et al., 1978; Tawn et al., 1989; Tawn, 1992; Tomasin et al., 2008). The independence between astronomical high tides and skew surges can be reasonably assumed (Williams et al., 2016) compared to the independence between astronomical tides and surges. Hence, the use of skew surges instead of surges makes the convolution easier because the interactions between both components of maximum sea levels can be neglected (Mazas et al., 2014). Moreover, according to Arns et al. (2015), Batstone et al. (2013) and Wahl et al. (2015), the skew surge is a better indicator of the meteorological impact on sea level than the surge.

The integration of historical information allows to increase the sample size, to enrich the data set in the right tail of the distribution and then, to reduce the estimation uncertainties of the statistical distribution (Benito et al., 2004; Gaál et al., 2010; Hamdi et al., 2015; Ouarda

et al., 1998a ; Payrastre et al., 2011 ; Reis et al., 2005). In the context of coastal analysis, historical events are the record maximum sea levels that occurred before the beginning of the systematic observation period - i.e. period during which tide gauge recordings are available - and that may be retrieved from archives or field surveys. The skew surges corresponding to these records can be estimated, but some extreme skew surges can easily remain unnoticed if they are combined with low or moderate astronomical high tides and do not generate extreme maximum sea levels (Outten et al., 2020). This is visible with the measured systematic data sets : some extreme skew surges, even the largest, can be missed when extreme maximum sea levels are sampled (see Figure 3.1 for an example). Then, the exhaustiveness of historical information for the calibration of a skew surge statistical method, which is essential for an unbiased statistical inference (Gaume, 2018), cannot be guaranteed in the case of skew surges. Frau et al. (2018) and Hamdi et al. (2015) attempt to overcome the issue of the historical skew surges exhaustiveness but respectively present some positive and negative bias demonstrated through Monte Carlo simulations in Saint Criq et al. (2022a), hereinafter referred to as SQ22. A large number of random samples was simulated with the same characteristics based on four real case studies. Then the maximum likelihood estimates and the posterior credibility intervals were analyzed with boxplots and rank histograms (Nguyen et al., 2014).

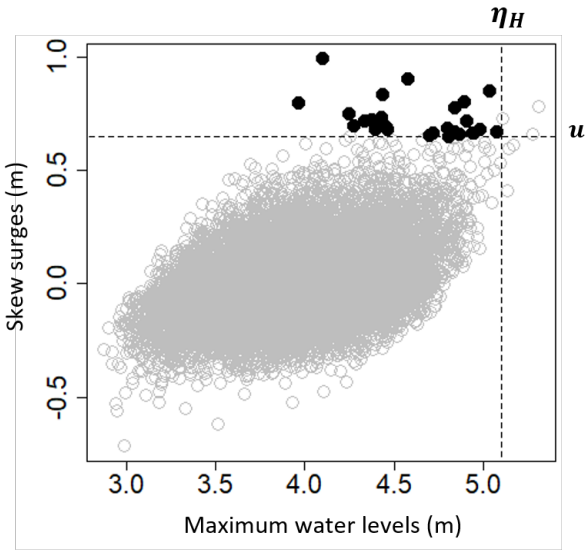

Figure 3.1 – Systematic events at Aberdeen (UK)
The black points represent the missed extreme skew surges (larger than u) when sampling the extreme maximum sea levels (larger than η_H).

SQ22 propose a new statistical inference procedure including the historical record maximum sea levels, instead of their corresponding skew surges. Indeed, the historical record maximum sea levels larger than a high enough threshold can reasonably be considered exhaustive during the historical period. For the calibration of the statistical distribution of skew surges, this method combines, in a single Bayesian inference procedure, information of two different natures : skew surges for the systematic period and extreme maximum sea levels for the historical period. The systematic skew surges are sub-sampled to a peaks-over-threshold (POT) sample and are modelled by a Generalized Pareto (GP) distribution. The statistical distribution of

the historical maximum sea levels is replaced in the likelihood by a numerical approximation which allows the implementation of this new inference procedure. This method, which will be called the HSL (Historical Sea Levels) method, is based on the hypotheses of independence between astronomical high tides and skew surges.

The HSL method appears reliable for the quantiles and parameters estimated by the maximum likelihood, as well as for the posterior credibility intervals of quantiles estimated in the Bayesian framework. The reduction of the averaged widths of the posterior credibility intervals (compared to the analysis of the systematic data only) shows the added value of the historical record maximum sea levels. The HSL method is applied to some case studies selecting a historical threshold that is not exceeded during the historical period according to the available information. This deterioration of the historical information is only moderately observable on the obtained posterior credibility intervals. This means that knowing that a sea level has not been exceeded - e.g. a coastal infrastructure has not been submerged - during a historical period is a valuable information from a statistical point of view. This is an interesting result, especially at sites without available historical information. The present study aims to challenge the HSL method proposed in SQ22 and its conclusions with new case studies. The HSL method is summarized in Section 3.2.1, the likelihood formulation is adapted to consider various uncertainty levels affecting historical information - i.e. in case of uncertainties on historical information. Section 3.2.2 presents the evaluation methodology. The application case studies are presented in Section 3.2.3. The application results are illustrated and discussed in Section 3.3.

3.2 Method

3.2.1 Combination of skew surges and sea levels in the same likelihood

Saint Criq et al. (2022a) propose to combine in a single Bayesian inference, $X_{sys} = \{x_{sys,1}, x_{sys,2}, ..., x_{sys,m}\}$, the systematic POT sample of m skew surges exceeding the threshold u during the systematic period of w_S years and $Z_{hist} = \{z_{hist,1}, z_{hist,2}, ..., z_{hist,h_z}\}$, the h_z historical record maximum sea levels exceeding the threshold η_H during the historical period of duration w_H years. The global likelihood of the systematic skew surges and the historical record sea levels $L(X_{sys}, Z_{hist}|\theta)$ is given by the product of the likelihood of the systematic skew surge sample $L(X_{sys}|\theta)$ and the likelihood of the historical sea level sample $L(Z_{hist}|\theta)$:

Equation 3.1

$$L(X_{sys}, Z_{hist}|\theta) = L(X_{sys}|\theta) \ . \ L(Z_{hist}|\theta)$$

where $\theta = (\sigma, \xi, \lambda)$ **are the parameters to estimate**

Skew surges exceeding the threshold u are chosen to be modelled by a GP distribution of

scale parameter $\sigma > 0$ and shape parameter $\xi \in R$. The number of skew surges exceeding the threshold u per year follows a Poisson process of intensity λ (Coles, 2001).

$L(X_{sys}|\theta)$, the likelihood of the systematic skew surge sample is defined, $\forall\ i \in \{1, ..., m\}$, $x_{sys,i}$ independent and identically distributed (i.i.d), by :

Equation 3.2

$$L(X_{sys}|\theta) = P_\theta(M = m)\ .\prod_{i=1}^{m} f_\theta(x_{sys,i})$$

where $P_\theta(M = m) = \frac{(\lambda w_s)^m}{m!}\exp(-\lambda w_S)$ **is the probability of observing** m **skew surges exceeding** u **during a systematic period of** w_S **years**
f_θ **is the GP probability density function**

On average, there are 706 high tidal levels during a year so, there are $N_{w_H} = 706 \times w_H$ high tidal levels during the historical period. Here, two consecutive events are assumed to be independent, but a storm can last two or three days, especially on the French Atlantic coast (Bulteau et al., 2015 ; Kergadallan et al., 2014). Then, to consider the temporal dependence, the number of high tidal levels per year should be reduced. $L(Z_{hist}|\theta)$, the likelihood of the historical maximum sea levels, describes the $N_{w_H} - h_z$ maximum sea levels that do not exceed η_H and the h_z maximum sea levels that exceed η_H during the historical period of duration w_H years. $\forall\ i \in \{1, ..., h_z\}$, $z_{hist,i}$ i.i.d, $L(Z_{hist}|\theta)$ is defined by :

Equation 3.3

$$L(Z_{hist}|\theta) = \tilde{G}_\theta(\eta_H)^{N_{w_H}-h_z}\ .\ \left[1 - \tilde{G}_\theta(\eta_H)\right]^{h_z}\ .\ \prod_{i=1}^{h_z}\frac{\tilde{g}_\theta(z_{hist,i})}{1 - \tilde{G}_\theta(\eta_H)}$$

$\tilde{g}_\theta$ and $\tilde{G}_\theta$ are respectively the probability density and cumulative distribution functions of high tidal levels which can be numerically computed given the statistical distributions of astronomical high tides, skew surges lower than u and skew surges exceeding u (for more details, see Appendix 7 in Saint Criq et al., 2022a).

Likelihood 3.3 is valid if the historical maximum sea levels z_{hist} are considered to be accurately known. However, uncertainties affecting z_{hist} can be accounted for (see Equation 3.4 : (a) range data, the historical maximum sea levels are known with uncertainties, they are comprised between the perception threshold η_H and a value ϕ_H with $\phi_H > \eta_H$, (b) binomial censored data, it is known that the threshold η_H has been exceeded h_z times over the historical period but the corresponding maximum sea levels are unknown, (c) lower limit data, a limit value ϕ_H has not been exceeded during the historical period. Note that the range data likelihood 3.4(a) could be more precise taking into account uncertainties on each historical sea level such as $\forall\ i\ \{1, ..., h_z\}$, $z_{hist,i} \in [\eta_H^i, \phi_H^i]$.

EQUATION 3.4

$$L(Z_{hist}|\theta) = \begin{cases} \tilde{G}_\theta(\eta_H)^{N_{w_H}-h_z} \cdot \left[\tilde{G}_\theta(\phi_H) - \tilde{G}_\theta(\eta_H)\right]^{h_z} & \text{if (a) range data,} \\ \tilde{G}_\theta(\eta_H)^{N_{w_H}-h_z} \cdot \left[1 - \tilde{G}_\theta(\eta_H)\right]^{h_z} & \text{if (b) binomial censored data,} \\ \tilde{G}_\theta(\phi_H)^{N_{w_H}} & \text{if (c) lower limit data.} \end{cases}$$

3.2.2 Method

The RStan package was used to conduct Bayesian Markov Chain Monte Carlo inferences based on the formulated likelihood with non-informative priors. The results of the inference procedure consist in the posterior densities for the calibrated parameters $\theta = (\sigma, \xi, \lambda)$ and of the corresponding skew surge quantiles. Note that Stan model related to the likelihood based on systematic skew surges and historical maximum sea levels (Equation 3.3) was made available within the scope of SQ22 at https://doi.org/10.5281/zenodo.6260203.

The HSL method is challenged with different evaluation criteria based on several tide gauges covering a variety of situations by their systematic and historical characteristics (see Section 3.2.3). First, the HSL method is implemented on observed systematic skew surges and exact historical maximum sea levels to measure the possible reduction of uncertainties by the integration of historical record maximum sea levels. The exact historical maximum sea levels are supposed to be perfectly known without any uncertainty. Then, uncertainties on historical maximum sea levels have to be accounted for to be in a more realistic context (see Equation 3.4). Then, the HSL method is implemented on observed systematic skew surges and historical information according to its accuracy (exact data, range data, binomial censored data and lower limit data) to evaluate the sensitivity of the accuracy historical information on the inference results, especially of the width of the posterior credibility intervals. In the cases of range data and lower limit data, the limit value ϕ_H is chosen as the maximum of the observed historical sea level added to 0.01 ($\phi_H = \max(z_{hist}) + 0.01$). Finally, the objective is to evaluate the most relevant descriptive parameters of the historical information. Then, from the observed data sets, a sensitivity analysis is conducted to the length of the historical duration w_H and to the limit value ϕ_H on the posterior credibility intervals. In the case of exact data (likelihood 3.3), w_H is taken as $w_H + \alpha$ with α the duration per historical record event. There are uncertainties to estimate w_H and in the worst case, the bias on w_H is around α years. In the cases of range data (likelihood 3.4(a) and lower limit data (likelihood 3.4(c), ϕ_H is taken as $\max(z_{hist}) + \beta$, with $\max(z_{hist})$ the maximum record historical sea level and β varying in $\{0.01, 0.5, 1, 2\}$.

3.2.3 Case study

Within the scope of this study, a database is developed, selecting tide gauges whose historical information is available or with long systematic series that can be split, for sake of illustration,

into two periods (systematic and historical) to create artificial historical information as was done for Brest and Saint Nazaire in SQ22. This database contains nine tide gauges : Calais, Cherbourg, Le Havre and Saint Malo on the English Channel coast, Nieuport and Oostende on the Belgium North coast, Aberdeen on the UK North coast, and Delfzijl and Vlissingen on the Netherlands North coast (Woodworth et al., 2007 ; Sterl et al., 2009 ; Haigh et al., 2010 ; Bernardara et al., 2011 ; Haigh et al., 2016). Figure 3.2 shows their geographic location.

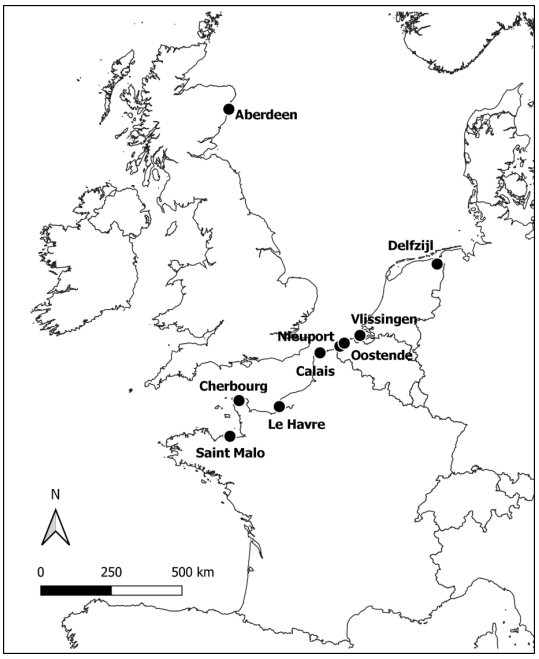

Figure 3.2 – Geographic location of selected tide gauges

3.2.3.1 Systematic data sets

The French Hydrographical and Oceanographical Service (data.shom.fr), the Flemish Agency for Maritime and Coastal Services (meetnetvlaamsebanken.be), the British Oceanographic Data Centre (bodc.ac.uk) and the Ministery of Infrastructure and Water Management of the Netherlands (rijkswaterstaat.nl) make available the hourly tide gauge data at the mentioned sites. These data are processed with a harmonic analysis through the R package *TideHarmonics* (Stephenson, 2015). As tidal predictions are calculated for the present time, to obtain the actual surges of past periods, the data must be corrected for a possible eustatism. If there is a significant trend in the temporal evolution of the annual mean of sea levels (calculated according to the Permanent Service for Mean Sea Level recommendations), then the series of observed sea levels is adjusted so that the corresponding series of annual means is stationary. The hourly astronomical tidal levels are computed, then, the series of astronomical high tides and skew surges can be extracted. Finally, the GP parameter stability criterion - based on fitting the model at a range of thresholds (Coles, 2001) - helps to select the POT threshold u (see Table 3.1) and to build the POT sample. The nine POT samples obtained are verified to be i.i.d. The independence between skew surges and astronomical high tides, which is a

necessary hypothesis to apply the HSL method, is tested for the nine tide gauges through the approach proposed by Arns et al. (2020) (see Appendix 9.2).

The systematic data sets for the nine selected tide gauges have different characteristics (see Table 3.1). The systematic period is more or less well documented (the systematic duration varies between 20.18 years and 50.72 years and the POT sample size varies between 23 and 69), the orders of magnitude for the skew surges are different (the POT threshold varies between 0.44m and 1.71m) and there are various patterns for the astronomical high tide component. For the nine tidal gauges, a tide surge ratio higher than 2 confirms the need to model separately the astronomical high tides and the skew surges as shown in Haigh et al. (2010). Saint Malo has a very high tide surge ratio and its highest astronomical high tide is very important compared to the other tide gauges, then the astronomical high tide appears to be the dominant component for record maximum sea levels. In this case, the HSL method is particularly interesting since the historical skew surges are certainly non-exhaustive and also particularly challenged because of the limited weigh of the extreme skew surges on the historical extreme sea level distribution. Calais, Cherbourg, Le Havre and Brest (SQ22) have similar values of tide surge ratio, lowest and highest astronomical high tide which testify of the relative importance of the high tide compared to the skew surge. At Aberdeen, Nieuport and Oostende, the astronomical high tide component is even more moderate, the tide surge ratio is about 13. Finally, at Delfzijl and Vlissingen, the maximum sea levels are clearly driven by the skew surge. Indeed, their tide surge ratios are reduced and the POT threshold is higher than the lowest astronomical high tide which is especially visible at Delfzijl. Then, at these stations, record maximum sea levels are related to record skew surges and the use of HSL method would be less essential than at Saint Malo since historical record skew surges would tend to be (or very closed to be) exhaustive and the method proposed by Hamdi et al. (2015) could then be used with probable limited bias.

Table 3.1 – Characteristics of the systematic data sets

Site	Tide gauge recording period	w_S (years)	u (m)	n	Tide surge ratio*	LAHT (m)	HAHT (m)
Aberdeen	1990-2021	24.61	0.65	26	12.50	3.05	4.85
Calais	1941-2021	42.56	0.60	43	25.20	5.16	7.84
Cherbourg	1943-2020	46.40	0.44	45	28.26	4.38	7.13
Delfzijl	1987-2021	34.53	1.71	33	2.05	0.81	1.84
Le Havre	1938-2021	50.72	0.60	69	25.59	5.92	8.55
Nieuport	2000-2020	20.18	0.71	26	13.65	3.28	5.43
Oostende	2000-2020	20.26	0.75	23	12.63	3.19	5.26
Saint Malo	1986-2021	26.64	0.50	30	47.62	7.81	13.52
Vlissingen	1987-2021	34.54	1.00	29	5.41	0.89	2.92

LHAT is the lowest astronomical high tide and HAHT the highest astronomical high tide. The systematic duration w_S does not account for the period of missing values. *Ratio of the 98% astronomical high tide to the 98% skew surge quantile (Dixon et al., 1999).

3.2.3.2 Historical data sets

Historical record maximum sea levels are provided by a database developed by the French Institute for Radiological Protection and Nuclear Safety (Giloy et al., 2018) for Belgium and French tide gauges and by a UK database developed by the British Oceanographic Data Centre from 1915 (Haigh et al., 2017) for Aberdeen. The systematic series of Delfzijl and Vlissingen start respectively in 1879 and 1863, present a measuring gap between 1960 and 1987. Then, they are split into a systematic sample (after 1987) and a historical sample (before 1960). For both Dutch tide gauges, the historical record maximum sea levels above 4m are extracted. The hypothesis of stationary is accepted for the complete series of Delfzijl (from 1879 to 2021), but rejected for the complete series of Vlissingen (from 1863 to 2021). Indeed, the two highest skew surges occurred during the historical period and are very large compared to the other skew surges of the complete series. The complete series contains 43 skew surges at Delfzijl and 47 at Vlissingen.

The nine tide gauges also present various situations for the historical period (see Tables 3.2 and 9.1) : the length of the historical period (from 17.84 years to 130 years), the number of historical record maximum sea levels (from 1 event to 5 events) and the height of the record maximum sea levels (η_H varies between 4.05m and 12.96m) which is directly related to the astronomical high tidal range (see Table 3.1). The historical duration w_H is chosen larger than the time laps between the first historical record and the beginning of the systematic period. $P(\mathrm{A}|X_{sys})$ and $P(\mathrm{B}|X_{sys})$ are computed to test the consistency of historical samples according to the systematic data sets, on the assumption that skew surges are following a GP distribution. At Aberdeen, Calais, Delfzijl, Le Havre and Saint Malo, the historical data set seems to be consistent with the distribution adjusted on the systematic skew surges ($P(\mathrm{A}|X_{sys})$ and $P(\mathrm{B}|X_{sys})$ close to one). In these cases, the systematic and historical data sets seem consistent and the systematic data sets do not seem to impose strong constraints on the skew surge distribution. At Cherbourg, Nieuport and Oostende, according to the systematic data sets, the threshold η_H can be easily exceeded h_z times during the historical period ($P(\mathrm{A}|X_{sys})$ high), but the maximum historical observed sea level can hardly be exceeded during the historical period ($P(\mathrm{B}|X_{sys}) = 0$). At Vlissingen, the sea level distribution estimated only on systematic skew surges can hardly allow the realization of the record maximum sea levels observed during the historical period ($P(\mathrm{A}|X_{sys}) = P(\mathrm{B}|X_{sys}) = 0$). The statistical consistency between systematic and historical data sets is highly questionable if we assume that the skew surges follow a GP distribution. Mixing both datasets in the same statistical inference procedure is likewise questionable and may result in problematic outcomes as will be illustrated hereafter.

Tide gauges can sometimes be defective as it was the case at Le Havre in 1984 when a major event occurred but could not be recorded (see Table 9.1). This observation is integrated as historical information in the HSL method. The 1984 event is very extreme and it appears reasonable to suppose that, if another event would have exceeded it during the systematic period but not measured, this event would have been retrieved. Then, the historical duration associated to this event is taken as the sum of the gap measures between 1938 and 2021. Consequently, at Le Havre, two historical periods have been defined (see Table 3.2).

Table 3.2 – Characteristics of the historical data sets

Site	Range	w_H (years)	η_H (m)	ϕ_H (m)	h_z	$P(\mathrm{A}\|X_{sys})$	$P(\mathrm{B}\|X_{sys})$	w_H/w_S
Aberdeen	1915-1990	80	5.10	5.10	2	1.00	1.00	3.25
Calais	1905-1941	50	7.70	7.70	1	1.00	1.00	1.17
Cherbourg	1821-1943	130	7.17	7.96	2	1.00	0.00	2.80
Delfzijl	1879-1960	28.15	4.34	4.34	1	0.96	0.96	0.82
Le Havre	1882-1938	70	8.40	8.55	3	1.00	1.00	1.38
Le Havre	1938-2021	33.26	9.28	9.28	1	0.00	0.00	0.66
Nieuport	1932-2000	80	6.08	6.73	5	0.99	0.00	3.96
Oostende	1932-2000	80	6.01	6.66	4	0.82	0.00	3.95
Saint Malo	1877-1986	100	12.96	12.96	1	1.00	1.00	3.75
Vlissingen	1863-1960	17.84	4.05	4.54	3	0.00	0.00	0.52

η_H and ϕ_H are the observed minimum and maximum historical sea levels. $\mathbf{A}|X_{sys}$ (respectively $\mathbf{B}|X_{sys}$) represents the event "η_H (respectively ϕ_H) is exceeded at least h_z (respectively 1) time(s) during the historical period knowing the systematic data set". Then, $P(\mathbf{A}|X_{sys}) = 1 - \sum_{i=0}^{h_z-1} \tilde{G}_{\hat{\theta}}(\eta_H)^{N-i}$ and $P(\mathbf{B}|X_{sys}) = 1 - \tilde{G}_{\hat{\theta}}(\phi_H)^N$ are computed with the parameters $\hat{\theta}$ estimated on systematic data sets by the maximum likelihood.

3.3 Application of the HSL method to observed data sets

The HSL method is applied to observed data sets. In Section 3.3.1, the historical record sea levels retrieved from archives (see Table 9.1) are supposed to be precisely known.

3.3.1 Exact data

At Delfzijl and Vlissingen, as the complete skew surge series are available (see Section 3.2.3.2), it is possible to compare the results of the HSL method with the ideal case - i.e. perfect knowledge of the historical skew surges. The adjusted credibility intervals with the HSL method are very similar to those obtained in the ideal case, and even if narrower, they are consistent with the data sets since they contain the complete skew surges series (see Figure 3.3). This result is very satisfactory since a large number of historical events is processed in the inference for the ideal case compared to the HSL historical samples : 43 (respectively 18) historical skew surges versus 1 (respectively 3) historical maximum sea levels at Delfzijl (respectively Vlissingen). This and similar results obtained in SQ22 for the French tide gauges of Brest and Saint Nazaire allow to validate the HSL method.

The inclusion of the exact historical record maximum sea levels leads to a significant reduction of the width of the posterior credibility intervals for all tide gauges except for Nieuport and Vlissingen, but to a redirection of the posterior credibility intervals, and for the last case, a significant increase of the estimated quantile (see Figure 3.3). At Nieuport and Vlissingen, this result was expected because of statistical inconsistency of the systematic and historical data sets. The reduction of uncertainties for the skew surge quantiles - i.e. reduction of the posterior credibility interval width - is discussed in light of the consistency between systematic

and historical samples (see $P(\mathrm{A}|X_{sys})$ and $P(\mathrm{B}|X_{sys})$ in Table 3.2). For all tide gauges and all methods, the median adjustments are in the lower part of the posterior credibility intervals. It is interesting to notice that the median adjustments obtained with the HSL method and without historical information are almost superposed.

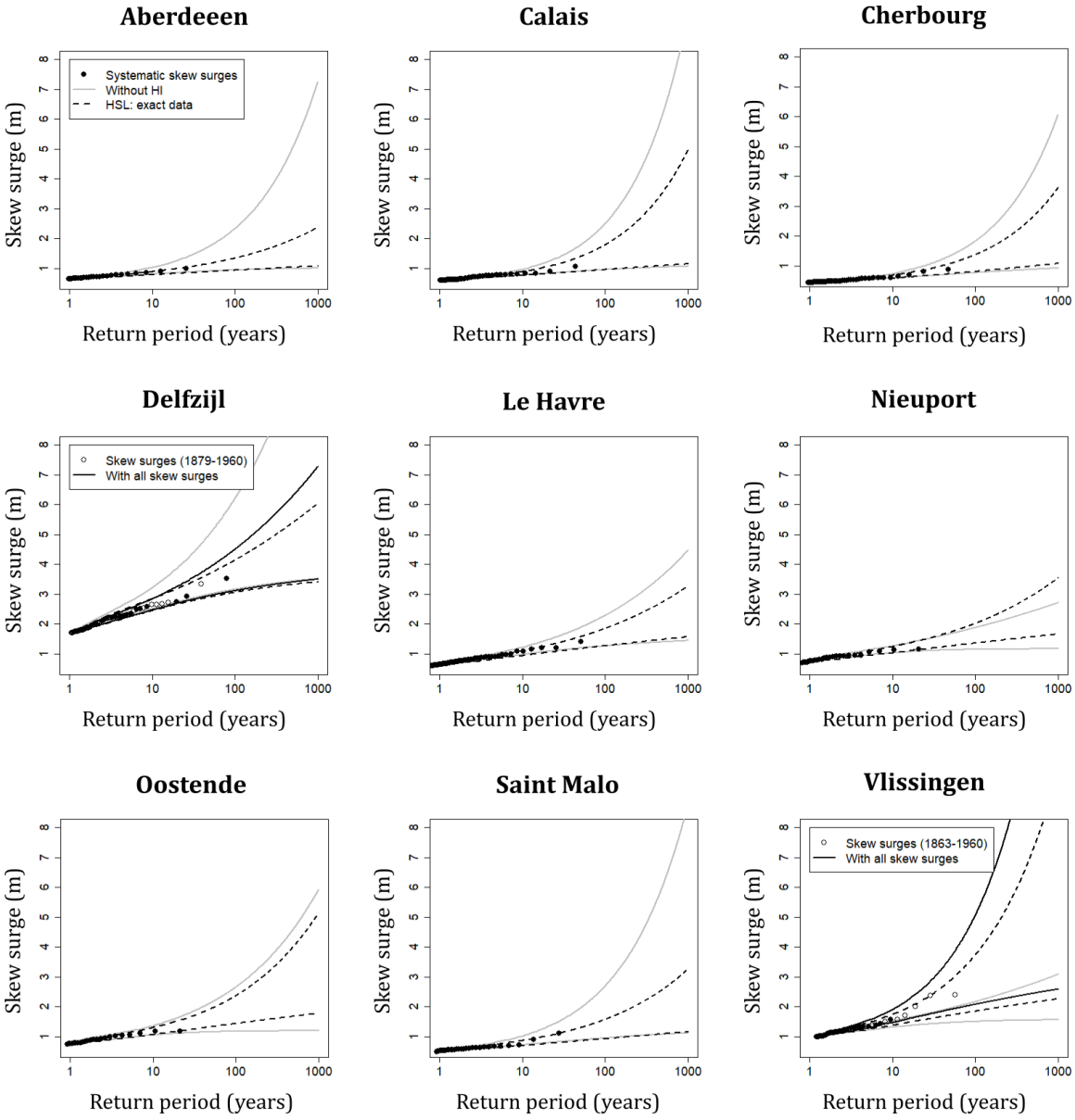

Figure 3.3 – 90% skew surge posterior credibility intervals
They are obtained without historical information (HI), based on the systematic data (grey line), integrating the historical record sea levels as exact data (black dotted line) and in the ideal case, when all skew surges are known during the systematic and historical periods (black line) for Delfzijl and Vlissingen. The dotted lines represent the median estimates of each method.

At Aberdeen, Calais, Delfzijl and Saint Malo, the systematic and historical data sets appear statistically consistent and the posterior credibility intervals are significantly narrower in comparison to the other sites. Moreover, at Aberdeen and Saint Malo, the historical duration is at least three times longer than the systematic duration which helps to significantly lower the upper bound of the posterior credibility interval. At Calais, due to equivalent lengths of the

systematic and historical periods, the uncertainties could not be as reduced as for Aberdeen and Saint Malo. At Delfzijl, the historical duration is slightly lower than the systematic duration, but the strong reduction of uncertainties (as for Aberdeen and Saint Malo) may be allowed because of the very high initial uncertainties - i.e. the posterior credibility interval based on the systematic skew surges is very large. At Cherbourg and Oostende, the historical sample appears to contain, at least, one exceptional event clearly not consistent with the systematic sample ($P(\mathrm{B}|X_{sys}) = 0$ in Table 3.2), so the integration of historical maximum sea levels only allows to slightly reduce the uncertainties. A similar phenomenon is observed at Le Havre, for the second historical period (1938-2021).

As a first conclusion, these analyses indicate that some factors have an influence on the reduction of the credibility intervals, like the consistency between systematic and historical samples, the initial uncertainties and the length of the historical duration compared to the systematic duration. Note that the most important reductions (at Aberdeen, Calais, Delfzijl and Saint Malo) are obtained with only one or two record maximum sea levels exceeding the historical perception threshold, whereas the least reduced posterior credibility intervals (at Le Havre, Cherbourg and Oostende) are obtained with three or four record maximum sea levels (see Table 3.2 and Figure 3.3).

The inconsistency between systematic and historical data sets at Vlissingen and Nieuport leads to a redirection of the posterior statistical distributions and credibility intervals. Indeed, at Vlissingen, three very extreme maximum sea levels (see Table 3.2) are reported during a very short historical period compared to the systematic duration ($w_H \approx \frac{w_S}{2}$). At Nieuport, extreme events are also observed, but during a relatively long historical period ($w_H \approx 4 \times w_S$). Their empirical frequency is more in accordance with the systematic observations, then the redirection of the posterior credibility intervals is more limited than at Vlissingen.

3.3.2 Sensitivity analysis of historical information quality

Accounting for the possible uncertainties affecting the historical information (range data, binomial censored data or lower limit data instead of exact data) has an impact that is only moderately observable on the posterior credibility intervals except in some particular cases and an almost invisible impact on the median adjustments (see Figure 3.4). This is consistent with the conclusions drawn by Payrastre et al. (2011) on river discharge series : the length of the historical period has more impact on the inference results than the number and accuracy of documented historical events.

At Aberdeen, Calais and Saint Malo, the posterior credibility intervals produced with any type of historical information are mostly superposed which means that no matter the accuracy of historical records, the information content is almost the same. Indeed, there is only one exceedance at Calais and Saint Malo and two exceedances of same value at Aberdeen. At Delfzijl, there is also one exceedance, the historical posterior credibility intervals are also very close except for binomial censored data, for which the upper bound is quite higher than the other ones. Indeed, this type of historical information is the least restrictive for the magnitude of historical maximum sea levels and leads to the highest upper bound as it is observed at most

of the tide gauges (Aberdeen, Calais, Delfzijl, Le Havre, Nieuport, Oostende and Vlissingen). There are also some particularities directly related to the samples.

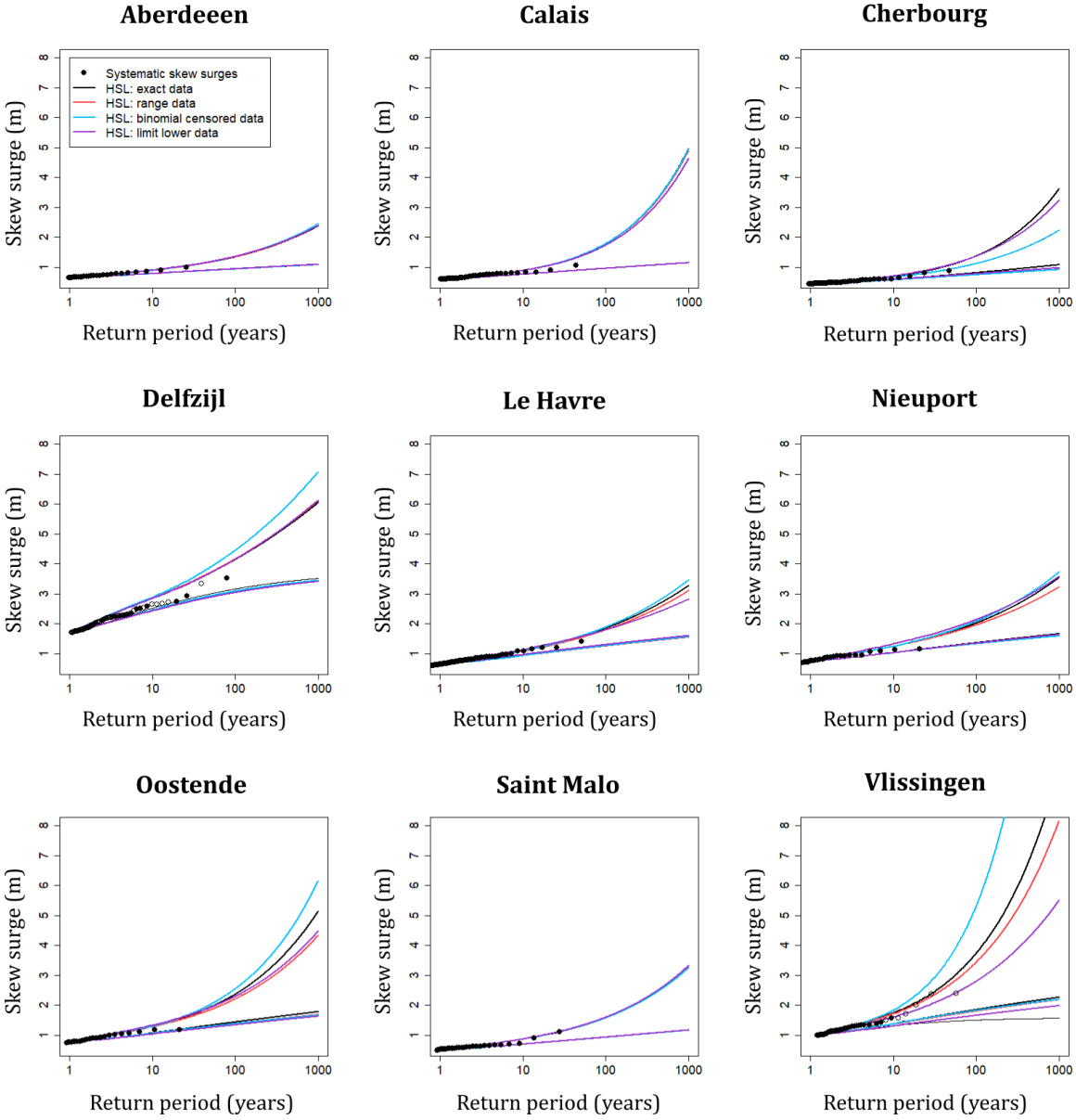

Figure 3.4 – 90% posterior skew surge posterior credibility intervals

They are based on the systematic data and on historical maximum sea levels as exact data (black line), range data (red line), binomial censored data (blue line) or lower limit data (purple line).

At Le Havre and Nieuport, the four posterior credibility intervals are quite close. The case of Oostende is similar with a higher scattering. At Cherbourg, the posterior credibility intervals are superposed except the one obtained with binomial censored data. Indeed, in this case, the highest historical sea level seems highly improbable according to the systematic data set (see Table 3.2), pulling up the calibrated statistical distribution. The binomial censored data method relaxes the constraint imposed to the calibration by this extreme historical record.

The case of Vlissingen is very special compared to the other ones since the systematic and historical data sets appear extremely inconsistent (see Section 3.2.3.2). The strong sensitivity to the uncertainties on the historical data, and then to the weight given to the historical data in the adjustment, reflects this statistical inconsistency.

3.3.3 Complementary analysis

Some complementary analyses are conducted to evaluate the sensitivity of the inference outcomes to 1) the estimated historical duration w_H, 2) the estimated limit value ϕ_H for historical record maximum sea levels, when the "range data" likelihood is used or 3) when the "lower limit data" likelihood is used. Similar results are obtained for all nine sites. For the sake of simplification, only the results of Aberdeen are presented herein (see Figure 3.5). This data set has been selected because of the statistical consistency between systematic and historical data sets.

The historical duration w_H has to be estimated. It is, at least, the time laps between the first historical record and the last one or between the first historical record and the beginning of the systematic period. But, it is common to select a slightly larger value for w_H to avoid introducing biases as discussed by Schendel et al. (2017). According to these considerations, at Aberdeen, the historical duration has been estimated to $w_H = 80$ years. The historical inventory covers the period 1915-1990 and there are two reported record maximum sea levels, then the empirical return period of these records is about 30 years. Figure 3.5-1) shows the posterior credibility intervals, in the case of exact data, when the historical duration w_H varies in a reasonable range of 80 ± 30 years. The historical duration appears to have a moderate impact on the statistical inference results, the longer estimated historical duration, the lower are the uncertainties. Yet, the additional information content increases with the length of the estimated historical duration.

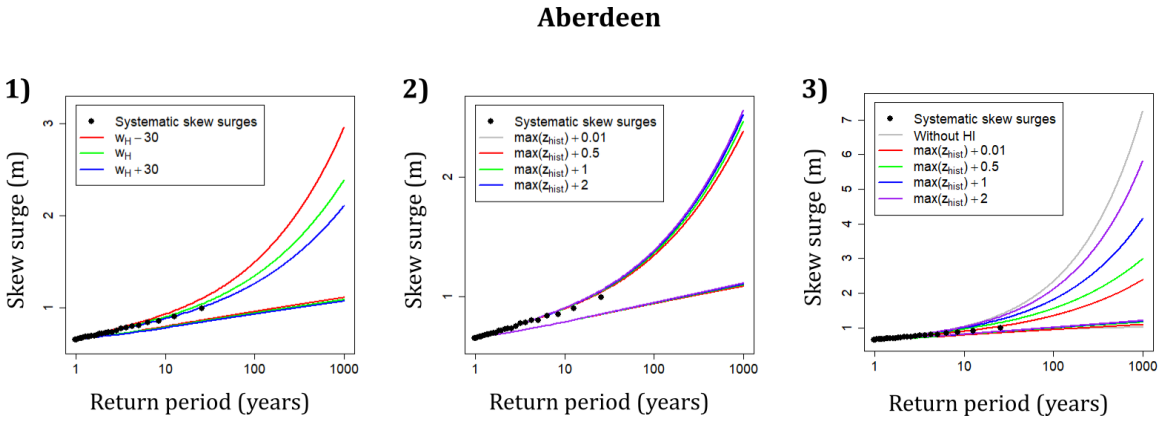

Figure 3.5 – 90% posterior skew surge posterior credibility intervals

They are based on the systematic data and the historical record maximum sea levels as 1) exact value adjusting the historical duration (likelihood 3.3), 2) range value adjusting the upper bound of the interval ϕ_H (likelihood 3.4(a)) and 3) lower limit data adjusting the value not exceeded ϕ_H (likelihood 3.4(c)).

As expected, in the case of range data, the posterior credibility intervals are relatively insensitive to uncertainties affecting the estimated limit value ϕ_H for historical record sea levels (see Figure 3.5-2)).

Finally, in the case of lower limit data, the posterior credibility intervals are very sensitive to the estimated limit value ϕ_H (see Figure 3.5-3)). The lower the limit value, the more informative is the added historical content. Yet, the possible range of the historical maximum sea levels is reduced leading to narrower posterior credibility intervals. When the lower limit value ϕ_H tends to infinity, the added value of the historical information is very reduced and the obtained adjustments tend to the ones obtained with systematic data only. Yet, a very high ϕ_H is not informative at all in the case of lower limit data.

Based on all previous analyses and Payrastre et al. (2011), the most determining information included in the historical data set appears to be the years without observed records. Then, a particular attention must be given to the determination of the value w_H. This conclusion is valid provided that the historical and systematic data sets appear consistent at the light of the calibrated statistical distribution. If it is not the case, it does not mean that the historical data is useless. On the contrary, it questions the adequacy of the statistical distribution and hence the basics of the risk assessment method. But this last issue goes far beyond the objectives of this paper.

3.4 Conclusion

SQ22 proposed a new statistical inference procedure to properly integrate historical information about extreme maximum sea levels in skew surge statistical analyses, to overcome the issue of non-exhaustiveness of the skew surge variable. The procedure consists in combining data sets of different natures : skew surges for the recent period and maximum sea levels for the historical period. This new method is valid under the assumption of independence between astronomical high tides and skew surges and it is implemented by replacing the analytic expression of the probability density and cumulative functions of maximum sea levels by numerical approximations in the likelihood formulations. The flexibility of the likelihood formulation allows to consider different levels of uncertainties affecting the historical information (see Section 3.2.1) and several historical periods.

The method proposed in SQ22 was implemented herein on nine additional case studies with different characteristics. The comparison with results based on a perfect knowledge of historical skew surges, when this information was available, confirm the relevance of the proposed approach. Indeed, the posterior credibility intervals appear unbiased and very close to those obtained with a perfect knowledge of the historical skew surges. The results of the present study indicate that all data, being recorded by tide gauges or not, are informative, deserve to be integrated in statistical analyses, on the condition of being exhaustive. The integration of historical information should lead to reduce the estimation uncertainties on condition that the systematic and historical data sets appear statistically consistent, at the light of the calibrated distribution. Otherwise, the historical information, if criticized and confirmed, still

should be considered as of crucial importance. It will not help reducing statistical inference uncertainties but will clearly question the adequacy of the statistical distribution and hence the basics of the risk assessment method. In any case, even if less accurate than systematic measurements, historical information should be considered in risk assessment procedures.

The sensitivity analyses conducted reveal some key features for useful historical record series. First, the duration of the period covered by the historical inventory w_H appears to be of primary importance. The level of accuracy of the historical record maximum sea levels has little influence on the statistical inference results. Second, the limit value ϕ_H, which it has not been exceeded during the historical period, is decisive. Its underestimation will introduce significant biases in the inference procedure and should be avoided. But its overestimation, for sake of prudence, will reduce the historical information content. It is of course possible to consider several historical periods differing by their content and accuracy. Future efforts should focus on the integration of expert knowledge such as coastal structure with known altitude which has not been submerged during a considered historical period. This is very promising for sites with high uncertainties.

The HSL method presents good properties, but should be improved by considering the skew surge – high tide dependence and the temporal dependence between two consecutive events. One weakness of this method is that historical information is only available at a few tide gauges as historical data collection is difficult and expensive. Consequently, the use of expert knowledge and the integration of other types of information should be highly considered.

Chapitre 4

Article 3

Titre original : "Regional frequency analysis of extreme skew surges at ungauged locations"

Titre en français : "Analyse fréquentielle régionale des surcotes de pleine mer extrêmes à des sites non jaugés"

Laurie Saint Criq[1,2] (L.S.C.), Taha B.M.J. Ouarda[2] (T.B.M.J.O.), Eric Gaume[3] (E.G.), Yasser Hamdi[1] (Y.H.)

[1]Institut de Radioprotection et de Sûreté Nucléaire, Fontenay-aux-Roses, France

[2]Institut National de la Recherche Scientifique, Quebec City, QC, Canada

[3]Université Gustave Eiffel, Champs-sur-Marne, France

Cet article a été soumis le 13 octobre 2022 à la revue "Scientific Reports".

Pour ce troisième article, la conception a été pensée par L.S.C, E.G, Y.H et T.B.M.J.O., la méthodologie a été développée par L.S.C. et T.B.M.J.O., la partie programmation informatique incluant la préparation des données a été réalisée par L.S.C., les résultats ont été analysés par L.S.C., T.B.M.J.O. et E.G., la première version de l'article a été préliminairement rédigée par L.S.C. qui a ensuite été révisée par T.B.M.J.O., E.G. et Y.H.. Ce travail a été encadré par T.B.M.J.O., E.G. et Y.H.. Tous les auteur.e.s ont approuvé la version soumise de l'article.

Les deux premiers articles ont permis de proposer et de valider une méthode intégrant de l'information historique pour l'estimation des surcotes de pleine mer extrêmes. Ces deux premiers articles permettent donc de répondre à la première problématique de cette thèse.

La deuxième problématique est l'utilisation de l'information régionale. Ainsi, le troisième article se concentre sur le développement de modèles régionaux basés sur des variables physiographiques et météorologiques pour estimer les quantiles de surcotes de pleine mer à des sites non jaugés. Pour cela, une première partie de cet article se concentre sur l'identification de potentielles covariables. Ensuite, des modèles régionaux basés sur les covariables identifiées sont testés et appliqués à une base de données contenant 78 marégraphes européens.

Abstract

Regional frequency analysis using physiographic and meteorological variables is introduced for the estimation of skew surge quantiles at ungauged sites. A regional model is the combination of a delineation method of homogeneous regions and a regional estimation method. The hierarchical cluster analysis, canonical correlation analysis and region of influence approaches are tested for the definition of homogeneous regions. The regional skew surge quantile estimate is computed based on either the multiple linear regression or the generalized additive model. The regional models are implemented on a data set of 78 European tide gauges located on the Atlantic, English Channel, Irish and North coasts. This study identifies a number of explanatory physiographic and meteorological variables such as the width of the continental shelf, the 100-year quantile of the wind speed, the 100-year quantile of the low mean sea level pressure and the angle between the prevailing wind direction and the continental shelf direction. Results show that the approaches based on the generalized additive model outperform the approaches based on the multiple linear regression. The region of influence approach appears as the delineation method leading to the best performances.

4.1 Main

Coastal flooding events have important consequences on human society. Knowledge of extreme sea levels is important for the design of coastal facilities at gauged sites, but also at locations where little or no observed sea level series are available. Sea levels at high tides can be defined as the combination of the astronomical high tide and the skew surge which is the difference between the observed maximum sea level and the predicted astronomical high tide during a tidal cycle. The astronomical high tide, caused by gravitational forces, is a deterministic and predictable variable, and the skew surge, caused by meteorological phenomena, is a stochastic variable. It is therefore common to focus on skew surges to estimate extreme sea levels.

Regional frequency analysis (RFA) is commonly used to estimate extreme events at a target site where series of observations are short or unavailable. Spatial information, available data at gauged sites close to the target site, is used to compensate for the lack of local data. RFA is generally composed of two main steps : the delineation of homogeneous regions and regional estimation. RFA was initially introduced in hydrology with the index flood method (Dalrymple, 1960 ; GREHYS, 1996a ; GREHYS, 1996b ; Cunnane, 1988 ; Potter et al., 1990 ; Grover et al., 2002 ; Wazneh et al., 2013), then applied to other fields like coastal analysis (Andreevsky et al., 2020 ; Bardet et al., 2011 ; Bernardara et al., 2011 ; Frau et al., 2018 ; Hamdi et al., 2019 ; Mai Van et al., 2007 ; Van Gelder et al., 1998 ; Weiss et al., 2012 ; Weiss et al., 2013a). The index flood method assumes that, within a statistically homogeneous region, all local events are identically distributed except for a site scaling factor (Hosking et al., 1997).

In hydrology, explanatory physiographic or meteorological variables may be used for both, the delineation of homogeneous regions and the regional estimation of flood quantiles at ungauged sites. The methods to delineate regions can lead to fixed homogeneous regions exclusive of one

another (e.g. hierarchical cluster analysis (HCA)) or to neighborhoods of gauged sites centered around the target sites (e.g. region of influence (ROI), canonical correlation analysis (CCA)). The HCA identifies sites that are similar with one another based on the distance between sites within the physiographic-meteorological space (Rencher et al., 2012 ; Ouarda et al., 2018). The ROI method identifies the neighborhood of each target site by computing a similarity measure between it and the other gauged sites (Burn, 1990b ; Zrinji et al., 1994 ; Holmes et al., 2002 ; Holmes et al., 2005 ; Ouarda, 2016 ; Burn, 1990a). The CCA method allows to describe the linear combination between two sets of random variables within the same group, for which the canonical correlation is maximal (Ribeiro-Corréa et al., 1995 ; Ouarda et al., 2000 ; Ouarda et al., 2001 ; Chokmani et al., 2004 ; Shu et al., 2007 ; Nezhad et al., 2010 ; Ouali et al., 2017 ; Ouali et al., 2016 ; Han et al., 2020 ; Desai et al., 2021). The two main methods for the quantile estimation are the multiple linear regression (MLR) and the generalized additive model (GAM). MLR assumes a linear relation between the response variables and the explanatory variables (Ouarda et al., 2006 ; Shu et al., 2004 ; Shu et al., 2008 ; Mediero et al., 2014), GAM assumes a nonlinear relation and uses non parametric smooth functions to link the response variables to the explanatory variables (Ouarda, 2016 ; Ouali et al., 2017 ; Hastie et al., 1986). The GAM method can be regarded as more flexible than MLR.

A number of studies highlight the possible effects of the physiography and meteorology on the high sea levels or skew surges quantiles. Exposed sites (in front of open sea) lead to larger quantiles with high return periods than protected sites (behind islands, in an estuary...) on the Netherlands coasts (Van Gelder et al., 1998). Strong surges are linked to a limited water depth and a long fetch along Vietnamese coast, in the South China Sea (Mai Van et al., 2007). The local effects of amplification or extenuation of the surges like the bathymetry, the topography and the prevailing wind should be better considered on the French coasts (Bardet et al., 2011). The storm track characteristics (trace and size of the storms) can also provide valuable information to find the right explanatory variables of the skew surge (Haigh et al., 2016 ; Stephens et al., 2019 ; Enríquez et al., 2020). However, to the knowledge of the authors, there is no published RFA coastal study involving physiographic or meteorological characteristics to estimate the skew surge quantiles at ungauged sites.

The present study aims to identify the most relevant physiographic-meteorological variables, and to develop RFA models based on covariates for the estimation of skew surge quantiles at ungauged locations. The HCA, CCA and ROI methods are tested and optimized for the delineation of the homogeneous regions, the HCA and ROI methods are also used with the geographic distance. The MLR and GAM methods are tested for the regional estimation on the homogeneous regions and also considering all tide gauges without delineation of homogeneous regions(ALL). This study is implemented on a data set of 78 European tide gauges located on the Atlantic, English Channel, Irish and North coasts.

4.1.1 Explanatory variables of the skew surge

In total, eight physiographic and meteorological variables possibly related to the skew surge statistics are selected : the latitude (LAT), the longitude (LON), the 100-year quantile of the low mean sea level pressure (100-MSLP), the 100-year wind speed quantile (100-WS), the width of the continental shelf (WCS), the angle between the prevailing wind direction and the continental shelf direction (ANGLE), the area (AREA) and the perimeter (PERIM) of the maritime zone in a 20km-square centered on the considered location. 100-MLSP and 100-WS are chosen because it is well known that the combination of strong winds and low pressures favors the occurrence of storms and high skew surge values (Muis et al., 2016). ANGLE is chosen to characterize the orientation of the main storm track relatively to the continental shelf direction. Its value is included between 0 and 1 ; if the prevailing wind and the continental shelf directions are similar then ANGLE is equal to 0, if they are perpendicular then ANGLE is equal to 0.5 and if they are opposite then ANGLE is equal to 1. The variables AREA and PERIM are introduced because the coastline morphology could be important for the skew surge amplitude (Bardet et al., 2011 ; Bernardara et al., 2011 ; Van Gelder et al., 1998 ; Weiss et al., 2013b). . Complex coastlines need a large number of different storm surge clusters to represent the spatial footprints of storm surges (Enríquez et al., 2020). The choice of AREA and PERIM is inspired by the physiographic variables characterizing the catchment basin shape in hydrology like the circularity ratio (Msilini et al., 2022) which is also used for the analysis of changes in coastline morphology in the Bohai Sea in China (Fu et al., 2017). The variables AREA and PERIM are illustrated for three typical cases in Figure 10.1 in the Supplementary Information. The distance of 20km for the definition of the variables AREA and PERIM is the result of a compromise.

The spatial distribution of the physiographic-meteorological variables is illustrated in Figure 4.1 hereafter and their descriptive statistics are summarized in Table 10.1 in the Supplementary Information. According to the meteorological variables (100-MLSP and 100-WS), the European tide gauges, except those located in Spain and South-Western France, should be at risk of important storms (see Figure 4.1a)). As expected, 100-MSLP seems to be very correlated with LAT, but skew surge quantiles are more correlated with 100-MSLP than with LAT (see Figure 4.2 and Supplementary Figure 10.2). WCS appears logically correlated with LON as the Eastern tide gauges have a strong WCS, and quantile skew surges are more correlated with WCS than with LON (see Figure 4.1b) and Supplementary Figure 10.2). Then, giving the geographical position of the tide gauge, LAT and LON are indirectly informative, but not as much as more specific physiographic and meteorological variables (e.g. WCS and 100-MSLP). ANGLE is very low for a number of tide gauges located on the English Channel : the prevailing wind and the continental shelf come from the West South-West direction (see Figure 4.1c)). There is a large variety of coastline shapes (AREA and PERIM) along the European coasts (see Figure 4.1d)). The largest skew surges (see Figure 10.2 in the Supplementary Information) seem to be generated at sites exposed to a combined effect of low pressures and high-speed winds, and with wide continental shelfs (high WCS).

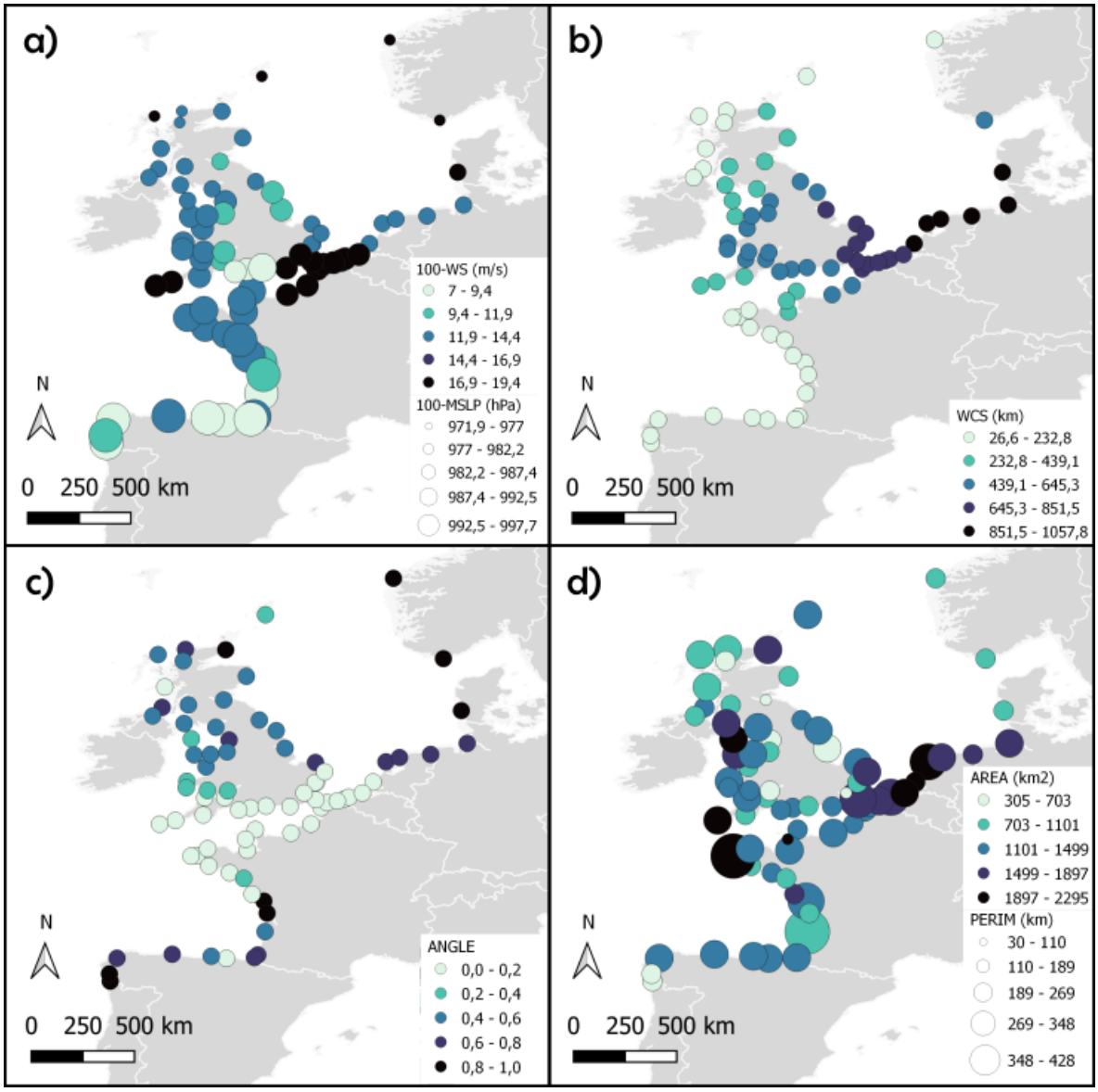

Figure 4.1 – Physiographic and meteorological variables at the European tide gauges

a) 100-WS and 100-MSLP, b) WCS, c) ANGLE and d) AREA and PERIM

A correlation analysis is carried out in order to investigate the relations between the physiographic-meteorological variables and the locally estimated 10-year, 50-year and 100-year skew surge quantiles (see Figure 4.2). WCS appears to be the most correlated variable to the skew surge quantiles. LON is another important variable, but both WCS and LON are also significantly correlated. The variables 100-MSLP, 100-WS and LAT seem to be quite important based on this simple correlation analysis, but to a lesser extent. The correlation between LAT and 100-MSLP appears also extremely high.

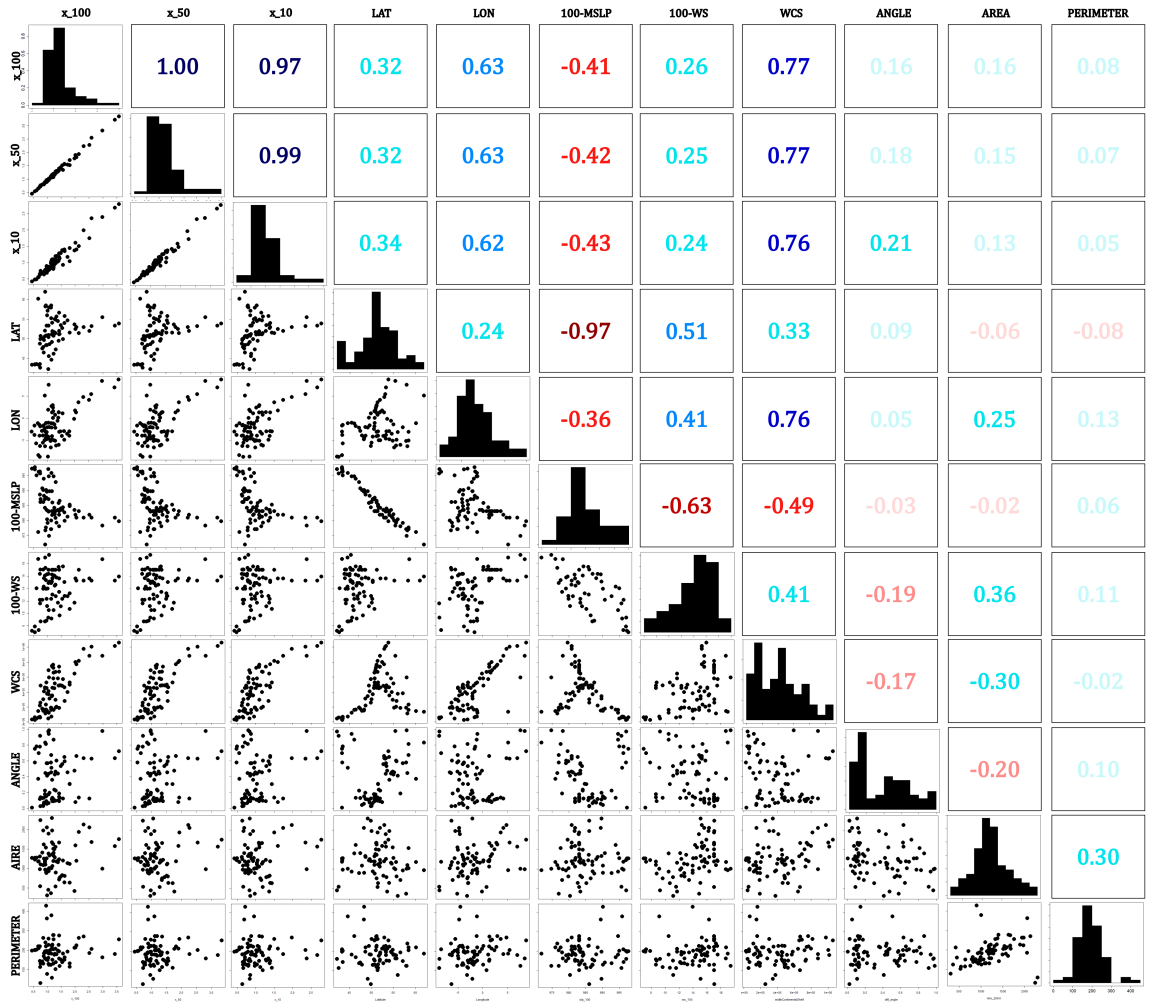

Figure 4.2 – Variable histograms, correlation coefficients and interrelations

For the explanatory physiographic-meteorological variables and the locally estimated 10,50,100-year skew surge quantiles.

4.1.2 Physiographic and meteorological variables for MLR and GAM

Figure 4.3 shows the physiographic and meteorological variables retained and their relative importance following the backward stepwise procedure (see Section 4.3.2) on all tide gauges for each specific skew surge quantile separately and for each estimation method MLR and GAM (see Section 4.2.2). The WCS largely appears as the most important explanatory variable whatever the quantile and the method. This is consistent with the computed correlation coefficients (see Figure 4.2). However, the addition of other retained variables helps improving the performances of estimation methods compared to an analysis based only on the WCS (see Table 10.1 in Supplementary Information). With a lower importance, the ANGLE is also selected for every model, but the correlation coefficient may not have allowed to anticipate this result. For MLR, with an almost insignificant importance, LON is selected for all quantiles and 100-MSLP and 100-WS are selected for x_{10}. Despite the strong correlation between the skew surges quantiles and the variables LON and 100-MSLP, their importance in the models is low or even null. This can be explained as LON and 100-MSLP are also highly correlated

with WCS which is systematically selected. Finally, LAT and PERIM are not retained by any model. As expected, for GAM, there are more variables involved than for MLR such as 100-WS, AREA and ANGLE.

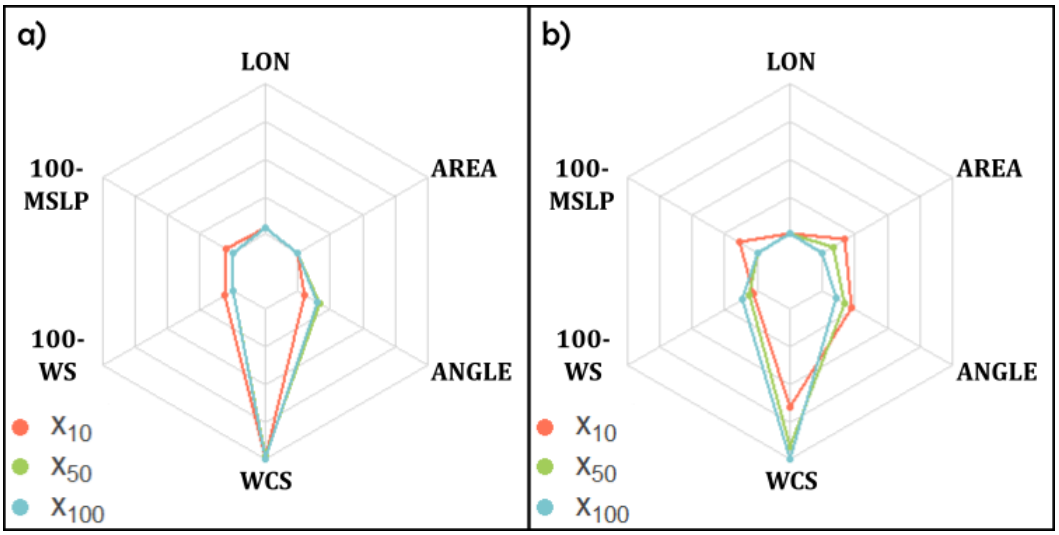

Figure 4.3 – Relative importance (%) of variables retained in a) MLR and b) GAM

LAT and PERIM are not represented because they were not retained by any model.

Figure 4.4 illustrates the smooth functions of the response variables as a function of the explanatory variables selected for x_{10} (see Figures 10.3 and 10.4 for x_{10} and x_{50} in the Supplementary Information). Smooth functions (see Section 4.2.2.2) allow to interpret the influence of each variable without the effect of the others. The variables WCS and ANGLE are the only ones presenting a linear relation, so their freedom degrees are equal to 1. The other physiographic and meteorological variables show nonlinear relations. The correlation coefficients (see Figure 4.2) explain the linear relation between WCS and skew surge quantiles (x_{10}, x_{50} and x_{100}) as well as the high freedom degrees of AREA for x_{50} and x_{100} (see Figures 10.3 and 10.4 in the Supplementary Information). For the other variables, the correlation coefficients are not sufficient to draw conclusions.

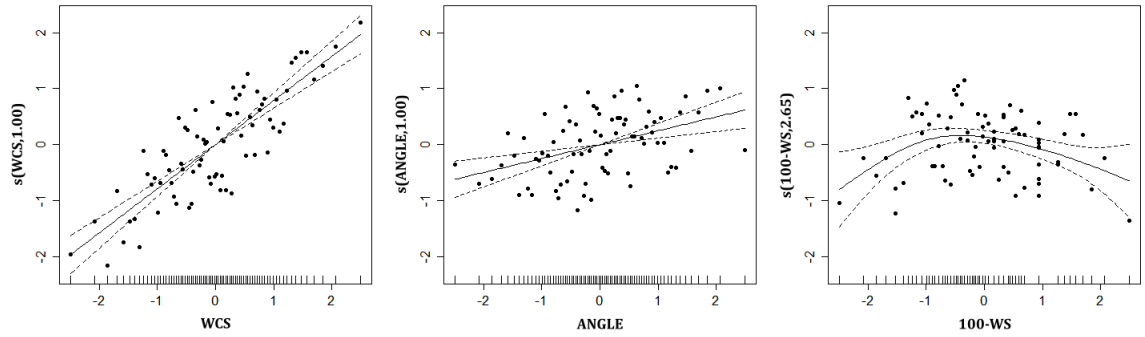

Figure 4.4 – Smooth functions of 100-year skew surge quantile x_{100} for the explanatory variables included in the regional model ALL + GAM (see Section 4.3.1). The dotted lines represent the 95% confidence intervals. The vertical axes are named s(var,edf), var is the name of the explanatory variable and edf is the estimated freedom degree of the smooth function.

4.1.3 Delineation of regions with HCA, ROI and CCA

The optimization procedure is implemented to find the weighted Euclidean distance function of the HCA method leading to the lowest RMSE for the 10-year skew surge quantile (see Section 4.3.1). The optimal distance functions obtained for MLR and GAM are respectively $d_{HCA/MLR}$ and $d_{HCA/GAM}$:

Equation 4.1

$$\mathrm{d_{HCA/MLR}} = \frac{3}{8}\mathrm{AREA} + \frac{2}{8}\mathrm{LON} + \frac{1}{8}\mathrm{LAT} + \frac{1}{8}\text{100-MSLP} + \frac{1}{8}\mathrm{PERIM}$$

Equation 4.2

$$\mathrm{d_{HCA/GAM}} = \frac{3}{8}\mathrm{ANGLE} + \frac{1}{8}\mathrm{LON} + \frac{1}{8}\text{100-WS} + \frac{1}{8}\text{100-MSLP} + \frac{1}{8}\mathrm{AREA} + \frac{1}{8}\mathrm{WCS}$$

The optimum distances are different from the geographic distance, computed as $d_{geog} = \frac{1}{2}\mathrm{LAT} + \frac{1}{2}\mathrm{LON}$, and lead to different fixed regions (see Figure 4.5). The clustering based on geographic distance leads to three regions : the green one covers the North-East of the study area, the blue one covers the UK with the exception of the South coast and the red one covers the South-West of the study area. With the MLR optimal distance, the green region remains the same, and the tide gauges of the red and blue regions are redistributed into two new regions keeping the Southwestern tide gauges in the same region. With the GAM optimal distance, only two regions are defined. If compared to the clustering based on geographical distances, with some exceptions, the red region is slightly shifted to the East but globally maintained, and the green and blue regions are combined into a single one.

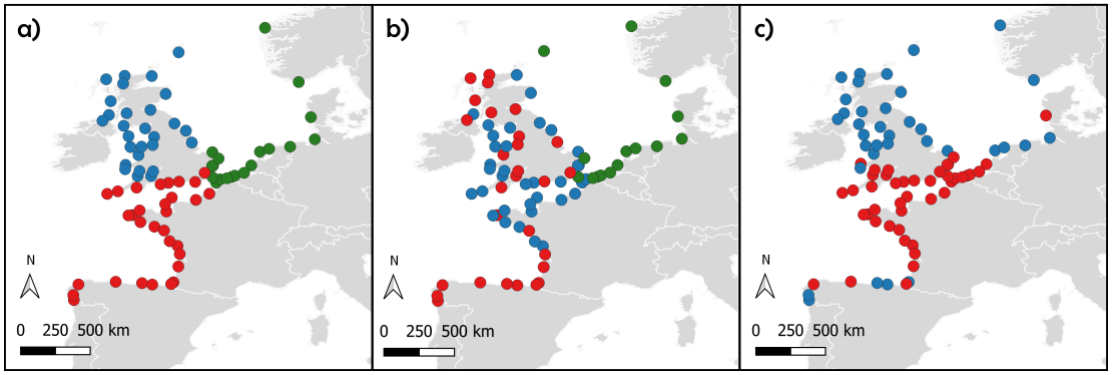

Figure 4.5 – Homogeneous regions formed through HCA with three different distances

a) d_{geog} **the geographic distance, b)** $d_{HCA/MLR}$ **the optimal distance obtained for MLR and c)** $d_{HCA/GAM}$ **the optimal distance obtained for GAM.**

For the ROI method, the optimization procedure provides the distance function and the threshold leading to the lowest RMSE for the 10-year skew surge quantile (see Section 4.3.1). The optimal thresholds obtained for MLR and GAM are such that the optimal neighborhood should contain 50% of the tide gauges of the whole dataset. The optimal distance functions obtained for MLR and GAM are respectively $d_{ROI/MLR}$ and $d_{ROI/GAM}$:

Equation 4.3

$$\mathrm{d_{ROI/MLR}} = \frac{6}{8}\mathrm{WCS} + \frac{1}{8}\mathrm{LAT} + \frac{1}{8}\mathrm{100\text{-}MSLP}$$

Equation 4.4

$$\mathrm{d_{ROI/GAM}} = \frac{2}{8}\mathrm{LAT} + \frac{2}{8}\mathrm{AREA} + \frac{1}{8}\mathrm{100\text{-}MSLP} + \frac{1}{8}\mathrm{WCS} + \frac{1}{8}\mathrm{ANGLE} + \frac{1}{8}\mathrm{PERIM}$$

In the case of CCA, the optimization procedure leads to the identification of the confidence level α and the selection of the most relevant physiographic and meteorological variables for the 10-year skew surge quantile (see Section 4.3.1). The optimal value of the confidence level obtained is $\alpha = 0.03$. The variables retained are LAT, LON, 100-MSLP and PERIM for MLR and LAT, LON, 100-WS and WCS for GAM. It is interesting to notice that the combination of LAT and LON with other variables is pertinent to form homogeneous regions with CCA, but not with HCA and ROI.

The sites included in the region of influence are geographically close to the target site for the model ROI+MLR, but a little bit more dispersed for the ROI+GAM model (see Figure 10.8 in the Supplementary Information). The regions obtained with CCA are large especially for MLR (see Figure 10.9 in the Supplementary Information). Whether for HCA, ROI or CCA, the physiographic and meteorological variables retained to delineate the homogeneous regions

are not necessarily the same as the variables used for the estimation methods MLR and GAM. For instance, the variable WCS is systematically retained for the estimation step but not for the delineation step.

4.1.4 Comparison of the regional models

The results of the jackknife procedure (see Section 4.3.3) for all regional models are presented in Figure 4.6 hereafter and in Figures 10.5, 10.6 and 10.7 in the Supplementary Information. The best overall performances are obtained with ROI + GAM according to the highest NASH values (more than 0.80) and the lowest RMSE and rRMSE values. More precisely, GAM outperforms MLR for combinations using the same delineation approach (ALL, CCA, HCA or ROI). For instance, the NASH criterion is systematically close to 0.80 or even larger for x_{10} which is the quantile for which the methods are optimized. This may be explained by the ability of GAM to consider the possible nonlinear relations between physiographic-meteorological variables and the skew surge quantiles, and by the impact of the new variables included in GAM compared to MLR. ROI appears to be the most efficient regional delineation approach, this is consistent with the conclusion of several previous works on flood quantiles (Ouarda et al., 2018 ; Msilini et al., 2022) and on low-flows (Ouarda et al., 2018).

According to the NASH, RMSE and rRMSE criteria, ALL (all tide gauges without delineation of homogeneous regions) and CCA appear equivalent for combinations using the same estimation method (MLR or GAM). Moreover, the models based on CCA have larger biases. In a number of hydrological studies (Ouarda et al., 2018 ; Ouarda et al., 2001 ; Han et al., 2020), the use of CCA to delineate homogeneous regions improves the estimations in comparison with the ALL approach (when there is no delineation step). In these previously quoted studies, there are at least 106 sites in the whole dataset, in contrast with the 78 sites of the present study. CCA is more complex than the other approaches (HCA and ROI) and requires rich data sets to be implemented properly, but here some tide gauge situations may not be well represented because of the limited number of sites. Even the fixed regions approach (HCA) shows better results than CCA and in particular for x_{10}.

As expected, for each regional model, all the criteria, except the rBias, are the best for x_{10} and deteriorate for x_{50} and x_{100}, because the delineations of homogeneous regions are optimized for x_{10}. Generally, the bias (both Bias and rBias) is low compared to the error (RMSE and rRMSE). The relation between the criteria and the physiographic-meteorological variables was investigated. However, it was not possible to conclude about any similar characteristic for the tide gauges for which the skew surge quantiles are under-estimated.

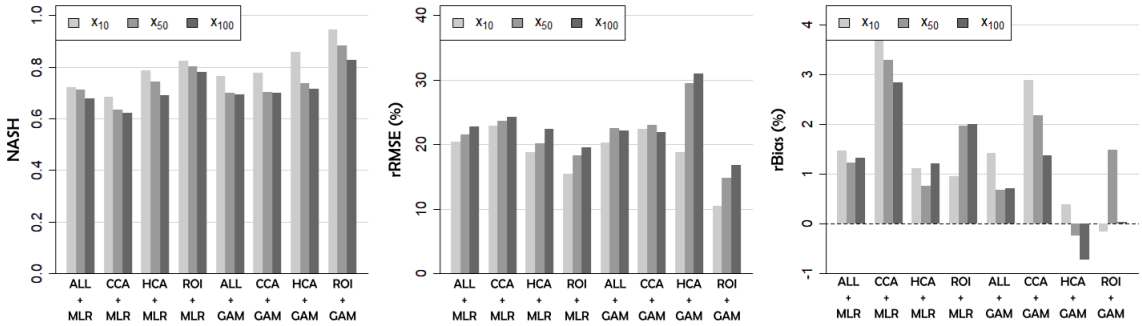

Figure 4.6 – NASH, RMSE, rRMSE, Bias and rBias
The criteria of the optimized regional models depending on the skew surge quantiles.

4.1.5 Conclusion

The purpose of the present study is to identify explanatory physiographic and meteorological variables of the skew surge quantiles and then to develop regional frequency analysis models for the estimation of skew surge quantiles at ungauged locations. Two estimation methods (multiple linear regression and general additive model) are implemented within homogeneous regions delineated by using three different methods (hierarchical clustering analysis, region of influence approach and canonical correlation analysis) and also to all tide gauges without the delineation of homogeneous regions. The comparison of these regional models is based on 78 European tide gauges.

Some variables, namely WCS, 100-WS, 100-MLSP and ANGLE, appear particularly important for the determination of skew surge quantiles in the considered area. LAT and LON are also useful especially for the delineation step. AREA and PERIM appear negligible, suggesting that either the coastline morphology may not have an important impact on the skew surge quantiles or that AREA and PERIM may not be the relevant variables to describe the coastline morphology for the case study. As expected, regional estimations are more efficient with the GAM than with the MLR estimation method. The delineation of homogeneous regions conducted with the CCA approach does not provide satisfactory results in this case study, probably because the sample of tide gauges used is too limited. Methods with the distances based on physiographic and meteorological variables (HCA and ROI) have better performances than CCA, especially ROI providing an estimated homogeneous region adapted to each target site. In general, the combination of the methods GAM and ROI provides the best overall results.

This is the first application, on skew surges, of the regional frequency analysis involving external explanatory variables such as physiographic and meteorological characteristics. Further efforts will be required to consolidate these results, but this study opens a wide and promising research field. Some physiographic and meteorological variables are identified, and could be specified in future works. To improve the explanatory power of the covariates, it could be useful to combine them, by summing them for example. Other variables for the description of the coastline morphology should be probably tested instead of AREA and PERIM. The

results of this study could be improved by applying other statistical techniques, already used in other fields. The existing literature provides a large range of possibilities like kriging approaches (Chokmani et al., 2004 ; Ouarda et al., 2008 ; Yin et al., 2018 ; Das et al., 2020). The paradigm could be changed by regionalizing the parameters of the skew surge distribution instead of the quantiles. This would ensure a consistency between the quantiles estimated for various return periods. Regionalizing the quantiles, as it is carried out in this work, does not guarantee that the quantiles increase with the return period, because the values are estimated independently for each return period (Ahn et al., 2016 ; Haddad et al., 2012). However, the dependency between the distribution parameters, should absolutely be considered, to obtain consistent results. This is a particularly challenging task. Likewise, the index method already implemented for the estimation of skew surge distributions could be improved if combined with the delineation of homogeneous regions based on the physiographic and meteorological variables. It is important to notice that the regionalization of the parameters of the distribution was found to be problematic in some cases. For instance, the estimation of the shape parameter of the GEV distribution with the parameter regression model can be unstable, leading to erroneous estimations of extreme quantiles (Odry et al., 2017).

Future efforts can also focus on the development of models especially destined for partially gauged locations, with a limited amount of information that is not sufficient to carry out a local frequency analysis. This situation is quite frequent as it is common to install a tidal gauge at a location where a project is planned, leading to the availability of a short series of observations. CCA is especially adapted for this purpose as it can directly integrate any observations at the target site in the estimation of the canonical variables. It would also be relevant to develop regional estimation approaches that are capable of integrating available historical information along with regional systematic skew surge observations (Saint Criq et al., 2022a). The use of valuable historical information should lead to significant improvements in the estimation of skew surges at partially gauged and ungauged locations.

4.2 Methods

4.2.1 Delineation of homogeneous regions

4.2.1.1 Hierarchical cluster analysis (HCA)

Hierarchical cluster analysis consists in delineating fixed homogeneous regions according to the local physiographic-meteorological variables of the sites (Ouarda et al., 2008). It is necessary to select the most relevant physiographic-meteorological variables and the distance function to compute the similarity between each pair of sites. In HCA, stations are grouped into a binary hierarchical cluster tree. Each station is initially assigned to its own singleton cluster by using a linkage function which is based on the distance information. In an iterative way, the two most similar clusters are joined into a new one until there is only one overall cluster. The result can be represented in a dendrogram.

4.2.1.2 Region of influence (ROI)

The identification of the sites to be included in the ROI of a target site is based on the similitude of sites with the target site according to their local attributes (Burn, 1990b). The site i is included in the ROI of the target site t if $D_{it} \leq \theta_t$, with θ_t the threshold and D_{it} the distance between the sites i and t. The value of θ_t should be set such that there is a good compromise between the number of sites in the ROI and the homogeneity of the selected sites. A large θ_t increases the number of sites included in the ROI and decreases the homogeneity. Conversely, a smaller θ_t increases the homogeneity, but the transferred information is decreased due to the small number of stations.

4.2.1.3 Canonical correlation analysis (CCA)

The canonical correlation analysis is a statistical multivariate method which allows to describe a linear relationship between two sets of random variables observed on the same subjects (Muirhead, 1982). Let X and Y be two sets of random variables $X = \{X_1, X_2, ..., X_n\}$ and $Y = \{Y_1, Y_2, ..., Y_r\}$ with $n \leq r$. X can contain the physiographic-meteorological variables and Y the skew surge quantiles. All variables should be standardized and transformed for normality. We consider the linear combinations

Equation 4.5

$$V_i = a_i' X \text{ and } W_i = b_i' Y$$

where a_i' **and** b_i' **are transposes of vector** a **and** b **respectively**

C is the covariance matrix of X and Y :

Equation 4.6

$$C = \begin{pmatrix} C_{XX} & C_{XY} \\ C_{XY}' & C_{YY} \end{pmatrix}$$

The correlation coefficient between V_i and W_i is :

Equation 4.7

$$\rho_i = \frac{a_i' C b_i}{\sqrt{a_i' C_{XX} a_i b_i' C_{YY} b_i}}$$

The objective of CCA is to find the vectors a_i et b_i maximizing ρ_i subject to the constraint that V_i and W_i must have unit variance. Once the first pair of canonical variables (V_1, W_1) is obtained, other pairs of canonical variables can be obtained in the uncorrelated directions under the constraints of unit variance and maximum correlation between pairs of canonical

variables. If p is the rank of the matrix C_{XY}, $a*$ and $b*$ can be identified such that the correlation coefficients $\lambda_i = corr(V_i, W_i)$, $i = 1, ..., p$ are maximized. It has been proven that the solutions $a*$ et $b*$ are eigenvectors of $C_{XX}^{-1} C_{XY} C_{YY}^{-1} C'_{XY}$ and $C_{YY}^{-1} C'_{XY} C_{XX}^{-1} C_{XY}$ respectively. The results are p triplets solutions (λ_i, a_i, b_i). $V_1, V_2, ..., V_p$ and $W_1, W_2, ..., W_p$ are the canonical variables and $\lambda_1, \lambda_2, ..., \lambda_p$ are the canonical correlation coefficients.

The CCA can be used for the delineation of homogeneous regions around a target site (Ouarda et al., 2001). The physio-meteorological canonical score v_0 is known and the canonical score w_0 is unknown for the target site. The approximation of w_0 can be obtained with a $100(1-\alpha)\%$ confidence interval, through Λv_0, $\Lambda = \text{diag}(\lambda_1, ..., \lambda_p)$. The distances to the mean position Λv_0 in the canonical space are given by :

Equation 4.8

$$D^2 = (W - \Lambda v_0)'(I_p - \Lambda\Lambda)^{-1}(W - \Lambda v_0)$$

where I_p **is the** $p \times p$ **identity matrix**

D^2 is a Mahalanobis distance and follows a Chi squared distribution with p degrees of freedom. The neighborhood of the target site can be defined selecting the sites such as their realisations w are close to the mean position Λv_0 of the target site, in other words, such as $D^2 \leq \chi^2_{\alpha,p}$, with α the confidence level.

4.2.2 Regional estimation methods

4.2.2.1 Multiple linear regression (MLR)

In the multiple linear regression, the relation between the random variables $X = \{X_1, X_2, ..., X_n\}$ and $Y = \{Y_1, Y_2, ..., Y_r\}$ is described by the following model :

Equation 4.9

$$Y = \beta_0 X_1^{\beta_1} X_2^{\beta_2} ... X_n^{\beta_n} \epsilon$$

where $\beta_0, \beta_1, ..., \beta_n$ **are the model parameters**
ϵ **the error term which is assumed to be normally distributed**

The previous equation is generally linearized with a logarithmic transformation :

Equation 4.10

$$\log(Y) = \log(\beta_0) + \beta_1 \log(X_1) + \beta_2 \log(X_2) + ... + \beta_n \log(X_n) + \log(\epsilon)$$

But, the logarithmic transformation introduces a bias (Girard et al., 2004) :

Equation 4.11

$$\mathbf{E}[Y] = \mathbf{E}[\exp(\log Y)] \neq \exp[\mathbf{E}(\log Y)]$$

4.2.2.2 Generalized Additive Model (GAM)

The Generalized Linear Model (GLM) is a generalization of the MLR and is defined by :

Equation 4.12

$$g(Y) = \beta_0 + \sum_{j=1}^{r} \beta_j X_j + \epsilon$$

where g **is a link function**
β_j **are unknown parameters**
ϵ **is the error term**

The Generalized Additive Model (Hastie et al. (1986)) is an extension of the GLM but more flexible because the linear predictor is replaced by a set of smooth functions. It is defined by :

Equation 4.13

$$g(Y) = \beta_0 + \sum_{j=1}^{r} f_j(X_j) + \epsilon$$

where f_j **are smooth functions of** X_j

The smooth functions are represented by splines which are piecewise polynomial functions joined together at a set of points called knots. In general, a smooth function can be represented by a linear combination of basis functions :

Equation 4.14

$$f_j(x) = \sum_{i=1}^{q_j} \beta_{ij} b_{ij}(x)$$

where $b_{ij}(x_j)$ **is the** i^{th} **basis function of the** j^{th} **explanatory variable evaluated at** x_i
q_j **is the number of basis functions for the** j^{th} **explanatory variable**
β_{ij} **are unknown parameters**

To avoid overfitting, the estimator $\hat{\beta}$ of β is obtained by maximizing the penalized log-likelihood :

Equation 4.15

$$l_p(\beta) = l(\beta) - \frac{1}{2}\sum_{j=1}^{m} \lambda_j \beta^T S_j \beta$$

where λ_j **is the smoothing parameter of the** j^{th} **smooth function** f_j **and it controls the smoothness degree of the curve** f_j
S_j **is a matrix with known coefficients**

4.3 Methodology

4.3.1 Regional models

The methods for the delineation of homogeneous regions (HCA, CCA and ROI, see Section 4.2.1) are used in conjunction with the regional estimation methods (MLR and GAM, see Section 4.2.2). The regional estimation methods are also tested considering all tide gauges (ALL) to evaluate the added value of the delineation of homogeneous regions. This results in eight regional models denoted by ALL + MLR, ALL + GAM, CCA + MLR, CCA + GAM, HCA + MLR, HCA + GAM, ROI + MLR and ROI + GAM. A backward stepwise regression method (see Section 4.3.2), applied to all stations (ALL), is used to select the optimal explanatory variables to be used with the estimation methods MLR and GAM for the skew surge quantiles x_{10}, x_{50} and x_{100}. In this study, the R package *mgcv* (Wood, 2017) is used to estimate the MLR and GAM parameters.

For the implementation of HCA, the Ward's hierarchical clustering algorithm (Ward, 1963) is commonly chosen for the linkage function and it consists in : i) initially assigning each site to its own region and (ii) merging the closest pair of regions until there is only one region. The optimal number of homogeneous regions is computed by the Mojena's stopping rule (Mojena, 1977) which consists in getting the level in the hierarchy implying a significant jump in the dendrogram heights, indicative of the merging of two dissimilar clusters. The weighted Euclidean distance is chosen as the distance function to measure similarity between two sites :

Equation 4.16

$$D_{ij} = \sqrt{\sum_{k=1}^{p} W_k \left(X_{k,i} - X_{k,j}\right)^2}$$

where p **is the number of attributes considered**
$X_{k,i}$ **and** $X_{k,j}$ **are the values of the** k^{th} **attribute at sites** i **and** j **respectively**
W_k **is the weight applied to the** k^{th} **attribute**

The values of attributes are standardized to avoid some possible bias. Each $W_{k,k\in\{1,\ldots,p\}}$ can take any value within $\{0, \frac{1}{p}, \frac{2}{p}, \ldots 1\}$ such as $\sum_{k=1}^{p} W_k = 1$. A standard jackknife procedure (see

Section 4.3.3), applied for each estimation method MLR and GAM, is used to find the optimal weights $W_{k,k\in\{1,...,p\}}$.

The implementation of ROI requires setting the threshold θ_t such that the distance of the target site to the other sites to be included in the region of influence of the target site is lower than this threshold. Some values for θ_t are tested such that each region centered on the target site contains 25%, 30%, 35%, 40%, 45%, 50%, 55%, 60%, 70% or 75% of the tide gauges from the whole dataset. As for HCA, the weighted Euclidean distance is chosen. Then, the distance and threshold are jointly optimized with a standard jackknife procedure (see Section 4.3.3) for each estimation method MLR and GAM.

To apply CCA, the most relevant physiographic and meteorological variables need to be selected, as well as the confidence level α. All the possible combinations of physiographic and meteorological variables with different values of α within {0,0.01,...,0.40} are jointly tested with a standard jackknife procedure (see Section 4.3.2) for each estimation method MLR and GAM. CCA requires normality of the variables which is computed with the R package *bestNormalize* (Peterson, 2021 ; Peterson et al., 2020) before conducting the analysis.

The various features of the delineation methods (the weighted Euclidean distance for HCA, the weighted Euclidean distance and the threshold for ROI, and the relevant variables and the confidence level for CCA) are optimized for the 10-year quantile. The quantile x_{10}, corresponds to the lowest return period and can hence be considered as the most reliable quantile. The features optimized for x_{10}, are also used for the other quantiles x_{50} and x_{100}. The same physiographic and meteorological variables are used for both delineation and estimation steps.

4.3.2 Stepwise regression

A backward stepwise selection procedure (Msilini et al., 2022 ; Marra et al., 2011) is carried out to ensure an objective selection of the explanatory variables for each quantile (x_{10}, x_{50} and x_{100}) and for each estimation method (MLR and GAM). It starts with an initial model including all available explanatory variables. At each step, the estimation method is applied with the current model and the variable with the highest p-value (for the null hypothesis of the MLR parameter or the GAM smooth terms) is excluded. The procedure ends when the p-values of the remaining variables are under a given threshold (5%).

4.3.3 Validation

A jackknife procedure (also called leave one-out cross validation procedure) is employed to assess the performance of each regional model. It consists in considering, in turn, each gauged tide gauge as an ungauged one in order to carry out regional estimation using data from the remaining tide gauges. The regional estimates can be compared to the observed values and the performances of the regional models can be evaluated with the following five criteria : the Nash criterion (NASH), the root mean squared error (RMSE), the relative RMSE (rRMSE), the mean bias (BIAS) and the relative BIAS (rBIAS). The NASH gives a general assessment of the prediction quality, the RMSE and the rRMSE provide information about the absolute

and relative accuracy of the predictors, BIAS and rBIAS measure the absolute and relative magnitude of overestimation or underestimation of a model.

4.4 Data acquisition

4.4.1 Skew surge variables

The hourly tide gauge recordings are provided by the British Oceanographic Data Centre (bodc.ac.uk), the Flemish Agency for Maritime and Coastal Services (meetnetvlaamsebanken.be), the French Hydrographical and Oceanographical Service (data.shom.fr), the Global Extreme Sea Level Analysis project (gesla787883612.wordpress.com), the Ministery of Infrastructure and Water Management of the Netherlands (rijkswaterstaat.nl) and the Spanish Institute of Oceanography (ieo.es).

The hourly recorded sea levels are processed with a harmonic analysis through the R package *TideHarmonics* (Stephenson, 2015). Tidal predictions are calculated for the present time, then the data must be corrected from a possible eustatism to obtain the actual surges of past periods. Once the hourly astronomical tidal levels are computed, the series of astronomical high tides and skew surges can be extracted. The POT threshold u is selected according to the GP parameter stability criterion (Coles, 2001) and allows to build the POT samples. Then, a GP distribution is adjusted on each local POT sample through the maximum likelihood to estimate the local quantiles x_{10}, x_{50} and x_{100} corresponding to return periods of 10, 50 and 100 years. Descriptive characteristics of the obtained quantiles are summarized in Table 10.1 in the Supplementary Information.

4.4.2 Physiographic and meteorological variables

The NOAA CIRES DOE 20CRv3 reanalysis (`psl.noaa.gov/data/gridded/data.20thC_ReanV3.monolevel.html`) provides meteorological variables from 1836 to 2015 with 3-hourly values over a 1° latitude x 1° longitude global grid (360x181). From these reanalyses, the u and v wind components at 10m (to compute the wind speed and direction) and the mean sea level pressure are downloaded in the form of "Ensemble Mean" - i.e. the mean result of the 80 models used in the reanalysis. From each tide gauge, the meteorological variables are retrieved at the closest point on the grid. Then, the empirical 100-year quantiles of the mean sea level pressure (100-MSLP), the wind speed (100-WS) and the prevailing wind direction can be extracted. ETOPO (`ngdc.noaa.gov/mgg/global`) provides the bathymetric data all around the world with a spatial resolution of 1 arc-minute. The width of the continental shelf (WCS) is estimated as the shortest distance between the tide gauge and the continental slope, defined as the 1000-m isobath (Calafat et al., 2020). The R package *marmap* (Pante et al., 2013) allows to extract the width (WCS) and the direction of the continental shelf.

Chapitre 5

Article 4

Titre original : "Historical information in a Hierarchical Bayesian Analysis for extreme skew surge estimation"

Titre en français : "Informations historique et régionale pour l'estimation des surcotes de pleine mer extrêmes"

Laurie Saint Criq[1,2] (L.S.C.), Taha B.M.J. Ouarda[2] (T.B.M.J.O.), Eric Gaume[3] (E.G.), Yasser Hamdi[1] (Y.H.)

[1]Institut de Radioprotection et de Sûreté Nucléaire, Fontenay-aux-Roses, France

[2]Institut National de la Recherche Scientifique, Quebec City, QC, Canada

[3]Université Gustave Eiffel, Champs-sur-Marne, France

Cet article est prêt à être soumis.

Pour ce quatrième travail, la conception a été pensée par L.S.C, E.G, Y.H et T.B.M.J.O., la méthodologie a été développée par L.S.C, E.G et T.B.M.J.O., la partie programmation informatique incluant la préparation des données a été réalisée par L.S.C., les résultats ont été analysés par L.S.C., E.G et T.B.M.J.O., la première version de l'article a été préliminairement rédigée par L.S.C. qui a ensuite été révisée par T.B.M.J.O., E.G. et Y.H.. Ce travail a été encadré par T.B.M.J.O., E.G. et Y.H.. Tous les auteur.e.s ont approuvé la version prête à soumettre de l'article.

Le troisième article a permis d'identifier des variables physiographiques et météorologiques explicatives des quantiles de surcotes de pleine mer telles que la largeur du plateau continental, le quantile centennal de la vitesse du vent, le quantile de la pression moyenne basse au niveau de la mer, et l'angle entre la direction du vent dominant et la direction du plateau continental. Pour estimer les quantiles de surcotes de pleine mer à des sites non jaugés, des modèles régionaux basés sur ces co-variables ont été testés sur une base de données de 78 marégraphes. Chaque modèle régional est la combinaison d'une méthode pour la formation de régions homogènes (HCA, ROI et CCA) et d'une méthode pour l'estimation régionale (MLR et GAM). Cet article a montré l'utilité de l'analyse régionale fréquentielle basée sur des variables explicatives pour l'estimation des surcotes de pleine mer à des sites non jaugés.

Les résultats de ce troisième article sont prometteurs et ouvrent de nouvelles pistes de recherche pour l'utilisation de l'information régionale. La méthode de l'indice pourrait être combinée à une méthode de formation des régions avec les variables physiographiques et météorologiques identifiées. Ces caractéristiques locales pourraient aussi être utilisées pour régionaliser les paramètres des distributions des surcotes de pleine mer dans un cadre Bayésien. Ces nouvelles questions sont abordées dans ce quatrième article. Finalement, pour répondre au dernier objectif de la thèse, cet article propose une approche pour utiliser simultanément l'information locale, historique et régionale.

Abstract

Coastal floodings affect people around the world. Coastal management and planning with the necessary flooding protection measures are hence essential and require accurate estimations of extreme sea levels. This usually relies on fitting a probability distribution to extreme skew surges. Available data series are often short and characterized by the presence of gaps, and are therefore not informative enough on extreme events. They can be enriched by historical information (observations before the beginning of the tide gauge recordings) and/or regional information (data available at other sites). In this paper, two methods for integrating regional information are used : the index method combined with the region of influence approach based on the physiographic and meteorological variables of the sites, and the hierarchical Bayesian analysis. A new approach based on the latter method is developed to combine regional information with the local historical extreme sea levels. The analyses are conducted on a database composed of 78 tide gauges along the European coasts. Results show that the index method tends to underrate the estimation uncertainties. The hierachical Bayesian analyses provide accurate estimates, especially when the two types of information - regional and historical - are combined.

5.1 Introduction

Extreme sea levels directly affect population in coastal areas, while also having important ecological and economic impacts (Hinkel et al., 2014). Then, coastal infrastructure planning needs the estimation of extreme sea levels, and especially those occurring at high tide (maximum sea levels) which are the most likely to cause the worst damages. A maximum sea level can be defined as the combination of the predicted astronomical high tide and of the skew surge. The skew surge is the difference between the maximum observed sea level and the predicted astronomical high tide within a tidal cycle (Vries et al., 1995). The astronomical high tide is a deterministic component of the sea levels, while the skew surge is a meteorological and stochastic component. Then, the extreme sea levels are usually obtained after estimating a statistical distribution for the extreme skew surges (Batstone et al., 2013 ; Andreewsky et al., 2014 ; Mazas et al., 2014 ; Kergadallan et al., 2014 ; Hamdi et al., 2014).

The recorded tide gauge series are rarely informative enough to provide reliable extreme skew surge quantile estimates and this leads to large estimation uncertainties. Historical or regional additional information is frequently integrated in the statistical analysis to reduce the estimation uncertainties. The historical extension consists in integrating historical information, extreme events observed before the beginning of the tide gauge recordings (Bulteau et al., 2015 ; Hamdi et al., 2015 ; Frau et al., 2018 ; Hamdi, 2019 ; Saint Criq et al., 2022a ; Saint Criq et al., 2022b). The regional extension consists in valuating the available information at gauged sites belonging to the region of the target site and considered as statistically consistent (Van Gelder et al., 1998 ; Mai Van et al., 2007 ; Bernardara et al., 2011 ; Bardet et al., 2011 ; Weiss et al., 2012 ; Weiss et al., 2013a ; Frau et al., 2018 ; Hamdi et al., 2019 ; Andreevsky et al., 2020). Only two approaches have been published to combine both types

of information to estimate skew surges quantiles (Frau et al., 2018 ; Hamdi et al., 2019). The first consists in performing a regional analysis on the local series supplemented with historical information at the sites where this information is available. The latter consists in performing a historical analysis on a local series for which the gap measurements are supplemented with regional information through multiple linear regressions.

A very common approach for the integration of regional information is the regional frequency analysis (RFA) (Hosking et al., 1997) generally composed of two main steps : the delineation of homogeneous regions and the regional estimation. The RFA based on the index method (Dalrymple, 1960) assumes that sites belonging to a statistically homogeneous region have the same regional distribution except for a scaling factor, the local index. In coastal analysis, several studies (Weiss et al., 2012 ; Weiss et al., 2013b ; Hamdi et al., 2019 ; Andreevsky et al., 2020) use the inter-sites dependences of the extreme skew surges to delineate the regions. It consists in grouping sites having similar behaviours for the extreme skew surges in a same region. It is based on the pairwise probability that, in a given time interval (typically 24h), two sites have an extreme skew surge if one of them has one. The regions can then be fixed or centered around a target site. The main drawback of this approach is the requirement of long enough data series, which rarely occurs in practice. The approaches for delineating homogeneous regions can also be based on the proximity of the physiographic and meteorological characteristics between sites like the hierarchical cluster analysis (HCA), the canonical correlation analysis (CCA) or the region of influence (ROI) (Ouarda, 2016). These three approaches were recently applied to the skew surge quantiles and the ROI appeared to have the best performances (Saint Criq et al. (2022c)).

The Bayesian framework, thanks to the flexibility of the likelihood, is particularly suitable to integrate regional information. For example, Seidou et al. (2006) integrated with the local observations, the prior distributions obtained with a regional log linear regression model on a quantile and two quantile differences. Another approach for the spatial extension is the Hierarchical Bayesian Analysis (HBA) (Gelman et al., 2014). The HBA consists in simultaneously modelling the joint distribution with unknown parameters and modelling these parameters with spatial physiographic and meteorological information through regression models. The HBA has some noteworthy features compared to the index method. Indeed, the statistical homogeneity of the regions is not required, nor is the restrictive assumption of scale invariance. Moreover, the statistical inference proceeds in one step, without separating the inference process in several steps. This allows to simultaneously deal with the uncertainties. The HBA was applied to natural hazards such as precipitations (Cooley et al., 2007 ; Renard, 2011 ; Sharkey et al., 2019 ; Love et al., 2020), stream flows (Reza Najafi et al., 2013 ; Lima et al., 2016) or wave heights (Clancy et al., 2016). The HBA has been recently applied for the first time to extreme sea levels, particularly to extreme storm surges (Calafat et al., 2020), capturing the spatial dependence via a max-stable process.

This paper has two main purposes : i) implement the HBA on the skew surges to integrate regional information and compare its performances with those of the index method because it is the main regional estimation method used for the marine submersion hazard, and ii) propose

a method for combining the local, historical and regional information on skew surges, building on the historical approach developed by Saint Criq et al. (2022a) and Saint Criq et al. (2022b). The models are explained in Section 5.2. The analyses are conducted on 78 European tide gauges (see Section 5.3.2) and the results are illustrated and discussed in Section 5.4.

5.2 Models

5.2.1 Local analysis

At site j, a peaks-over-threshold (POT) sample of skew surges exceeding a threshold u_j during the recording period of w_j years is commonly modelled by a General Pareto (GP) distribution, with scale parameter $\sigma_j > 0$ and shape parameter $\xi_j \in R$, and n_j the number exceedances per year follows a Poisson process of intensity λ_j (Coles, 2001 ; Batstone et al., 2013). The GP cumulative distribution function F_{θ_j} is given by :

Equation 5.1

$$\forall\ x^j > u_j,\ F_{\theta_j}(x^j) = \begin{cases} 1 - \left[1 + \xi(\frac{x^j - u}{\sigma})\right]^{-\frac{1}{\xi_j}} & \text{if } \xi_j \neq 0, \\ 1 - \exp(\frac{x^j - u_j}{\sigma_j}) & \text{if } \xi_j = 0. \end{cases}$$

The likelihood of the recorded skew surges $x^j = \{x_1^j, x_2^j, ..., x_n^j\}$ independent and identically distributed can be written as :

Equation 5.2

$$L(X^j|\theta_j) = \prod_{i=1}^{n_j} f_{\theta_j}(x_i^j)$$

where f_{θ_j} **is the GP probability density function**
$\theta_j = (\sigma_j, \xi_j)$ **are the parameters to estimate**

In this study, the Poisson process intensity λ_j (average number of skew surges exceeding the threshold u per year) is chosen not to be estimated, so the likelihood does not include the probability of observing n_j skew surges exceeding the threshold u_j during a period of duration w_j years. Indeed, in this study, the POT threshold u_j is chosen such that λ_j is equal to 1 (see Section 5.3.2.1) for a trade-off between bias and variance for the index method (Bernardara et al., 2011 ; Weiss et al., 2014a ; Weiss et al., 2014b) and it allows to simplify the more complex following models.

5.2.2 Regional analysis

5.2.2.1 Index method

The index method (Dalrymple, 1960) assumes that observations at various sites of a statistically homogeneous region are identically distributed except for a local scaling factor : the local index. The index method was originally developed for the annual maxima series following a Generalized Extreme Value distribution and then extended to the POT series following a GP distribution (Madsen et al., 1997 ; Ribatet et al., 2007). The S local series of an homogeneous region are standardized by the local index chosen as the POT threshold and are pooled in a same regional sample $X_R = \{X^1/u_1, X^2/u_2, ..., X^S/u_S\}$. Then, the regional series X_R is supposed to follow a GP distribution of regional shape parameter ξ_R constant over the homogeneous region and regional scale parameter σ_R satisfying $\sigma_R = \sigma_j/u_j \ \forall j \in \{1, ..., S\}$. The likelihood of the regional sample X_R is given by :

Equation 5.3

$$L(X_R|\theta_R) = \prod_{j=1}^{S} \prod_{i=1}^{n_j} f_{\theta_R}\left(\frac{x_i^j}{u_j}\right)$$

where f_{θ_R} **is the regional GP probability density function**
$\theta_R = (\sigma_R, \xi_R)$ **are the regional parameters to be estimated**

The total regional period is $w_R = w_1 + w_2 + ... + w_S$. The likelihood definition 5.3 implies that x_i^j and $x_{i'}^{j'}$ are independent $\forall i \in \{1, ..n_j\}$, $\forall i' \in \{1, ..n_{j'}\}$ for any j and j'. This independence of the regional observations is rarely observed since a same storm can frequently impact several sites. Keeping all the observations and not accounting for the possible inter-dependences should not introduce any bias, but could lead to an underestimation of the estimation uncertainties (Stedinger, 1983 ; Hosking et al., 1988). To overcome this difficulty, it is common to only keep the maximum value among the dependent observations (Bernardara et al., 2011 ; Weiss et al., 2014a ; Weiss et al., 2014b ; Andreevsky et al., 2020). With Monte Carlo simulations based on six case studies, we showed that this could overestimate the quantiles (see Appendix 11.2). In this study, for the sake of simplicity, all the dependent observations are chosen to be kept even if this would generate the underestimation of the estimation uncertainties (confirmed by Monte Carlo simulations, see Appendix 11.2). However, the inter-dependencies should ideally be modelled.

5.2.2.2 Delineation of homogeneous regions : Region of influence

The region of influence (ROI) approach allows the delineation of physiographically and meteorologically homogeneous regions centered on a target site (Ouarda, 2016). The identification of the sites to be included in the ROI of a target site is based on the proximity of the target site with the other sites according to their local attributes (Burn, 1990b). The similarity measure between sites t and v is chosen as the weighted Euclidean distance (see Equation 5.3). The site v is included in the ROI of the target site t if $d_{tv} \leq \theta_t$, with θ_t set such that there is a

good compromise between the number of sites in the ROI and the homogeneity of the selected sites composing the ROI. A large θ_t increases the number of sites included in the ROI and decreases the homogeneity, and vice versa.

Equation 5.4

$$d_{tv} = \sqrt{\sum_{k=1}^{p} W_k (\Delta Y_{k,tv})^2}$$

where p **is the number of considered physiographic and meteorological attributes**
$\Delta Y_{k,tv}$ **is the difference between** $Y_{k,t}$ **and** $Y_{k,v}$ **the values of the** k^{th} **attribute at sites** t **and** v
W_k **is the weight applied to the** k^{th} **attribute**

The weighted Euclidean distance and the threshold value θ_t are jointly optimized with a standard jack-knife resampling procedure (see Section 5.3.1).

To be applied, the index method requires the statistical homogeneity of the region which can be checked through the procedure proposed by Hosking et al. (1997). This is based on the assumption that the L-moment ratios should be identical for the sites of a statistical homogeneous region. A site within a given region can be declared discordant if the discordancy measure D is larger than 3 and the region can be considered statistical homogeneous if the heterogeneity measure H is lower than 2. Then, the statistical homogeneity of the region delineated by the ROI approach is checked with the following process inspired by Weiss et al. (2014a) :

1. Compute the heterogeneity measure H of the regional sample obtained with the ROI approach. If $H < 2$ then go to 4, else go to 2.
2. Compute the discordance measures D of the regional sample. Remove the sites with $D > 3$ and compute a new heterogeneity measure H'. If $H' < 2$ then go to 4, else go to 3.
3. Remove the site v with the highest d_{tv} (i.e. the site furthest from the target site t) and go to 1.
4. The region is both physiographically, meteorologically and statistically homogeneous.

5.2.3 Hierarchical Bayesian Analysis (HBA)

In this study, the HBA is a three-level hierarchical model in a Bayesian framework and its corresponding likelihood is given by Equation 5.5. The first level, called data level, describes the joint distribution of observed skew surges with unknown GP distribution parameters. The second level, called process level, describes the spatial variability of the scale and shape parameters of the GP distribution using a regression model that links the parameters with physiographic and meteorological covariates through hyper-parameters. The third level, called prior level, describes the prior distribution of the hyper-parameters.

Equation 5.5

$$L(\theta|X) = L(X|\theta)\ .\ L(\theta|\beta)\ .\ L(\beta)$$

Equation 5.6 gives the joint likelihood of the S series of skew surges $X = \{X^1, X^2, ..., X^S\}$ of parameters $\theta = (\theta_1, \theta_2, ..., \theta_S)$, $\sigma = (\sigma_1, \sigma_2, ..., \sigma_S)$ and $\xi = (\xi_1, \xi_2, ..., \xi_S)$.

Equation 5.6

$$L(X|\theta) = \prod_{j=1}^{S} \prod_{i=1}^{n_j} f_{\theta_j}(x_i^j)$$

The scale and shape parameters of the GP distributions σ and ξ are defined by generalized linear models (GLMs) of the physiographic and meteorological covariates :

Equation 5.7

$$\sigma = \alpha_\sigma Y_\sigma + \epsilon_\sigma \quad \text{and } \xi = \alpha_\xi Y_\xi + \epsilon_\xi$$

where $Y_\sigma = (1, Y^1, ..., Y^{m_\sigma})$ **and** $Y_\xi = (1, Y^1, ..., Y^{m_\xi})$ **are the vectors of the** m_σ **and** m_ξ **physiographic and meteorological covariates for** σ **and** ξ
α_σ **and** α_ξ **represent the regression parameters**
ϵ_σ **and** ϵ_ξ **are the error terms**

The procedure to select the optimal physiographic and meteorological variables Y_σ and Y_ξ are detailed in Section 5.3.1. We have $\epsilon_\sigma \sim N(0, \tau_\sigma^2)$ and $\epsilon_\xi \sim N(0, \tau_\xi^2)$, then $\sigma \sim N(\alpha_\sigma Y_\sigma, \tau_\sigma^2)$ and $\xi \sim N(\alpha_\xi Y_\xi, \tau_\xi^2)$. The likelihood of the scale and shape parameters of the GP distribution σ and ξ, given the hyper-parameters $\beta = (\alpha_\sigma, \tau_\sigma, \alpha_\xi, \tau_\xi)$, is written as :

Equation 5.8

$$L(\theta|\beta) = N(\sigma|\alpha_\sigma Y_\sigma, \tau_\sigma^2).N(\xi|\alpha_\xi Y_\xi, \tau_\xi^2)$$

Finally, independent priors are assigned to the hyper-parameters β. A zero-centered normal distribution with variance equal to 10 is selected for α_σ and α_ξ, and a standard normal distribution is selected for τ_σ and τ_ξ. This can be translated into the likelihood 5.9. These priors are non-restrictive and are chosen to help the convergence of the inference Monte Carlo Markov Chains (see Section 5.3.1).

Equation 5.9

$$L(\beta) = N(\tau_\sigma|0,1).N(\alpha_\sigma|0,10).N(\tau_\xi|0,1).N(\alpha_\xi|0,10)$$

At the first level of the hierarchy, the distribution of each site j has its own parameters θ_j and the data are not required to be spatially independent. However, the parameters of the sites are spatially linked through physiographic and meteorological covariates in the second level of the hierarchy then, the data are indirectly dependent. This indirect inter-site dependence is nevertheless reduced if compared to the index method, then it is not considered in this study. In Calafat et al. (2020), the dependences modelled via a max-stable process to interpolate the estimates (parameters and quantiles) at ungauged locations.

5.2.4 Historical HBA

Saint Criq et al. (2022a) propose, in a local analysis, a method to combine systematic skew surges X^j and observed historical record sea levels Z^j_{hist} at site j in a consistent inference procedure. This consists in computing a global likelihood $L(X^j, Z^j_{hist}|\theta_j)$ equal to the product of the likelihood of the systematic skew surge sample $L(X^j|\theta_j)$ (see Equation 5.2) and the likelihood of the historical sea level sample $L(Z^j_{hist}|\theta_j)$ (see Equation 5.10). $L(Z^j_{hist}|\theta)$ is numerically estimated and represents the likelihood, for a historical observation period of duration w^j_H years, of all the maximum sea levels whether lower or larger than a perception threshold η^j_H. The historical maximum sea levels are often affected by uncertainties, but Saint Criq et al. (2022b) show that the level of accuracy of the historical maximum sea levels has a limited influence on the results. It has been considered herein, that the reported historical maximum sea levels h^j_z are comprised between the perception threshold η^j_H and a value ϕ^j_H with $\phi^j_H > \eta^j_H$:

Equation 5.10

$$L(Z^j_{hist}|\theta_j) = \tilde{G}_{\theta_j}(\eta^j_H)^{N^j_{w_H} - h^j_z} \cdot \left[\tilde{G}_{\theta_j}(\phi^j_H) - \tilde{G}_{\theta_j}(\eta^j_H)\right]^{h^j_z}$$

where $\tilde{G}_{\theta_j}$ **is the probability cumulative distribution function of high tidal levels numerically estimated**
$N^j_{w_H} = 706 \times w^j_H$ **because there are** 706 **high tidal cycles during a year**

This method can be straightforwardly used to integrate historical information in the HBA, already combining the local and regional data. The HBA inference is enriched with the historical information at sites where it is available. This consists in combining the HBA likelihood $L(\theta|X)$ and the historical likelihood $L(Z_{hist}|\theta)$ (see Equation 5.11) to obtain the full historical HBA likelihood $L(\theta|X, Z_{hist})$.

Equation 5.11

$$L(Z_{hist}|\theta) = \prod_{\substack{i=1 \\ H_j=1}}^{S} (Z^j_{hist}|\theta_j)$$

where $H_j = 1$ **if historical information is available at site** j **and** $H_j = 0$ **else**

5.3 Methodology

5.3.1 Models and settings

The index method for the regional estimation is combined with the ROI approach for the delineation of physiographic and meteorological homogeneous regions. The process to guarantee the regional statistical homogeneity is applied (see Section 5.2.2.2). The HBA does not require homogeneous regions. It is then implemented considering all tide gauges. This results in two regional models denoted by ROI + Index and HBA. The regional models are first settled (see Section 5.4.1). They are evaluated according to their performances and to the added value compared to the local analysis (see Section 5.4.2). The HBA is then used in combination with historical information (see Section 5.4.3). The index method was originally developed for the frequency analysis, but it is computed here within the Bayesian framework in order to be able to compare it to the HBA with the same criteria.

To identify Y_σ and Y_ξ, the covariates modelling the scale and shape parameters σ and ξ through GLMs in the HBA (see Equations 5.7), two independent standard jack-knife procedures (Marra et al., 2011 ; Msilini et al., 2022) have been applied. All the possible combinations of the physiographic and meteorological covariates are tested for Y_σ and Y_ξ. Each tide gauge is considered, in turn, as an ungauged one, in order to carry out the regional regression using data from the remaining tide gauges and evaluate the performance of the resulting regression model. The regional estimates of the 10-year skew surge quantile x_{10} are computed with a GP distribution from the regional predicted scale parameter σ (or shape parameter ξ) and the observed (i.e. local estimated) shape parameter ξ (or scale parameter σ). The regional estimates of the 10-year skew surge quantile can be compared to the local estimates, computing the root mean squared error (RMSE). The settings leading to the lowest RMSE are selected. If several combinations have similar results, the simplest one (with the fewest covariates) is selected. For the implementation ROI + Index, the threshold θ_t and the weighted Euclidean distance (see Equation 5.3) are jointly optimized with a standard jack-knife procedure. Each weight $W_{k=\{1,...,p\}}$ of the weighted Euclidean distance can take any value within $\{0, 1/p, 2/p, ...1\}$ such as $\sum_{k=1}^{p} W_k = 1$ and p is the total number of available physiographic and meteorological variables. The threshold value θ_t can take any value within {0.1,0.2,0.3,...,2.5}. The physiographic and meteorological variables are standardized to avoid potential bias.

Once the regional models are adjusted, their performances are assessed through a jack-knife procedure. The following five criteria are computed for the estimated skew surge quantiles

x_{10}, x_{50} and x_{100}, considering the locally estimated quantiles as reference : the Nash criterion (NASH), the root mean squared error (RMSE), the relative RMSE (rRMSE), the mean bias (BIAS) and the relative BIAS (rBIAS). The width of the credibility intervals of the quantiles and the parameters are also evaluated to measure the added value of each regional model compared to a local analysis.

The R Package *rstan* is used to conduct Bayesian MCMC (Monte Carlo Markov Chain) inferences for computing the posterior distributions of the different models. Three parallel chains of a length of 30000 iterations are run for each model and the first 25000 iterations are discarded as warmup. The convergence of the chains is reached if the scale reduction $\hat{R}$, which is the ratio between average within-chain and average between-chains variance of the likelihood, is lower than 1.05 (Gelman et al. (2014)).

5.3.2 Case study

5.3.2.1 Skew surges series

The data set used in this study is composed of 78 European tide gauges located on the Atlantic, English Channel, Irish and North coasts (see Figure 5.1). The hourly recordings of these tide gauges are made available by the British Oceanographic Data Centre (`bodc.ac.uk`), the Flemish Agency for Maritime and Coastal Services (`meetnetvlaamsebanken.be`), the French Hydrographical and Oceanographical Service (`data.shom.fr`), the Global Extreme Sea Level Analysis project (`gesla787883612.wordpress.com`), the Ministery of Infrastructure and Water Management of the Netherlands (`rijkswaterstaat.nl`) and the Spanish Institute of Oceanography (`ieo.es`). Tide gauge recording lengths last from 16 years to 160 years. The hourly astronomical tidal levels are obtained based on an harmonic analysis on the hourly recorded sea levels through the R package *TideHarmonics* (Stephenson, 2015), as well as a correction from a possible eustatism as tidal predictions are calculated for the present time. Then, the series of astronomical high tides and skew surges can be extracted. To built the POT sample at each site, a POT threshold u is selected such that there is on average 1 threshold exceedance per year for a trade-off between bias and variance for the index method (Bernardara et al., 2011 ; Weiss et al., 2014a ; Weiss et al., 2014b). A GP distribution is adjusted on each local POT sample through the maximum likelihood to estimate the local scale and shape parameters σ and ξ (see Table 5.2 for the descriptive characteristics of u, σ and ξ and see Figure 12.1 in the Supplementary Information for their values at the European tide gauges).

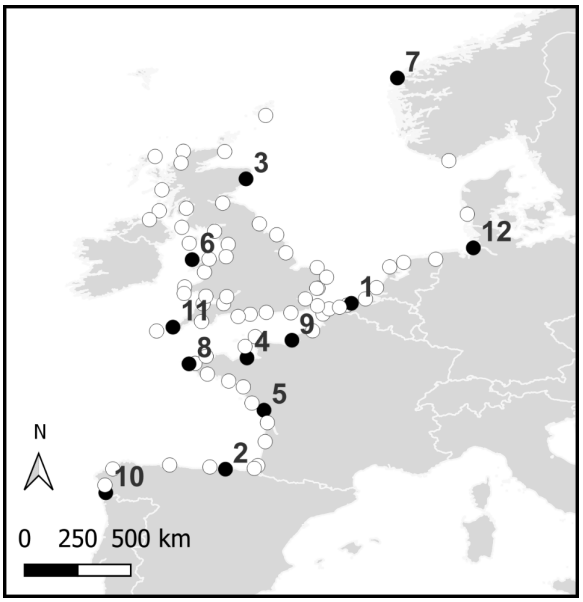

Figure 5.1 – Geographic location of European tide gauges

The black points represent the 12 randomly selected tide gauges for the result analysis : Oostende (1), Bilbao (2), Aberdeen (3), SaintMalo (4), LaRochelle (5), Holyhead (6), Maloy (7), LeConquet (8), LeHavre (9), Vigo (10), Newlyn (11) and Cuxhaven (12).

Historical record maximum sea levels are provided by the French Institute for Radiological Protection and Nuclear Safety (Giloy et al., 2018) and the British Oceanographic Data Centre (Haigh et al., 2017). From these two databases, the historical record maximum sea levels are available at 10 tide gauges (see Saint Criq et al. (2022a) for La Rochelle, Saint Criq et al. (2022b) for Aberdeen, Calais, Cherbourg, Le Havre, Nieuport, Oostende and Saint Malo, and Table 11.1 for Le Conquet and Le Crouesty). At Le Conquet and Le Crouesty, the historical maximum sea levels are observed during periods of missing data and the historical period duration is the rounded sum of the measurement holes since the beginning of the recordings. The main characteristics of the historical data sets to be used in the historical inference (see Equation 5.10) are summarized in Table 5.1. $P(\mathrm{A}|X^j)$ is a criterion proposed by Saint Criq et al. (2022b) to check the consistency of historical samples according to the systematic data sets, on the assumption that skew surges are following a GP distribution. Systematic and historical data sets appear very consistent at all tide gauges and quite consistent at La Rochelle.

Table 5.1 – Characteristics of the historical data sets

Site	w_H^j (years)	η_H^j (m)	ϕ_H^j (m)	h_z^j	$P(\mathrm{A}\|X^j)$
Nieuport	80	6.08	6.83	5	1.00
Oostende	80	6.01	6.76	4	0.96
Aberdeen	80	5.10	5.20	2	1.00
Calais	50	7.70	7.80	1	1.00
Cherbourg	130	7.17	8.06	2	1.00
La Rochelle	80	7.15	7.50	4	0.66
Le Conquet	20	7.63	7.83	1	1.00
Le Crouesty	30	5.87	6.69	3	1.00
Le Havre	105	8.40	9.38	4	1.00
Saint Malo	100	12.96	13.06	1	1.00

At the tide gauge j, there are h_z^j maximum historical sea levels observed between η_H^j and ϕ_H^j during the historical period of duration w_H^j years (see Section 5.2.4). $\mathrm{A}|X^j$ represents the event "η_H^j is exceeded at least h_z^j time(s) during the historical period of duration w_H^j years knowing the systematic data set" (Saint Criq et al., 2022b).

5.3.2.2 Physiographic and meteorological variables

The physiographic and meteorological covariates of the skew surges identified by Saint Criq et al. (2022b) are selected : the latitude (LAT), the longitude (LON), the 100-year quantile of the low mean sea level pressure (100-MSLP), the 100-year wind speed quantile (100-WS), the width of the continental shelf (WCS) and the angle between the prevailing wind direction and the continental shelf direction (ANGLE). Table 5.2 gives the descriptive characteristics of LAT, LON, 100-MSLP, 100-WS and WCS and Figure 1 in Saint Criq et al. (2022c) shows their values at the European tide gauges. The NOAA CIRES DOE 20CRv3 reanalysis (`psl.noaa.gov/data/gridded/data.20thC_ReanV3.monolevel.html`) provides meteorological variables from 1836 to 2015 with 3-hourly values over a 1° latitude x 1° longitude global grid (360x181). From these reanalyses, the u and v wind components at 10m (to compute the wind speed and direction) and the mean sea level pressure are downloaded in the form of "Ensemble Mean" - i.e. the mean result of the 80 models used in the reanalysis. From each tide gauge, the meteorological variables are retrieved at the closest point on the grid. Then, 100-MSLP, 100-WS and the prevailing wind direction (for ANGLE) can be extracted. ETOPO (`ngdc.noaa.gov/mgg/global`) provides the bathymetric data all around the world with a spatial resolution of 1 arc-minute. WCS is estimated as the shortest distance between the tide gauge and the continental slope, defined as the 1000-m isobath. The R package *marmap* (Pante et al., 2013) allows to extract the WCS and the direction of the continental shelf (for ANGLE).

Table 5.2 – Descriptive statistics of the variables.

Variable	Unit	Minimum	Maximum	Mean	Median	SD
LAT	°N	42.24	61.93	51.39	51.44	4.32
LON	°W	-8.77	8.72	-1.66	-2.16	3.90
100-MSLP	hPa	971.85	997.70	985.05	983.41	6.04
100-WS	$m.s^{-1}$	6.95	19.39	14.11	14.98	3.04
WCS	km	26.62	1057.78	421.17	409.28	272.44
ANGLE	°	0.02	0.99	0.50	0.52	0.31
u	m	0.33	1.88	0.70	0.62	0.31
σ	m	0.04	0.61	0.18	0.14	0.11
ξ	m	-1.05	0.31	-0.17	-0.12	0.27

5.4 Results

5.4.1 Settings of the models

Figure 5.2 shows the relative importance of the physiographic and meteorological variables selected to model the scale and shape parameters through GLMs for the HBA (see Equations 5.7). For the scale parameter σ, WCS is by far the most important covariate (around 90%) which is not surprising according to the high correlation between σ and WCS (see Figure 12.2 in the Supplementary information). Indeed, large continental shelves produce large skew surges (Pugh, 1987). The other covariates selected, 100-WS and 100-MSLP, are much less important (less than 1% for 100-MSLP, even not visible on the Figure 5.2). For the shape parameter ξ, the selected covariates are 100-WS, 100-MSLP and LAT which is very correlated with 100-MSLP (see Figure 12.2 in the Supplementary information). This is not surprising either because the combination of strong winds and low pressures favors the storms, and consequently extreme skew surges (Muis et al., 2016). Indeed, the shape parameter guides the right tail of the distribution. Finally, the physiographic covariates LON and ANGLE are not retained for any parameter.

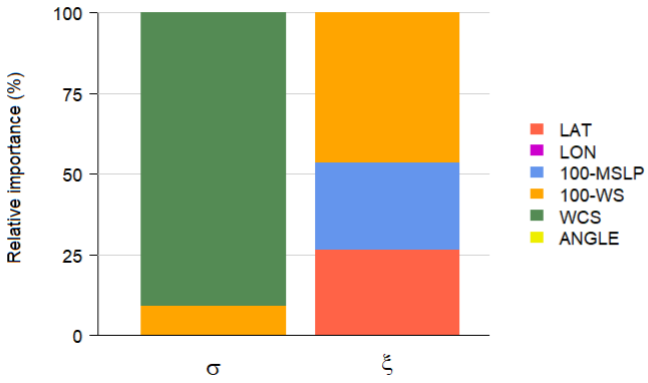

Figure 5.2 – Relative importance (%) variables retained in GLMs

In the case of ROI + Index, the weighted Euclidean distance function d_{tv} and the threshold θ_t are jointly optimized (see Section 5.3.1). The optimal distance function obtained is given by Equation 5.12, it is quite similar to the geographic distance (based on LAT and LON), but with a moderate contribution of the 100-MSLP. The sites v to be included in the ROI of the target site t should have a distance to the target sites equal or lower than 0.7 (i.e. $d_{tv} \leq \theta_t = 0.7$).

Equation 5.12

$$d_{tv} = \sqrt{\frac{2}{6}(\Delta\text{LAT}_{tv})^2 + \frac{3}{6}(\Delta\text{LON}_{tv})^2 + \frac{1}{6}(\Delta\text{100-MSLP}_{tv})^2}$$

5.4.2 Comparison of the regional models

Table 5.3 presents the results of the jack-knife procedure for the regional models. ROI + Index has the best overall performances (the highest NASH values and the lowest RMSE and rRMSE values), but presents a little bias, increasing with the return period compared to the HBA. The HBA has good performances as well.

Table 5.3 – Jack-knife results of the regional models

	Quantiles	ROI + Index	HBA
NASH	x_{10}	**0.97**	0.91
	x_{50}	**0.91**	0.82
	x_{100}	**0.87**	0.78
Bias (m)	x_{10}	0.02	**-0.01**
	x_{50}	0.08	**0.04**
	x_{100}	0.11	**0.07**
RMSE (m)	x_{10}	**0.08**	0.13
	x_{50}	**0.17**	0.22
	x_{100}	**0.22**	0.27
rBias (%)	x_{10}	2.98	**0.40**
	x_{50}	8.10	**5.01**
	x_{100}	10.48	**7.36**
rRMSE (%)	x_{10}	**7.74**	13.26
	x_{50}	**14.43**	20.69
	x_{100}	**18.20**	24.54

Best statistics are in bold characters.

ROI + Index systematically reduces the width of the credibility intervals of the skew surge quantiles and HBA in 92% of cases (72 out of 78 sites). This points the usefulness of integrating regional information to improve the estimate accuracy. Figure 5.3 shows the 95% credibility intervals of the parameters and quantiles of the local, ROI + Index and HBA models for 12 randomly selected tide gauges (see Figure 5.1). The credibility intervals are narrower with ROI

+ Index compared to HBA for both parameters or quantiles. With the regional information, the credibility intervals of the shape parameter are much narrower, this is particularly true for the tide gauges with short series. Consequently, the reduction of uncertainties is stronger for x_{100} than for x_{10}.

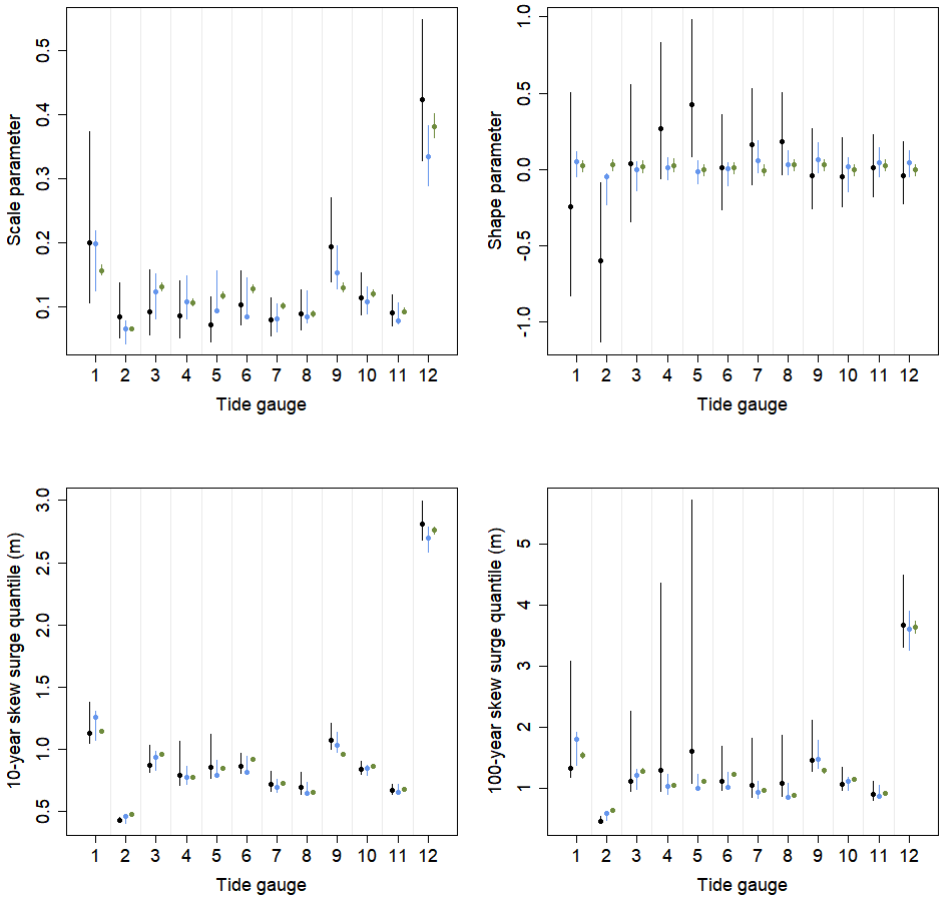

Figure 5.3 – 90% posterior credibility intervals of the parameters and quantiles

They are obtained with the local analysis (black), HBA (blue) and ROI + Index (green). The dots represent the maximum likelihood estimates. The tide gauges are arranged in ascending order of their local duration within {20, 22, 25, 27, 36, 41, 43, 47, 50, 72, 87, 97} years.

Figure 5.4 shows the credibility intervals obtained with a local analysis and with ROI + Index and HBA. The credibility intervals based on the local data can be very large for the highest return periods, which indicates the difficulty of accurately estimating extreme events with short duration series and justifies the use of additional information. The integration of regional information generally largely reduces the width of the credibility intervals and can sometimes reorientate the calibrated distribution (see Bilbao). The credibility intervals based on the HBA are consistent with the empirical data, since they contain the locally observed skew surges (black dots) except for some values appearing as outliers in the local sample like at Le Conquet. This is not systematically the case with ROI + Index, the widths of the

credibility intervals are narrower but the distributions do not always seem to be consistent with the data. To check the adequacy of the data observed to the distribution fitted with the ROI + Index model, Kolmogorov-Smirnov test were conducted and we could not reject the hypothesis of adequacy.

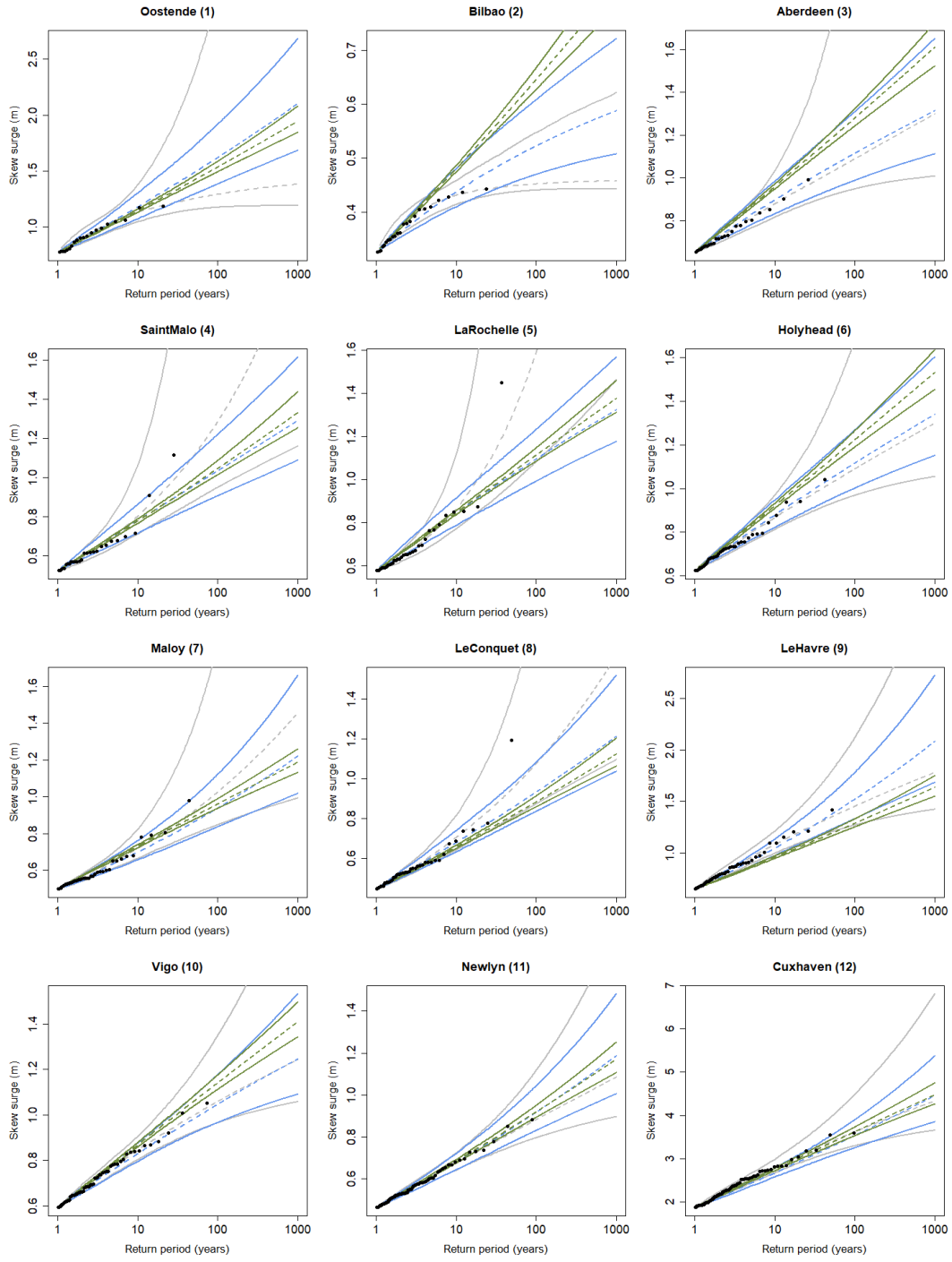

Figure 5.4 – 90% skew surge posterior credibility intervals
They are based on the local data (grey), on the ROI + index model (green) and on the HBA (blue). The dotted line represents the median estimates of each method.

As a conclusion, both models have good performances and allow to reduce the estimation

uncertainties compared to a local analysis. However, the credibility interval widths obtained with the ROI + Index are certainly more narrower than the actual regional content because of the inter-site dependencies. The HBA leads to larger credibility intervals than the index method probably also because it is more complex and requires the estimation of more parameters. This effect could be mitigated considering less variables in the GLMs (see the previous Section), the accuracy of the estimates would then be less, this is the principle of parsimony. Finally, the index method is discarded for the combination with the historical information to not worsen the issue of inter-site dependencies. The HBA model is then used in conjunction with historical information. Moreover, the HBA has the advantage to naturally give more weight to the local data than data from other sites compared to the index method.

5.4.3 Combination of historical and regional information

Figure 5.5 shows the posterior credibility intervals based on HBA with and without historical information. At Oostende, Aberdeen, Saint Malo, Maloy, Le Havre, Newlyn and Cuxhaven, the integration of the historical information in the HBA allows to decrease the uncertainties, it is the case for 17 tide gauges among the 78 (22% of the whole data set). For about 62% of the tide gauges, the credibility intervals are of similar widths with or without historical information, but they are slightly redirected upwards (see La Rochelle, Holyhead and Le Conquet). For the remaining tide gauges, the credibility intervals are redirected, especially the upper bound, and the uncertainties are increased (see Vigo and Bilbao).

The historical information added in the global inference of the HBA has an influence on the distribution of all tide gauges and not only those for which historical information is available. However, the seven sites where the uncertainties have been reduced the most are sites with available historical information, including Le Havre, Aberdeen, Oostende and Saint Malo. This is because the most important information is the local one for each tide gauge in the HBA.

The integration of the historical sea levels in the local analysis is confirmed to reduce the uncertainties compared to a simple local analysis (see sites with available historical information in Figures 5.4 and 5.5). The highest observed skew surges at Saint Malo, La Rochelle and Le Conquet are then included in the credibility intervals. It is interesting to notice that the inclusion of the regional information leads to narrower credibility intervals than the historical information.

The informative contents of the historical and regional data are different and the combination of both improves the estimation compared to the use of a single one. The results encourage the combination of local, historical and regional information, and the HBA provides an interesting and practical framework for that. More historical data series should be considered in the future.

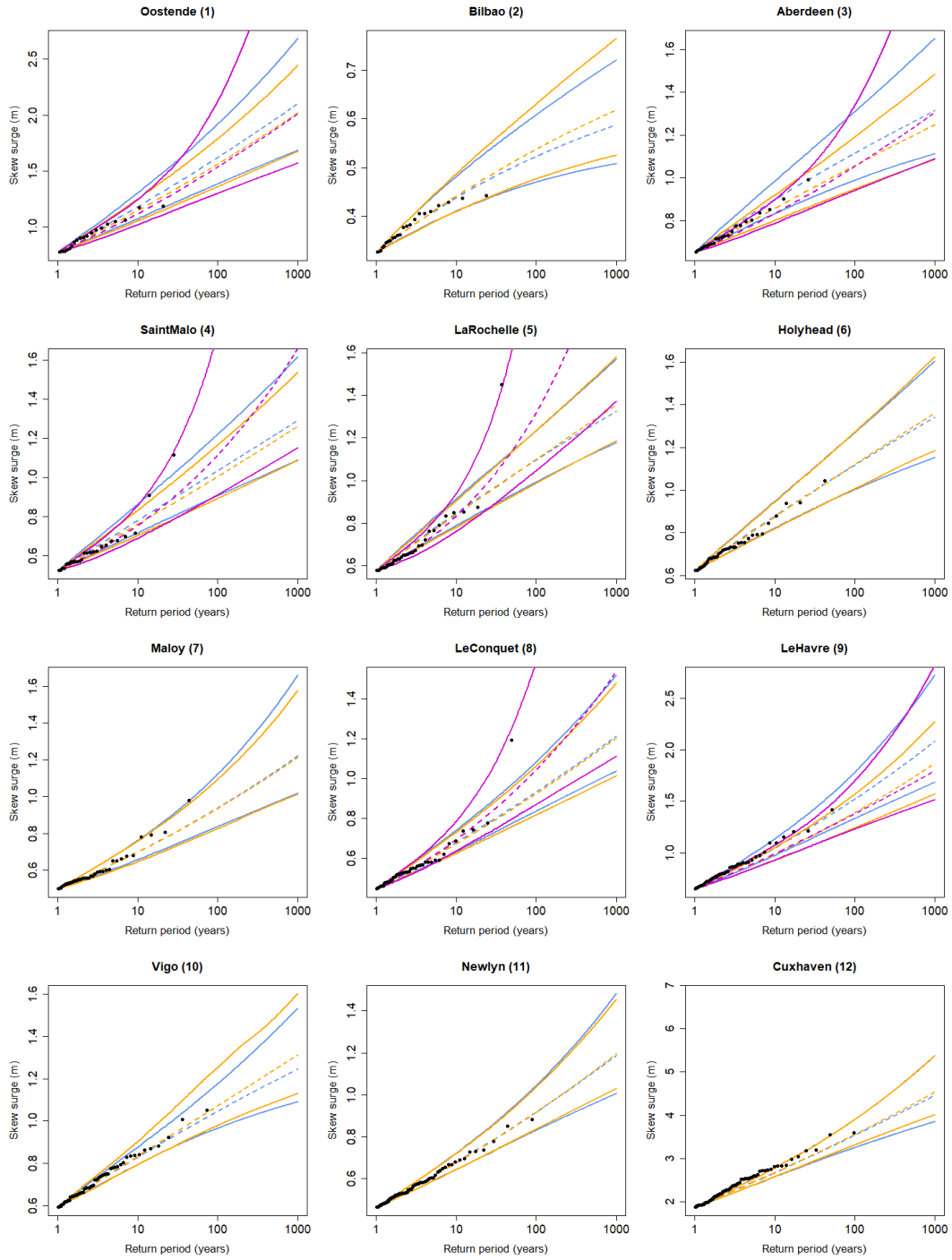

Figure 5.5 – 90% skew surge posterior credibility intervals
They are based on the HBA (blue), the historical HBA (orange) and on the local systematic skew surges and historical sea levels with the method developed by Saint Criq et al. (2022a) (purple). The dotted line represents the median estimates of each method.

5.5 Conclusion

In this study, a Hierarchical Bayesian Analysis (HBA) is applied to a data set of 78 European tide gauges in order to estimate the extreme skew surges sampled with the POT method

and fitted with the GP distribution. The scale and shape parameters are spatially linked to physiographic and meteorological variables with regressions. The HBA approach is compared to the classical index method in the Bayesian framework. The HBA approach is used to combine the regional skew surge series with historical extreme maximum sea levels through the method developed by Saint Criq et al. (2022a) and Saint Criq et al. (2022b).

For the index method, the ROI approach is used to delineate the homogeneous regions with a similarity measure based on the physiographic and meteorological variables. This allow to delineate regions centered on a target site even if the series are not long enough as the previously published approaches require (Hamdi et al., 2016; Hamdi et al., 2019; Andreevsky et al., 2020). The index method shows good performances in terms of the Nash criterion and errors, but at some stations, the fitted adjustments are visually completely inconsistent with the observed data. Moreover, the estimation uncertainties are artifically under estimated because the inter-site dependences are neglected.

For the HBA, the scale and shape parameters are modelled by generalized linear models in terms of physiographic and meteorological variables (WCS, 100-WS, 100-MSLP and LAT). The results show that the HBA also have good performances and improve the accuracy of the parameter and quantile estimates. The HBA appears as an alternative approach of the index method relaxing strong assumptions. This study confirms the interest of using physiographic and meteorological variables to spatialize the characteristics of the extreme skew surges, the parameters here and the quantiles in Saint Criq et al. (2022c). One limit of the present HBA can be the linear relation between parameters and covariates, it may be more realistic to use more complex relations.

The historical HBA is a powerful tool since the historical information at a given site helps to better estimate the extreme skew surges locally, but also at the other sites without locally available historical observations, compared to the simple HBA. Then, the HBA provides a particularly good framework to take into account local, historical and regional information. Combining all type of additional information is very helpful (Merz et al., 2008a; Merz et al., 2008b), however the literature is very poor (Frau et al., 2018; Hamdi et al., 2019 are the unique references in coastal analysis). This study is a contribution to this.

Other tests more specific to the Bayesian analysis should be conducted to rigorously check the reliability of the posterior credibility intervals. Sensitivity analyses should also be lead to test the effects of the observation durations for example. For further perspectives, the inference could be made more complex and informative taking into account the inter-site dependences. One possibility for this is to adapt the model of Calafat et al. (2020) developed for annual maxima series modelled by generalized extreme value distributions to peaks-over-threshold samples modelled by GP distributions. In the context of climate change, this is also essential to consider the non-stationarity.

Chapitre 6

Discussion générale et conclusion

Ce sixième chapitre conclut la thèse. Une synthèse des méthodes et des principaux résultats est d'abord présentée. Puis, les limites de ces travaux sont identifiées et des perspectives sont proposées pour de futures recherches.

6.1 Synthèse

Pour rappel, l'objectif de cette thèse était de développer des méthodes afin de prendre en compte proprement de l'information historique ou régionale, et la combinaison des deux pour l'analyse statistique des surcotes de pleine mer extrêmes. Voici une synthèse des méthodes développées.

6.1.1 Information historique

En réponse à la problématique d'exhaustivité de l'information historique liée spécifiquement à la variable de surcote de pleine mer, une nouvelle méthode a été proposée pendant cette thèse. Les niveaux marins extrêmes, plutôt que les surcotes de pleine mer extrêmes, sont évalués pour la période historique. En effet, il est plus facile d'avoir une connaissance exhaustive de tous les niveaux marins extrêmes (ayant dépassé un seuil) pendant une période donnée car ce sont des événements majeurs accessibles dans les archives. La méthode développée consiste alors à combiner, dans une seule inférence Bayésienne, les surcotes de pleine mer pour la période systématique et les niveaux marins extrêmes pour la période historique, afin de calibrer une distribution de probabilités sur les surcotes de pleine mer. Le caractère innovant de cette méthode tient dans la combinaison de variables de différentes natures (surcotes de pleine mer et niveaux marins).

La méthode repose sur l'hypothèse d'indépendance entre les surcotes de pleine mer et les marées hautes astronomiques. De plus, les distributions des niveaux marins historiques sont substituées par leurs approximations numériques. La flexibilité de la vraisemblance permet de considérer différents degrés de précision des niveaux marins historiques, leurs valeurs peuvent être connues exactement, connues avec des incertitudes ou inconnues mais ayant dépassé un seuil connu. On peut aussi inclure la connaissance qu'une valeur limite n'a pas été dépassée pendant une période donnée. La vraisemblance permet également de tenir compte de plusieurs périodes historiques avec des caractéristiques différentes. Cette méthode a été implémentée

avec l'interface R de Stan, le package *RStan* (**rstan**) et les codes ont été mis à disposition en libre accès à l'adresse suivante https://doi.org/10.5281/zenodo.6260203.

Des simulations de Monte Carlo basées sur des jeux de données observés ont montré que cette nouvelle méthode conduisait à des estimations précises et non biaisées, comparées aux estimations des "approches historiques" existantes pour l'analyse des surcotes de pleine mer. L'intégration de l'information historique devrait conduire à réduire les incertitudes d'estimation si les jeux de données systématiques et historiques apparaissent statistiquement consistants. La réduction des incertitudes est très peu influencée par le degré de précision des niveaux marins historiques, en revanche, la durée historique et la valeur limite non excédée sont très importantes. Finalement, la méthode a été appliquée avec succès à 13 marégraphes européens localisés sur le littoral Atlantique Français, de la Manche et de la Mer du Nord.

6.1.2 Information régionale

Une originalité de cette thèse est l'introduction de caractéristiques physiographiques et météorologiques pour l'estimation des surcotes de pleine mer dans le cadre d'une analyse régionale. Comme ce n'est pas une pratique courante dans le domaine maritime, on a tenté d'identifier des covariables physiographiques et météorologiques pertinentes explicatives de la surcote de pleine mer telles que la latitude (LAT), la longitude (LON), le quantile centennal de la pression basse moyenne au niveau de la mer (100-MSLP), le quantile centennal de la vitesse du vent (100-WS), la largeur du plateau continental (WCS), l'angle entre la direction du vent dominant et la direction du plateau continental (ANGLE), l'aire (AREA) et le périmètre (PERIM) de la zone maritime dans un carré de 20km de côté centré autour du site considéré. Ces covariables ont été utilisées, dans les approches régionales, pour définir les régions homogènes et pour régionaliser les caractéristiques des surcotes de pleine mer extrêmes, comme les quantiles ou les paramètres des distributions de probabilité, à une base de données composée de 78 marégraphes européens le long du littoral Atlantique, Manche et Mer du Nord.

Pour la délimitation des régions basées sur les covariables physiographiques et météorologiques, trois méthodes ont été testées et comparées : la classification ascendante hiérarchique, la région d'influence et l'analyse canonique des corrélations. L'approche de la région d'influence a été retenue pour ses performances évaluées avec une procédure de jack-knife. Elle permet d'obtenir une région homogène centrée autour d'un site cible avec une distance calculée à partir des covariables physiographiques et météorologiques. Les covariables offrent la possibilité de déterminer la région d'un site non jaugé, ce qui n'est pas faisable avec les méthodes de délimitation des régions classiques basées sur les séries locales enregistrées.

Les covariables physiographiques et météorologiques WCS, 100-WS, 100-MLSP et ANGLE apparaissent particulièrement importantes pour exprimer les quantiles des surcotes de pleine mer dans la zone considérée. Pour l'estimation des quantiles, deux modèles ont été testés et comparés : la régression linéaire et multiple, et le modèle additif généralisé. Le dernier modèle a été retenu pour ses performances évaluées avec une procédure de jack-knife. Finalement, le meilleur modèle régional pour estimer les quantiles des surcotes de pleine mer à des sites

non jaugés est la combinaison de l'approche région d'influence pour la formation des régions homogènes avec le modèle additif généralisé pour l'estimation.

Aux sites jaugés, l'approche de la région d'influence et de la méthode de l'index ont été utilisées conjointement dans le cadre de l'analyse régionale. On a montré que si les dépendances entre les observations des sites d'une région ne sont pas prises en compte, les incertitudes d'estimation sont sous-estimées. On a aussi montré que la pratique consistant à ne conserver que l'observation maximale parmi les observations dépendantes entraîne la surestimation des quantiles. Pour contourner cette problématique de dépendance, l'analyse hiérarchique Bayésienne est apparue comme une bonne alternative. Elle est beaucoup moins sensible aux dépendances inter-sites que la méthode de l'index et donne naturellement plus d'importance aux données locales qu'aux données des autres sites. De plus, elle ne nécessite pas l'étape de formation des régions homogènes. Les paramètres d'échelle et de forme des distributions sont spatialement reliés aux covariables physiographiques et météorologiques (WCS, 100-WS et 100-MSLP pour le paramètre d'échelle, et 100-WS, 100-MSLP et LAT pour le paramètre de forme). L'intégration de l'information régionale diminue les incertitudes d'estimation ainsi que la largeur des intervalles de crédibilité comparée à une analyse locale.

6.1.3 Combinaison information historique et régionale

Cette thèse confirme l'intérêt du cadre Bayésien pour le traitement et la combinaison de l'information additionnelle. Les données locales, régionales et historiques sont combinées en intégrant les données historiques aux sites où elles sont disponibles dans l'analyse hiérarchique Bayésienne grâce à la méthode historique développée. La combinaison de l'information historique et régionale permet de réduire encore plus les incertitudes d'estimation comparée à l'utilisation d'un seul type d'information additionnelle. Toute information additionnelle est importante et devrait être valorisée. Finalement, cette nouvelle approche apporte des propositions à tous les objectifs de la thèse.

6.2 Discussion et perspectives

Dans cette partie, on identifie les limites des méthodes développées et des résultats dans cette thèse, ainsi que des pistes de réflexions pour de futurs travaux.

La méthode développée pour l'intégration de l'information historique présente de bonnes propriétés, mais de futurs développements pourraient l'améliorer. La distribution des niveaux marins, telle qu'elle est implémentée, impose l'indépendance entre la surcote de pleine mer et la marée haute astronomique, ainsi que l'indépendance entre les observations de pleine mer consécutives (dépendance spatiale). Ces deux hypothèses simplificatrices ne remettent pas en cause la méthode, mais peuvent être questionnées pour prendre en compte ces possibles interactions et ainsi augmenter la précision de la méthode. Par exemple, l'indice extrémal apparaît être un bon indicateur pour mesurer les dépendances spatiales (Tawn et al., 1989 ; Tawn, 1992 ; Batstone et al., 2013 ; D'Arcy et al., 2022). Pour prendre en compte les dépendances entre les marées hautes astronomiques et les surcotes de pleine mer, D'Arcy et

al. (2022) proposent d'ajouter une covariable de marée au paramètre d'échelle et au paramètre du taux de dépassement du seuil POT. Un moyen de prendre en compte indirectement ces dépendances, est de prendre en compte la saisonnalité des deux variables, comme suggéré dans Williams et al. (2016).

La méthode historique développée permet de prendre en compte de l'information historique dégradée telle qu'une structure côtière avec une altitude connue n'a pas été submergée au cours d'une période historique donnée. Ce type d'information historique pourrait être obtenue grâce aux connaissances des populations locales ou des experts du terrain. Ainsi, cela permettrait de valoriser de l'information même aux marégraphes où les archives ne sont pas disponibles ou n'ont pas encore été fouillées.

Les covariables PERIM et AREA ont été imaginées pour décrire la forme du littoral. Cependant, elles n'ont pas été retenues comme importantes dans les analyses régionales menées. Le lien entre la morphologie du littoral et les surcotes de pleine doit être étudié plus précisément pour trouver des covariables plus pertinentes, ou pour éliminer définitivement l'utilisation de covariables de ce type. Pour améliorer le pouvoir explicatif des covariables, il pourrait être intéressant de les combiner, en les sommant par exemple.

Pour les approches régionales, de nouvelles méthodes existantes dans la littérature pour d'autres aléas pourraient être appliquées au domaine maritime. Par exemple, le krigeage qui combine les deux étapes de l'analyse régionale : la délimitation des régions homogènes et l'estimation régionale (Chokmani et al., 2004 ; Ouarda et al., 2008 ; Yin et al., 2018 ; Das et al., 2020).

Les problématiques des dépendances inter-sites pour l'analyse régionale ont été relevées mais n'ont pas été traitées dans cette thèse. Et même si ces dépendances ont beaucoup moins d'effets pour l'analyse hiérarchique Bayésienne que pour la méthode de l'index, elles devraient être idéalement prises en compte. En effet, cela permettrait notamment d'augmenter le contenu informatif des données régionales. Cela pourrait être possible par exemple avec les processus de max-stable comme dans Calafat et al. (2020) pour les maximums annuels, cependant cela demande des développements théoriques et numériques pour les dépassements de seuil.

Dans cette thèse, les effets du changement climatique ont été ignorés pour développer de nouvelles méthodes. Le changement climatique a deux impacts majeurs sur les niveaux marins extrêmes : l'élévation du niveau marin moyen, et des changements dans l'intensité et la fréquence des tempêtes, et donc des surcotes de pleine mer extrêmes. L'hypothèse de stationnarité nécessaire à la distribution statistique actuelle des surcotes de pleine mer est alors remise en question et sera de moins en moins en vérifiée avec le temps. La distribution statistique des surcotes de pleine mer devrait donc être corrigée, par exemple, en faisant varier les paramètres de la distribution statistique en fonction du temps ou d'une autre covariable. De plus, l'élévation du niveau marin devrait être intégrée dans la distribution empirique des marées astronomiques pour la méthode historique. Dans de futurs travaux, les méthodes intégrant l'information régionale et/ou historique devraient prendre en compte les effets du changement climatique pour s'y adapter. C'est le défi planétaire actuel.

Chapitre 7

Annexe de l'article 1

7.1 Estimation of $\tilde{g}_\theta$ and $\tilde{G}_\theta$

The maximum sea level Z is the sum of a skew surge X and an astronomical high tide Y. Both components are supposed to be independents (see Section 7.3). Hence,

Equation 7.1

$$P(Z < z) = \int_{\min(Y)}^{\max(Y)} q(y) P(X < z - y)\ dy$$

where $q(y)$ **is the probability density function of** Y
$\min(Y)$ **and** $\max(Y)$ **represent respectively the lowest and the highest astronomical high tide**
$\xi \in R$ **est le paramètre de forme**

The skew surge X may either be smaller or larger than the systematic threshold u. Therefore,

Equation 7.2

$$\tilde{G}_\theta(z) = P(Z < z) = P(X \leq u)\ P_{X \leq u}(Z < z) + [1 - P(X \leq u)]\, P_{X > u}(Z < z)$$

Considering that $P_{X>u}(X < x) = F_\theta(x)$ and $P(X > u) = \hat{\lambda}/706$ and combining Equations 7.1 and 7.2 leads to :

Equation 7.3

$$\tilde{G}_\theta(z) = \left(1 - \frac{\hat{\lambda}}{706}\right) \int_{\min(Y)}^{\max(Y)} q(y)\ P_{X \leq u}(X < z - y)\ dy + \frac{\hat{\lambda}}{706} \int_{\min(Y)}^{\max(Y)} q(y)\ F_\theta(z - y)\ dy$$

The two terms $q(y)$ and $P_{X\leq u}(X < z-y)$ can be estimated based on the observed systematic data set, prior to the implementation of the statistical inference procedure. The distribution of astronomical high tides is defined by the analysis of the predicted high tide values over a saros cycle (18,6 years). To enable the numeric computation of Equation 7.3, the range of possible values for Y is split into n_T intervals $Y_{k=\{1,\ldots,n_T\}}$ of 0.01m width. The vector of length n_T including the probability values $P(Y \in Y_k)$ is computed and the integrals in Equation 7.3 are approximated by finite sums, leading to :

Equation 7.4

$$\tilde{G}_\theta(z) \approx \left(1 - \frac{\hat{\lambda}}{706}\right) \sum_{k=1}^{n_T} P(Y \in Y_k)\ P_{X\leq u}(X < z - \mathrm{Med}(Y_k)) + \frac{\hat{\lambda}}{706} \sum_{k=1}^{n_T} P(Y \in Y_k)\ F_\theta(z - \mathrm{Med}(Y_k))$$

where $\mathbf{Med}(Y_k)$ **represents the median high tide value for interval** k

The term $P_{X\leq u}(X < z - \mathrm{Med}(Y_k))$ is estimated based on the empirical distribution of the measured sample of ordinary skew surges (i.e. skew surges lower than the threshold u). It is simply equal to the ratio of the number of observed ordinary skew surges lower than $(z - \mathrm{Med}(Y_k))$ to the total number of observed skew surges lower than u. Finally, an approximate value of the sea level z probability density function $\tilde{g}_\theta(z)$ is deduced from the cumulative density function $\tilde{G}_\theta(z)$:

Equation 7.5

$$\tilde{g}_\theta(z) \approx \left[\frac{\tilde{G}_\theta(z+h) - \tilde{G}_\theta(z)}{h}\right]$$

For the computations, h is set equal to $0.01z$.

7.2 Available historical information

Table 7.1 – Historical information at Brest

Date	1856	1877	1882	1888	1899	1913	1928	1936	1939	1940
Sea levels (m)	8.03	8.05	8.03	8.14	8.04	8.02	8.10	8.10	8.07	8.05
Skew surges (m)	(0.44)	0.91	(0.33)	0.72	(0.37)	0.69	(0.48)	(0.38)	(0.48)	(0.32)

In parenthesis, skew surges not exceeding u.

Table 7.2 – Historical information at Dunkerque

Date	1720	1763	1767	1807	1808	1846	1846	1953
Sea levels (m)	7.68	7.60	7.76	7.60	8.10	7.96	7.86	7.90
Skew surges (m)	1.68	1.94	1.71	1.40	2.20	1.95	2.25	2.17

Table 7.3 – Historical information at La Rochelle

Date	1866	1872	1890	1895	1924	1940
Sea levels (m)	(5.70)	(6.34)	7.30	7.15	7.15	7.40
Skew surges (m)	1.15	1.00	1.02	0.75	1.09	1.60

In parenthesis, sea levels not exceeding η_H.

Table 7.4 – Historical information at Saint Nazaire

Date	1864	1877	1894	1937	1940
Sea levels (m)	7.16	7.24	7.09	7.16	7.12
Skew surges (m)	0.90	1.25	1.35	0.82	1.41

7.3 Settings of the Monte Carlo runs

The independence between skew surges and astronomical high tides has to be verified to consider the sea levels as the sum of both components randomly sampled independently. To evaluate the interactions between astronomical high tides and skew surges, Williams et al. (2016) proposed to i) visually analyse the scatter plot of observed astronomical high tides versus the corresponding skew surges (Figure 7.1), and ii) conduct a Kendall test (Table **??**, the test is conducted on the largest skew surge values that are of particular interest here). Both indicate that there is no obvious correlation between astronomical high tides and skew surges. Especially, the skew surges exceeding u, correspond to diverse levels of high tides.

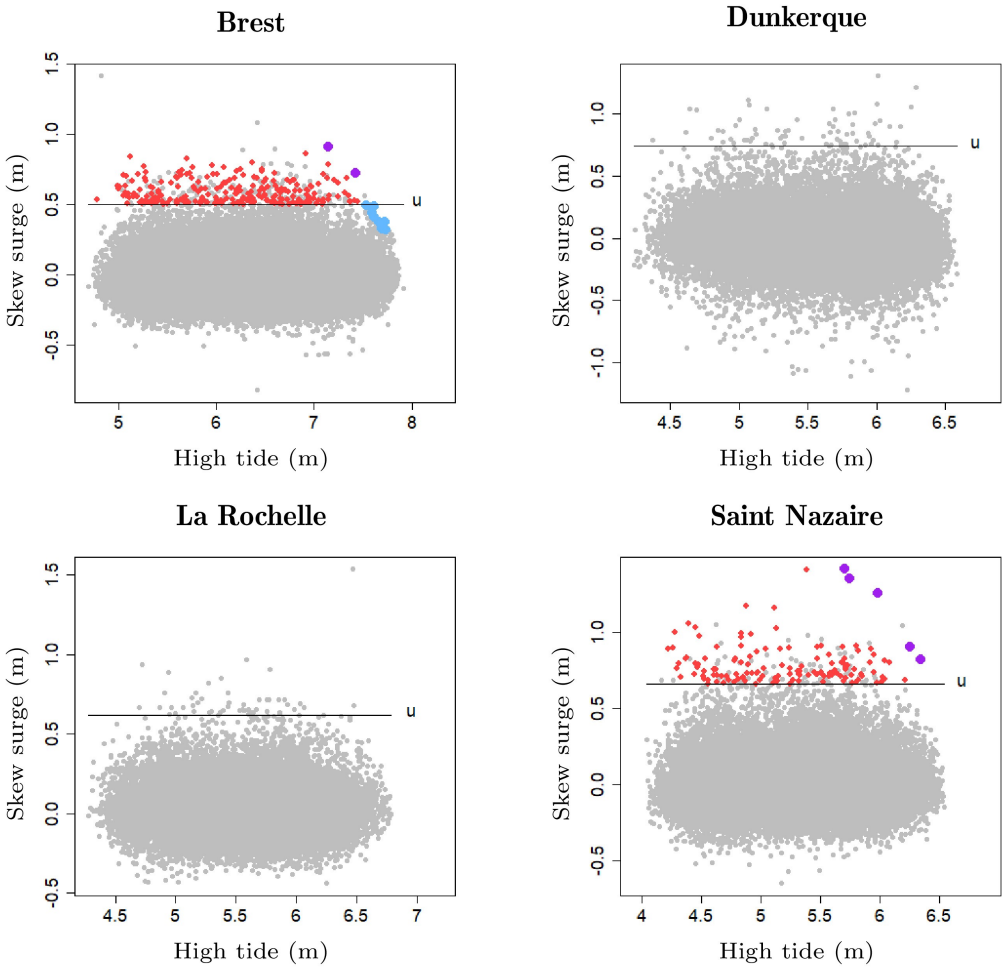

Figure 7.1 – Scatter plot of the high tide / skew surge samples
For Brest and Saint Nazaire, the red points represent the historical sample used in method 2 (ideal case), the blue points represent the historical sample used in method 3 (proposed method) and the purple points represent the observations common to both historical samples.

It is worth noting that the sample of historical events valuated in method 3 is a sub-set of the sample of events used in method 2 at Saint Nazaire. It furthermore includes 3 of the 4 largest observed skew surge events. At Brest, a station with a large tide/surge ratio, the samples used for the implementation of the two methods are almost totally different : they have only two events in common including only one of the largest observed skew surges.

Table 7.5 – Kendall's τ and p-value (5%) for the top 1% skew surges.

Site	τ	p-value
Brest	-0.023	0.257
Dunkerque	-0.009	0.806
La Rochelle	-0.021	0.628
Saint Nazaire	-0.45	0.65

The empirical distributions of astronomical high tides for the four case studies are shown in Figure 7.2. The number n_T intervals used to describe these distributions in the numerical implementation (see Section 7.1) depends on the range of high tide values at each station : 4.70m to 7.86m at Brest (317 intervals), 4.14m to 6.49m at Dunkerque (237 intervals), 4.26m to 6.71m at La Rochelle (247 intervals), 4.00m to 6.46m at Saint Nazaire (247 intervals).

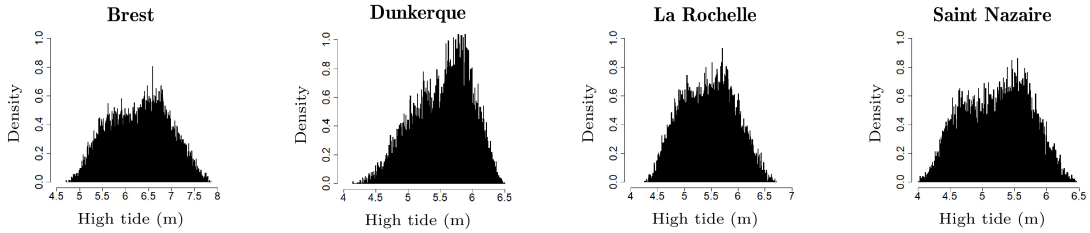

Figure 7.2 – Empirical distributions of astronomical high tides.

Chapitre 8

Information supplémentaire pour l'article 1

Supporting Information for "Extreme sea level estimation combining systematic observed skew surges and historical record sea levels"

Contents of this file

1. Figures S1 to S3
2. Tables S1 to S2

Introduction

This document includes the evaluation criteria of the tested methods, the 1000-year skew surge quantile estimates on the real datasets, and the maximum likelihood estimates of the parameters.

Table 8.1 – Relative bias, RSD and RRMSE of the ML estimated 100-year quantile

Station	Model	Relative bias	RSD	RRMSE
Brest	1	0.06	0.20	0.21
	2	0.02	0.11	0.11
	3	0.02	0.11	0.11
	4	-0.01	0.20	0.20
	5	0.17	0.22	0.26
	6	0.18	0.23	0.27
Dunkerque	1	0.15	0.41	0.43
	2	0.02	0.12	0.13
	3	0.03	0.14	0.14
	4	-0.08	0.15	0.18
	5	1.81	0.48	0.80
	6	0.12	0.35	0.36
La Rochelle	1	0.20	0.52	0.55
	2	0.05	0.21	0.21
	3	0.06	0.20	0.21
	4	-0.01	0.37	0.37
	5	0.84	0.63	0.78
	6	0.50	0.90	0.96
Saint Nazaire	1	0.06	0.19	0.20
	2	0.02	0.10	0.10
	3	0.08	0.11	0.14
	4	-0.07	0.13	0.15
	5	0.16	0.20	0.24
	6	0.05	0.18	0.19

Table 8.2 – 1000-year quantile estimations obtained from the real datasets

Site	Method	$\hat{x}_{1000}^{5\%}$ (m)	$\hat{x}_{1000}^{\mathrm{ML}}$ (m)	$\hat{x}_{1000}^{95\%}$ (m)	ΔCI (m)	$\Delta\mathrm{CI}/\hat{x}_{1000}^{\mathrm{ML}}$ (%)
Brest	1	1.28	1.85	4.11	2.83	152.39
	2	1.17	1.34	1.70	0.54	40.31
	3	1.21	1.58	2.30	1.09	69.10
	3*	1.22	1.60	2.36	1.14	71.27
Dunkerque	1	1.31	1.57	2.69	1.38	87.65
	3	2.37	3.44	5.55	3.17	92.22
	3*	1.56	1.95	2.70	1.14	58.53
LaRochelle	1	1.50	3.00	22.54	21.05	701.97
	3	1.47	2.41	5.23	3.77	156.12
	3*	1.41	2.22	4.65	3.24	146.03
SaintNazaire	1	1.07	1.26	2.18	1.11	88.52
	2	1.45	1.77	2.57	1.12	63.20
	3	1.41	1.96	3.19	1.77	90.58
	3*	1.31	1.62	2.36	1.06	65.13

In method 3*, the historical threshold is increased such as it is exceeded by no observed record (h_Z is 0, a particular case of binomial censored data) : η_H is set equal to 8.20m at Brest, 8.15m at Dunkerque, 7.45m at La Rochelle and 7.30m at Saint Nazaire.

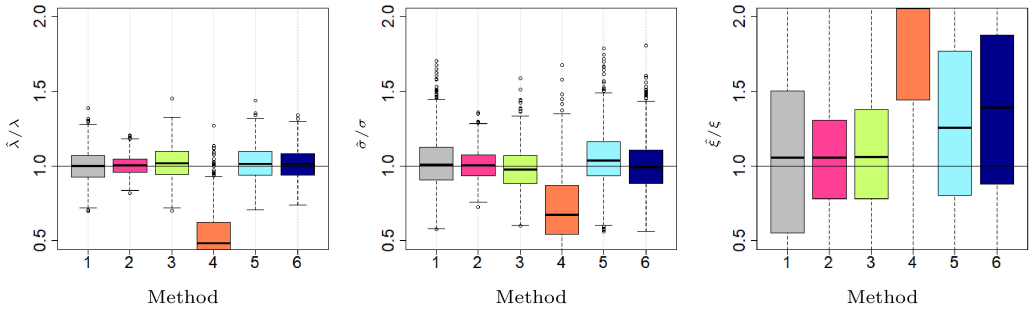

Figure 8.1 – Dispersion of the estimated parameters with ML at Brest

The parameters obtained from simulations are divided by the real values.

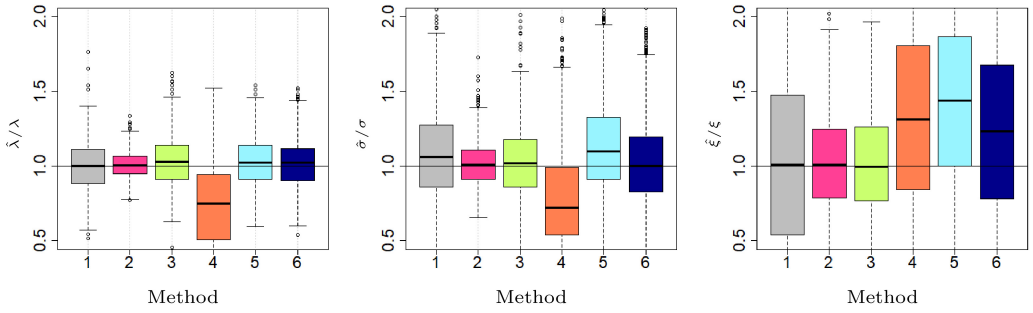

Figure 8.2 – Dispersion of the estimated parameters with ML at La Rochelle

The parameters obtained from simulations are divided by the real values.

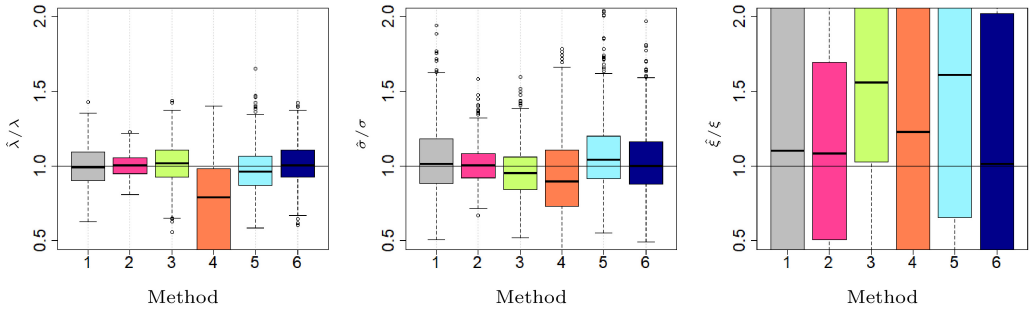

Figure 8.3 – Dispersion of the estimated parameters with ML at Saint Nazaire

The parameters obtained from simulations are divided by the real values.

Chapitre 9

Annexe de l'article 2

9.1 Historical information

Table 9.1 – Record historical maximum sea levels with their corresponding skew surges

Site	Date	Sea levels (m)	Skew surges (m)
Cherbourg	13-09-1821	7.96	1.28
Cherbourg	01-01-1877	7.17	0.71
Saint Malo	01-01-1877	12.96	0.43
Le Havre	27-10-1882	8.42	0.30
Le Havre	22-01-1890	8.55	0.55
Le Havre	06-12-1896	8.40	0.54
Calais	07-01-1905	7.70	0.56
Vlissingen	12-03-1906	4.05	1.49
Vlissingen	31-12-1910	4.33	2.37
Delfzijl	13-01-1916	4.34	3.34
Oostende	23-11-1930	6.19	1.64
Oostende	26-04-1944	6.01	1.81
Oostende	01-03-1949	6.04	1.57
Nieuport	01-02-1953	6.73	2.17
Oostende	01-02-1953	6.66	2.22
Vlissingen	01-02-1953	4.54	2.41
Nieuport	21-03-1961	6.10	1.39
Aberdeen	28-02-1967	5.10	0.49
Aberdeen	29-09-1969	5.10	0.64
Le Havre	23-11-1984	9.28	1.18
Nieuport	15-11-1993	6.14	0.95
Nieuport	28-01-1994	6.08	1.18
Nieuport	02-01-1995	6.08	1.13

9.2 Independence between skew surges and astronomical high tides

The independence between skew surges and astronomical high tides is verified, as in Arns et al., 2020, through the scatter plot of predicted astronomical high tides versus the corresponding skew surges and a Kendall test (see Figure 9.1). If the Kendall's value τ is equal to 0, there is no correlation between astronomical high tides and skew surges. On the other hand, if $|\tau| = 1$, astronomical high tides and skew surges are perfectly dependent.

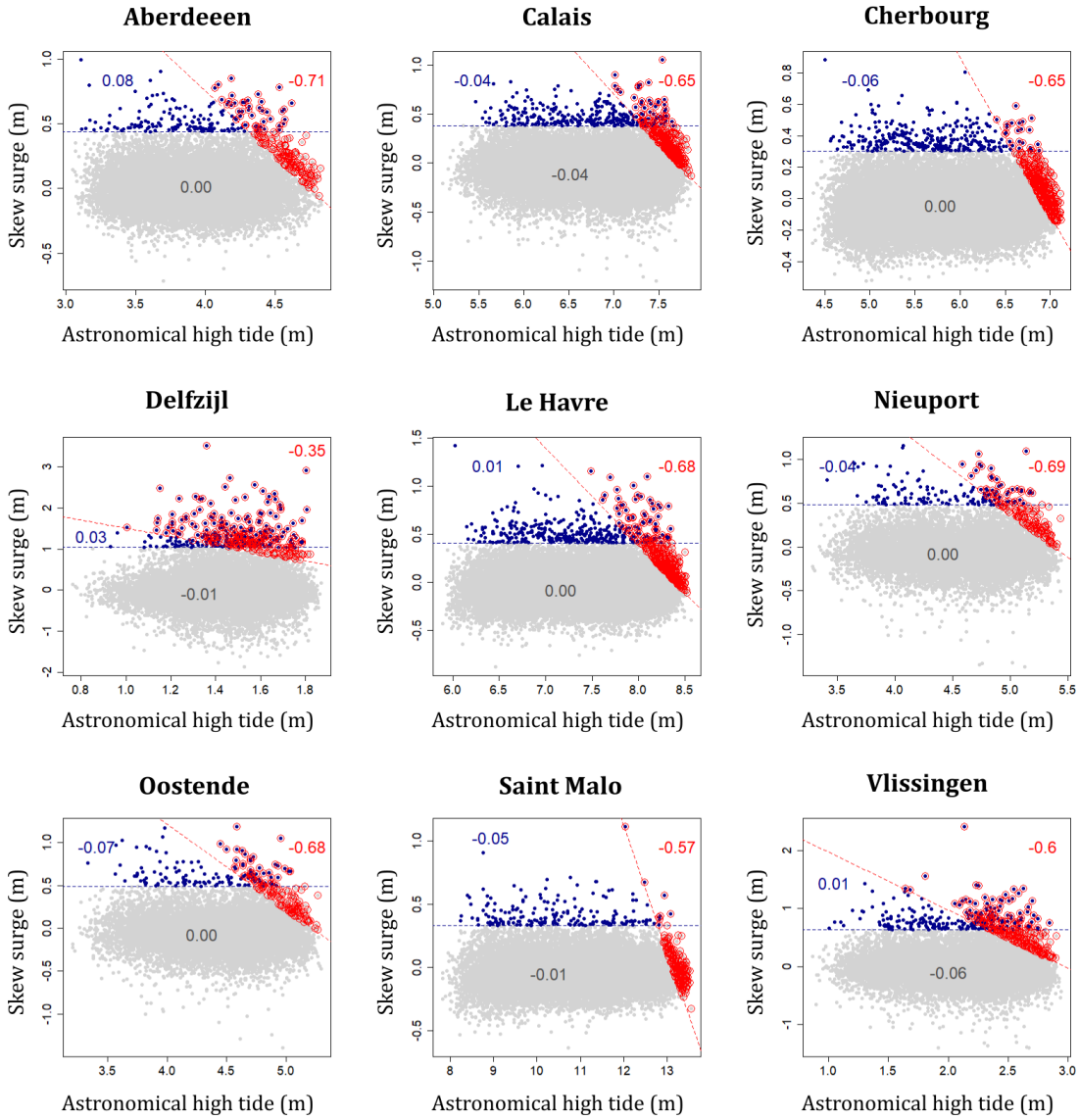

Figure 9.1 – Scatter plot of predicted astronomical high tides versus observed skew surges

The grey points represent all the maximum sea levels, the red points represent the 1% largest maximum sea levels and the blue points represent the maximum sea levels associated with the 1% largest skew surges. The colored numbers are the Kendall's τ values.

Chapitre 10

Information supplémentaire de l'article 3

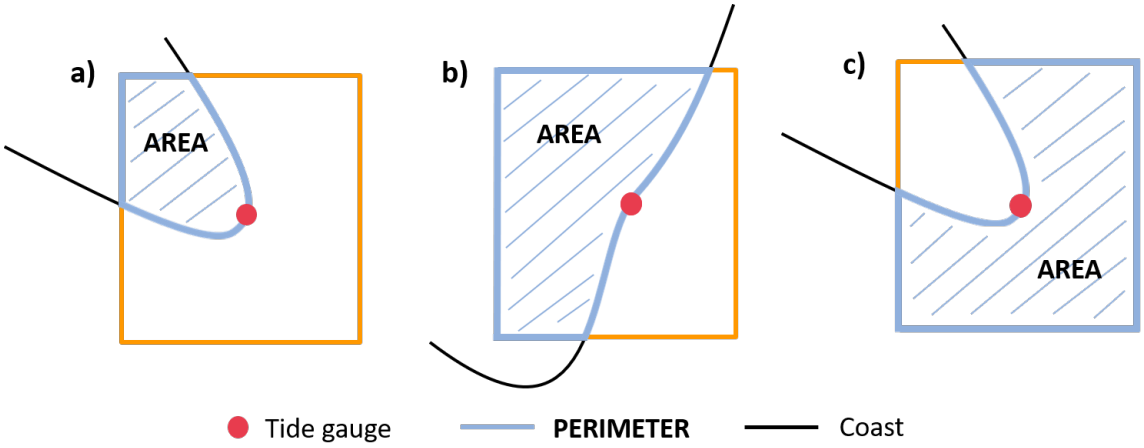

Figure 10.1 – AREA and PERIMETER in three typical cases
a) the tide gauge is inside a bay, b) the coastline is quite straight and c) the tide gauge is at a cape.

Table 10.1 – Descriptive statistics of the variables

Variable	Unit	Minimum	Maximum	Mean	Median	SD	Skewness	Kurtosis
LAT	°N	42.24	61.93	51.39	51.44	4.32	-0.18	2.86
LON	°W	-8.77	8.72	-1.66	-2.16	3.90	0.71	3.19
100-MSLP	hPa	971.85	997.70	985.05	983.41	6.04	0.52	2.62
100-WS	$m.s^{-1}$	6.95	19.39	14.11	14.98	3.04	-0.63	2.61
WCS	km	26.62	1057.78	421.17	409.28	272.44	0.45	2.32
ANGLE	°	0.02	0.99	0.50	0.52	0.31	0.00	1.61
AREA	km^2	305.17	2294.66	1232.71	1194.69	440.89	0.29	2.92
PERIM	km	30.23	427.77	190.50	189.93	64.45	0.84	5.39
x_{10}	m	0.42	2.78	1.03	0.91	0.47	1.91	7.07
x_{50}	m	0.45	3.34	1.22	1.10	0.56	1.86	7.00
x_{100}	m	0.45	3.57	1.30	1.17	0.60	1.80	6.75

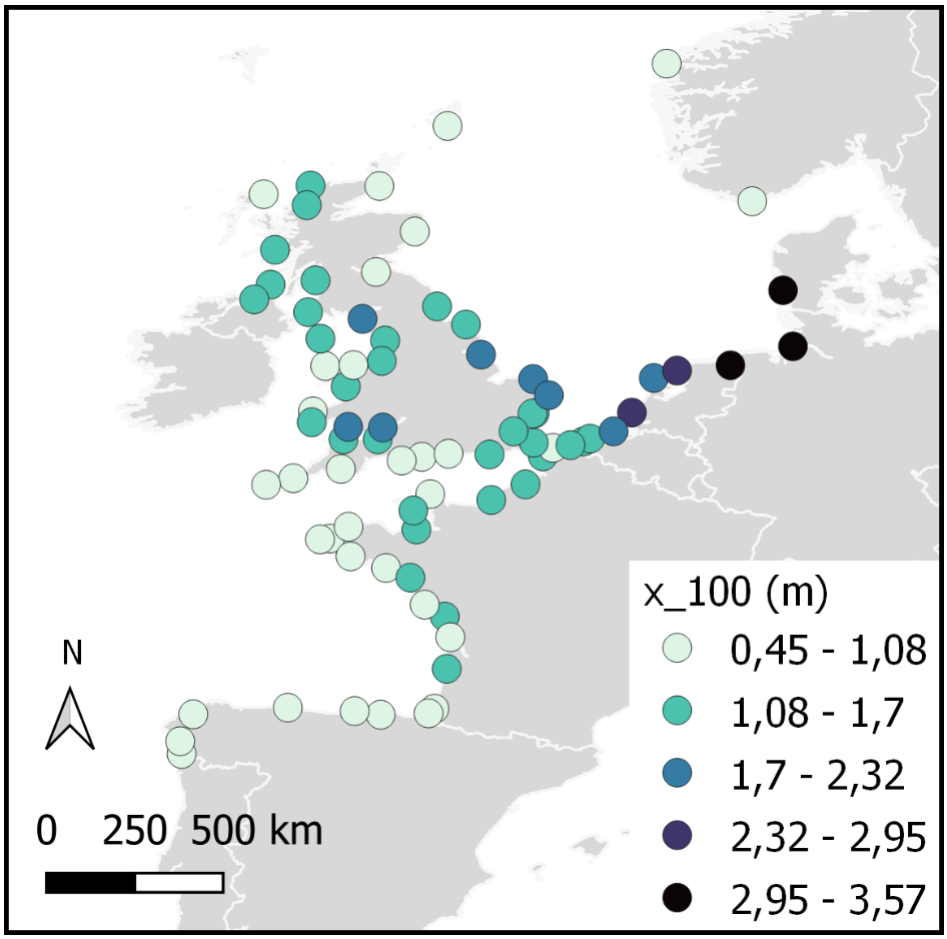

Figure 10.2 – 100-year skew surge quantile x_{100} at the European tide gauges

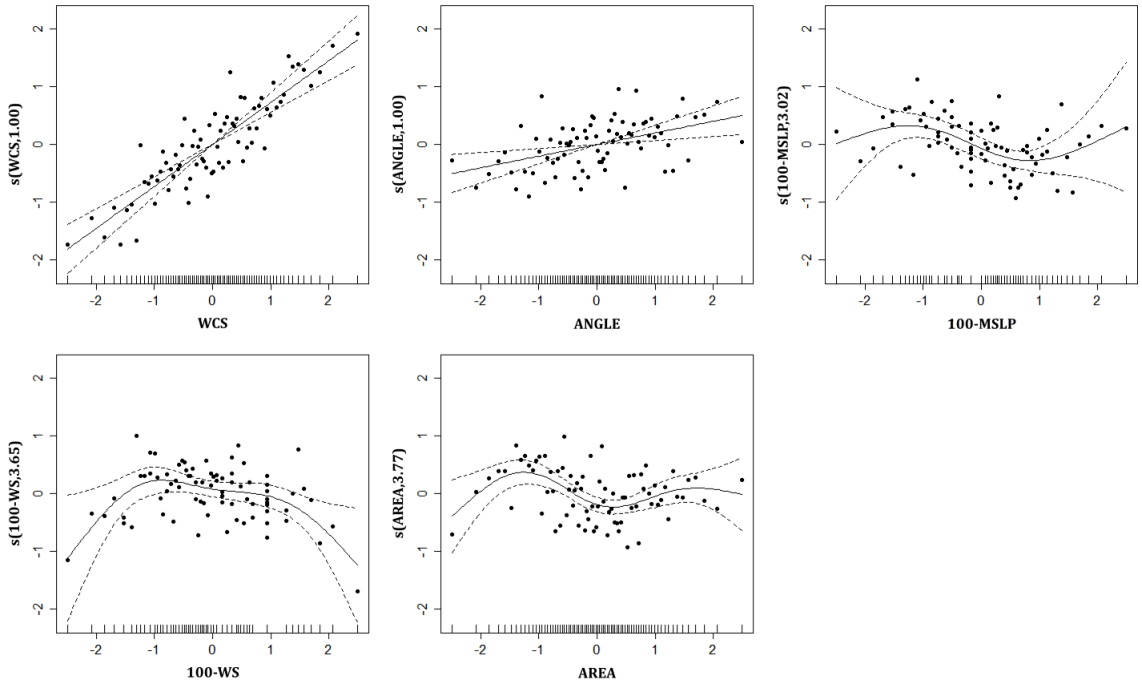

Figure 10.3 – Smooth functions of the 10-year skew surge quantile x_{10} for the explanatory variables included in the regional model ALL + GAM. The dotted lines represent the 95% confidence intervals. The vertical axes are named s(var,edf), var is the name of the explanatory variable and edf is the estimated degree of freedom of the smooth function.

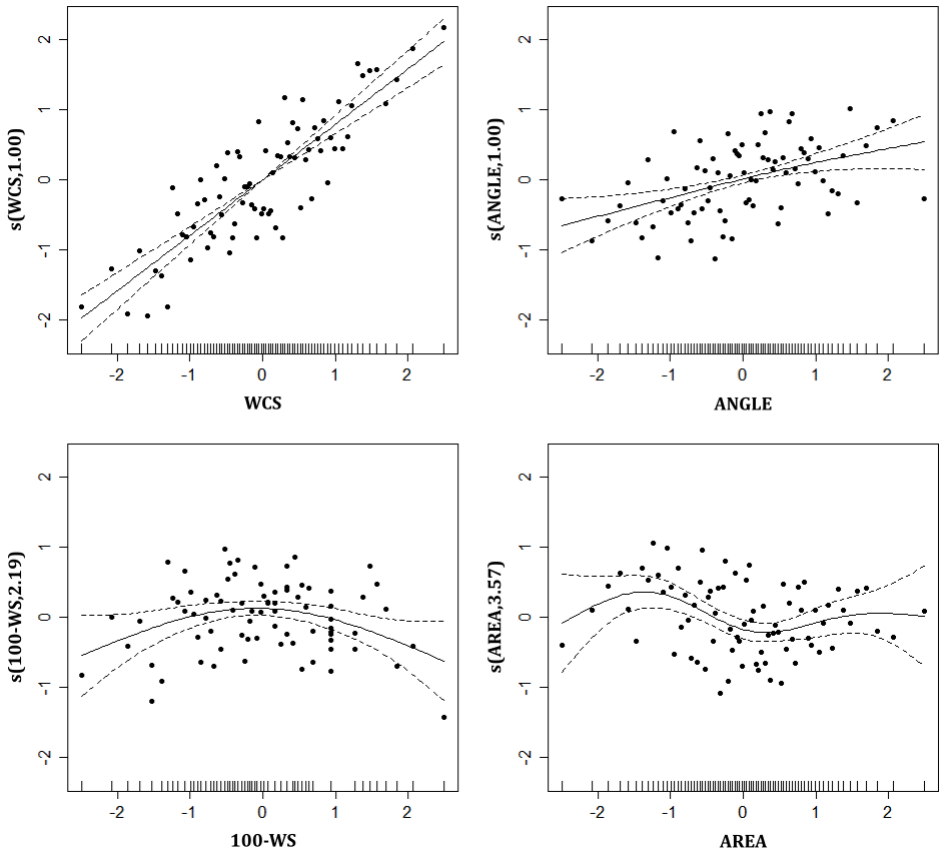

Figure 10.4 – Smooth functions of the 50-year skew surge quantile x_{50} for the explanatory variables included in the regional model ALL + GAM. The dotted lines represent the 95% confidence intervals. The vertical axes are named s(var,edf), var is the name of the explanatory variable and edf is the estimated degree of freedom of the smooth function.

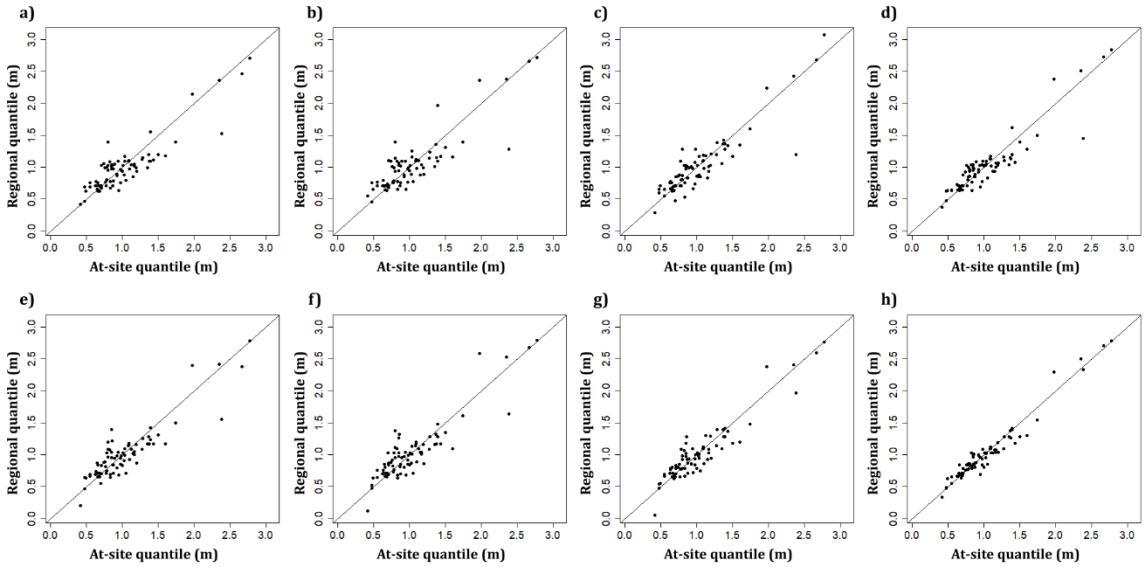

Figure 10.5 – Regional versus at-site skew surges quantiles x_{10}

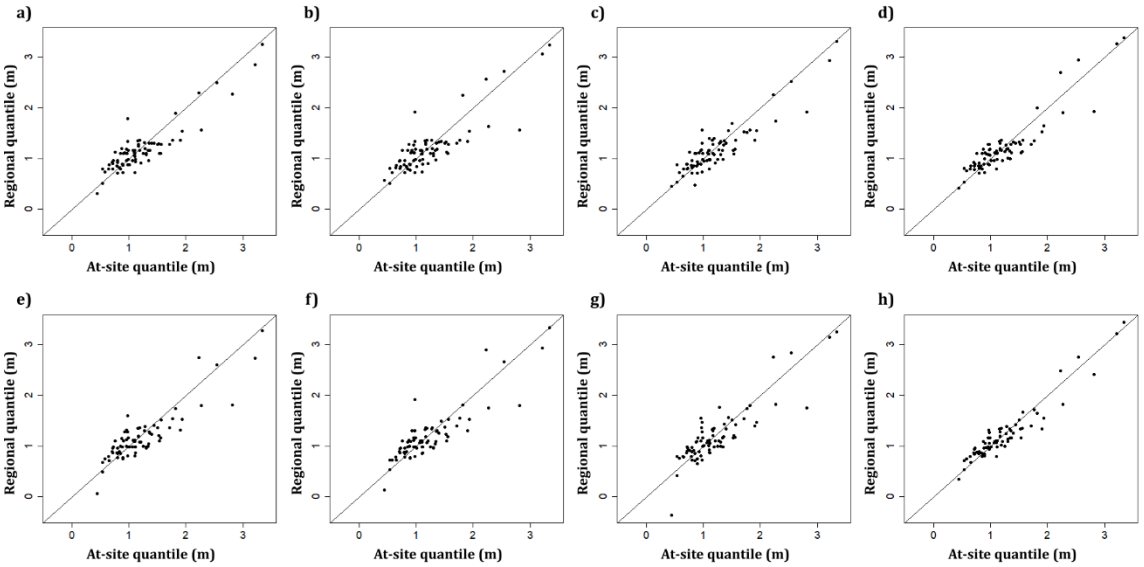

Figure 10.6 – Regional versus at-site skew surges quantiles x_{50}

a) ALL + MLR, b) CCA + MLR, c) HCA + MLR, d) ROI + MLR, e) ALL + GAM, f) CCA + GAM, g) HCA + GAM and h) ROI + GAM.

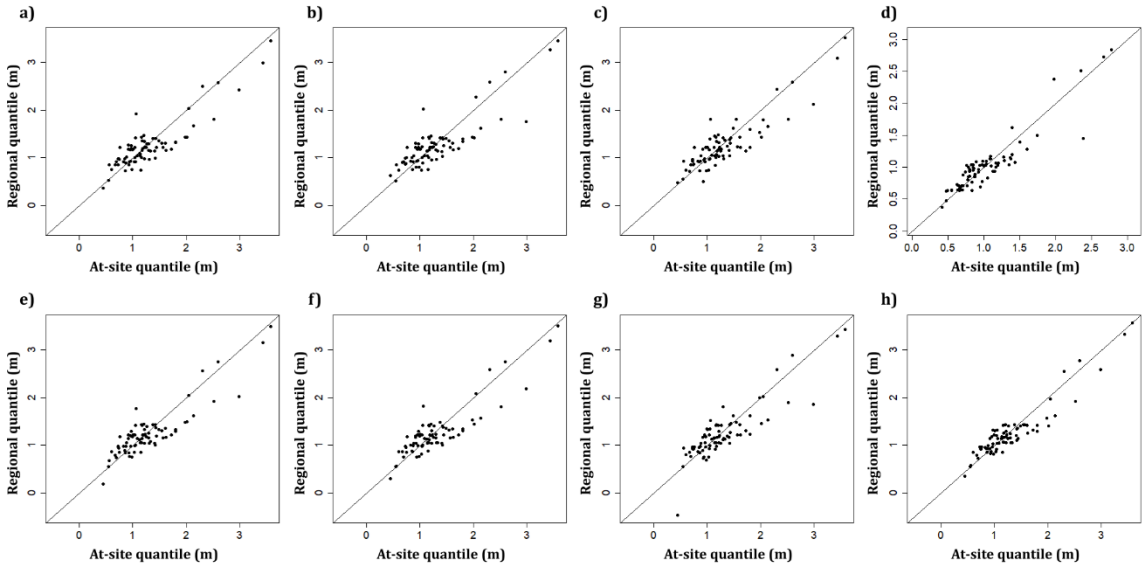

Figure 10.7 – Regional versus at-site skew surges quantiles x_{100}

a) ALL + MLR, b) CCA + MLR, c) HCA + MLR, d) ROI + MLR, e) ALL + GAM, f) CCA + GAM, g) HCA + GAM and h) ROI + GAM.

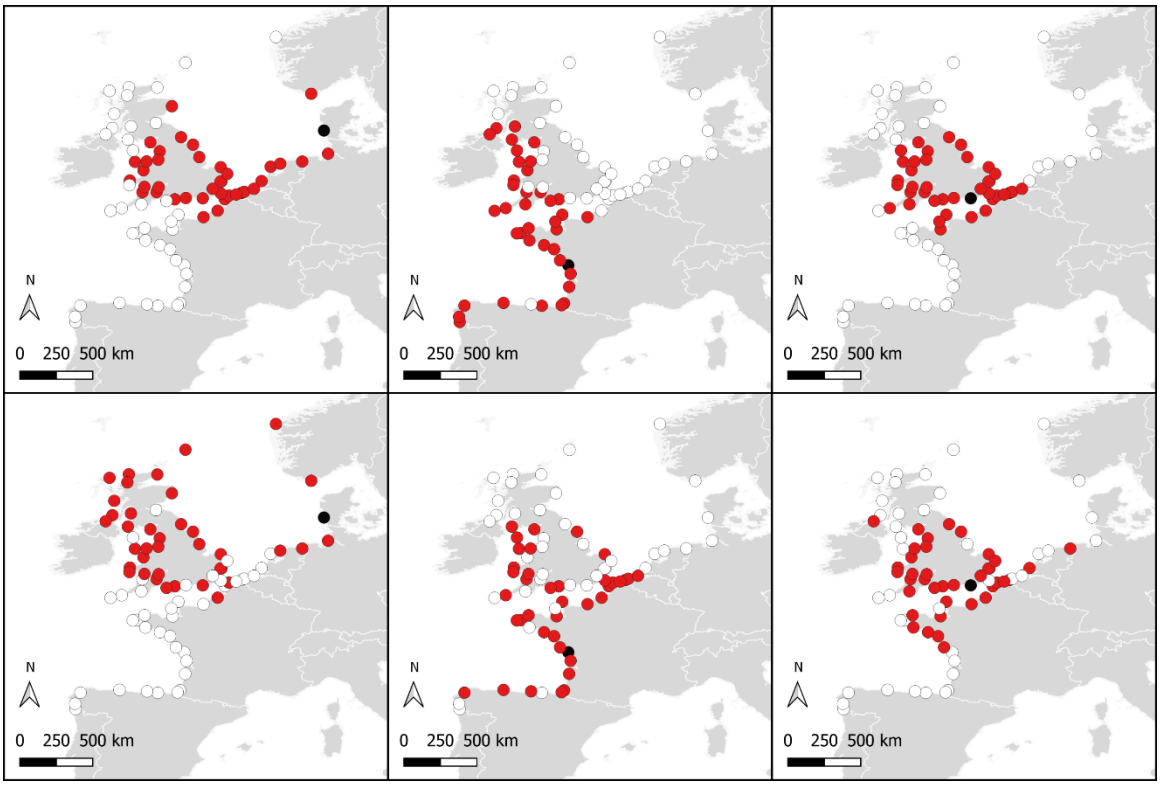

Figure 10.8 – Homogeneous regions centered on three tide gauges formed through ROI

Esbjerg (first column), La Rochelle (second column) and Newheaven (third column). $d_{ROI/MLR}$ the optimal distance obtained for MLR (first line) and $d_{ROI/GAM}$ the optimal distance obtained for GAM (second line).

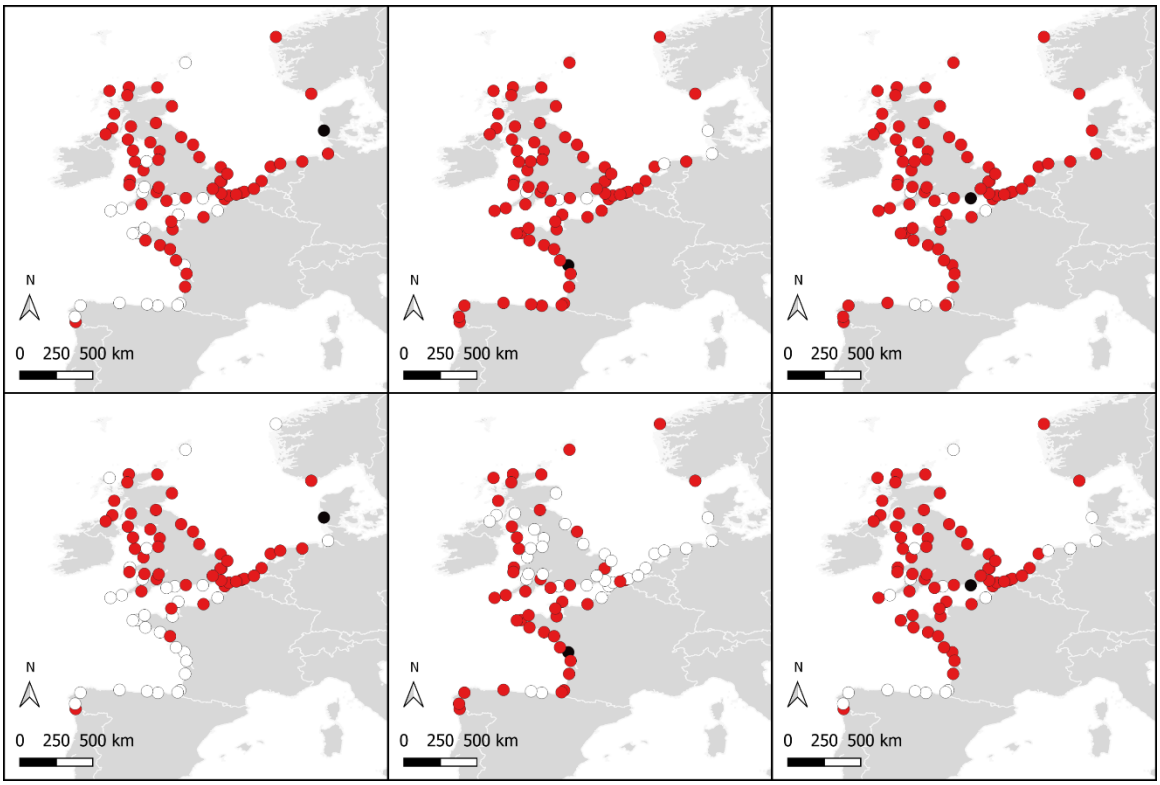

Figure 10.9 – Homogeneous regions centered on three tide gauges Esbjerg (first column), La Rochelle (second column) and Newheaven (third column). The variables retained for MLR (first line) and the variables retained for GAM (second line).

Chapitre 11

Annexe de l'article 4

11.1 Historical information

Table 11.1 – Record historical sea levels with their corresponding skew surges

Site	Date	Sea levels (m)	Skew surges (m)
Le Conquet	24-12-1999	7.63	0.54
Le Crouesty	08-12-2006	5.97	0.75
Le Crouesty	10-03-2008	6.59	0.80
Le Crouesty	09-02-2009	5.87	0.38

11.2 How to deal with dependent observations ?

The observations of the regional sample of the index method should be independent, but a same storm can frequently impact several sites and cause dependence between regional observations. In order to respect the hypothesis of independence of the observations in the regional sample, it is common to only keep the highest observation and discard the other ones within a certain period of time like 72h (Andreevsky et al., 2020 ; Bernardara et al., 2011 ; Weiss et al., 2014a ; Weiss et al., 2014b). This choice is suspected to lead to an overestimation of the quantile estimates. On the contrary, keeping all the dependent observations could introduce too much information and then underestimate the estimation uncertainties. These two methods for dealing with dependent observations are called MAX method (only the highest value is kept) and ALL method (all values are kept).

The comparison of the MAX and ALL methods is based on 1000 random samples generated through Monte Carlo simulations to evaluate the accuracy of the posterior credibility intervals inspired by six case studies. Figure 11.1a) shows the position (in the parameter space) of the six selected parameter sets (σ, ξ) among the 78 available. Each sample contains two series of length $n = 30$, $\alpha \times n$ observations are fully independent and $(1 - \alpha) \times n$ observations are dependent, α takes the following values 0.1, 0.5 and 0.9. The independent parts of both series are independently and randomly drawn by a GP(σ, ξ). The dependent parts of both series are randomly drawn by a bivariate GP (σ, ξ) with an extremal dependency function

approximating the Gumbel copula (see Figure 11.1b)). The R package *POT* (Ribatet, 2006) is used for the bivariate GPD

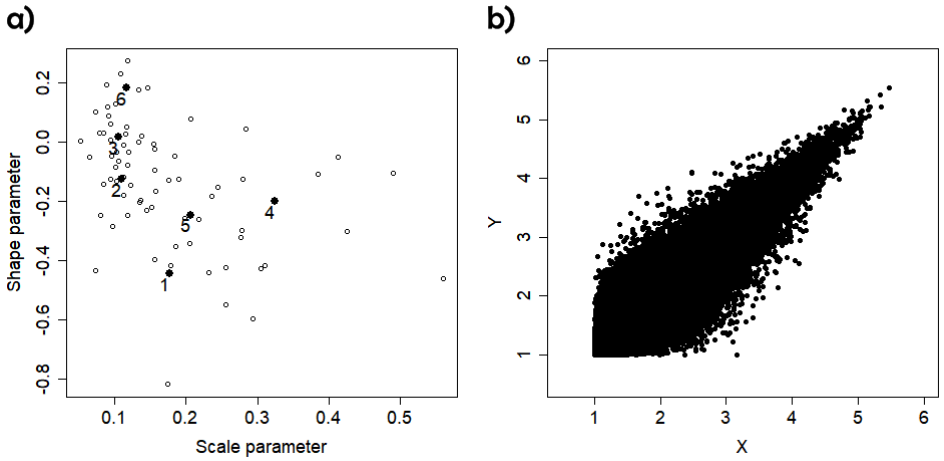

Figure 11.1 – Settings for simulations

a) Locally estimated parameters of the European tide gauges, the filled dots represent the selected tide gauges. b) Dependence function between two local series X and Y.

Similar results are obtained for all six parameter sets. For the sake of simplification, only the results of the sixth parameter set are presented herein (see Figure 11.2). For the same dependent part, the MAX method appears to overestimate the 100-year skew surge quantiles compared to the ALL method. The larger the dependent part, the larger the positive bias for the MAX method. As expected, the posterior credibility intervals obtained with the ALL method are too narrow and especially when the dependent part increases. In this present study, we choose to keep all the dependent observations (ALL method) to have an unbiased inference at the risk of minimizing uncertainties.

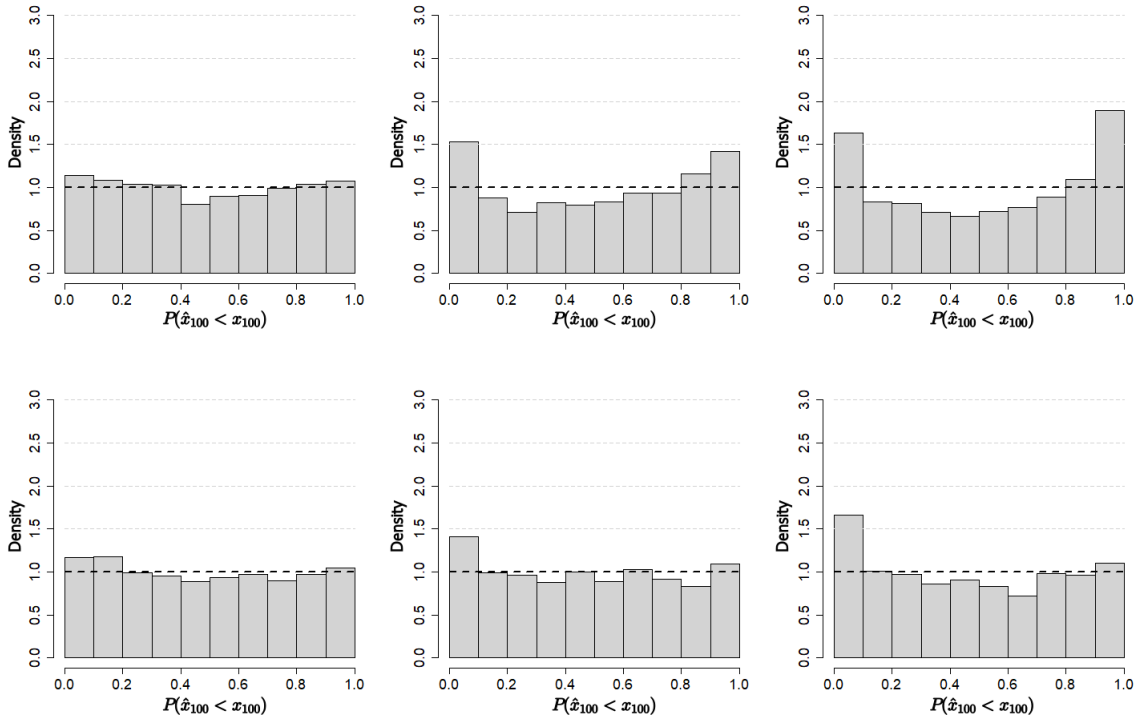

Figure 11.2 – Uniformity tests for the credibility intervals

Methods ALL (first line) and MAX (second line) according to the dependent part $\alpha = 0.1$ (first column), 0.5 (second column) and 0.9 (third column).

Chapitre 12

Information supplémentaire de l'article 4

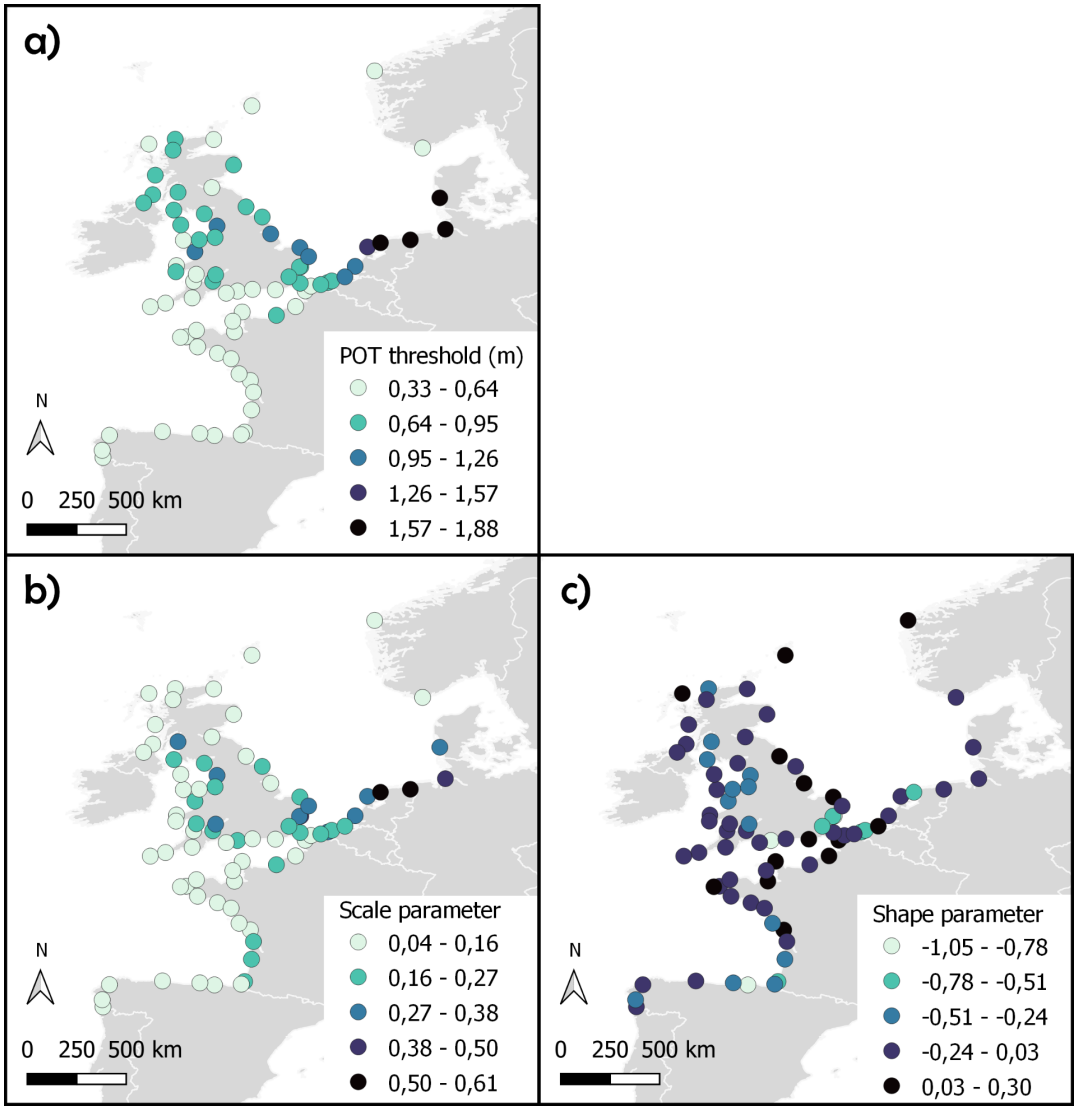

Figure 12.1 – Spatial distribution of the parameters at the European tide gauges

a) POT threshold u, b) GP scale parameter σ and c) GP shape parameter ξ

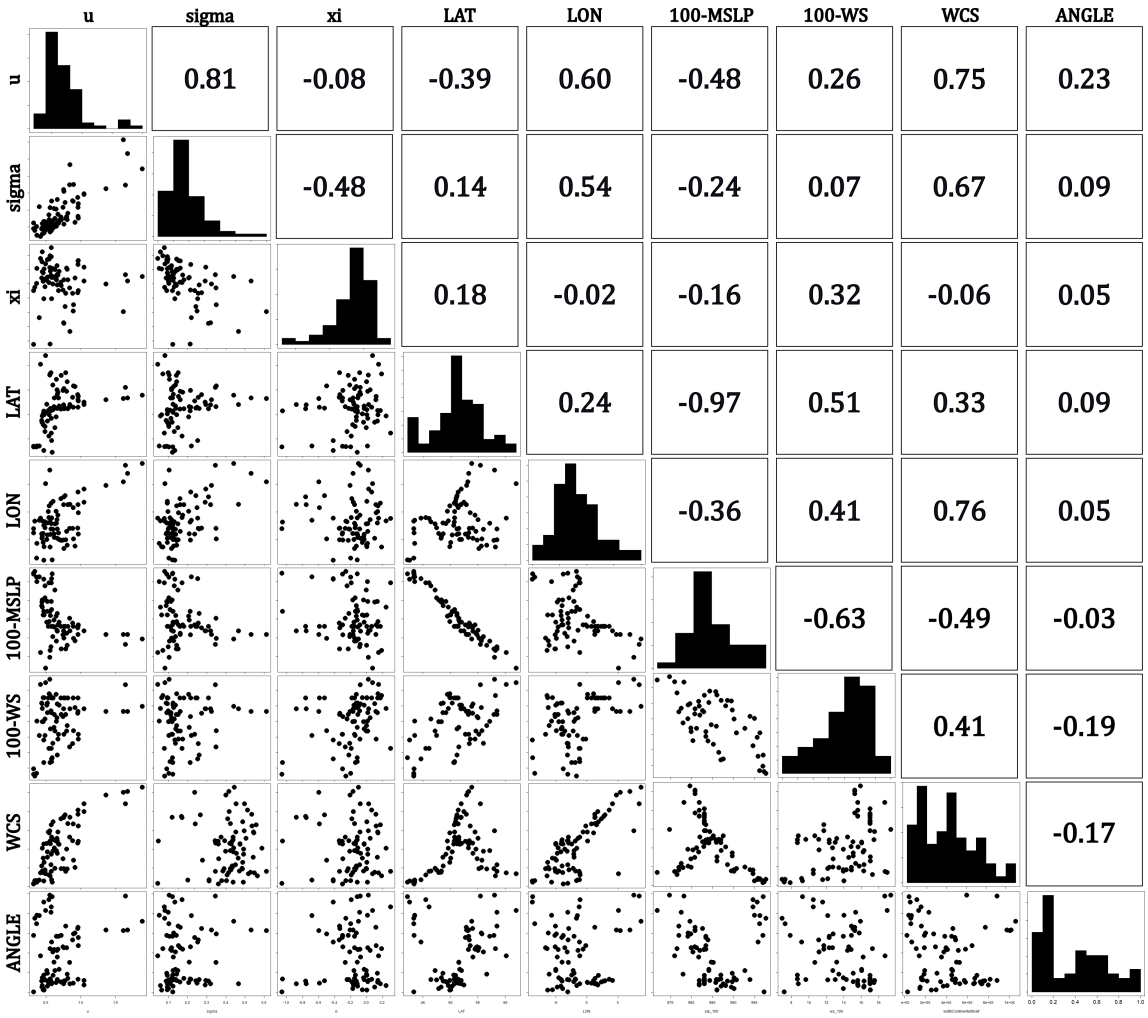

Figure 12.2 – Variable histograms, correlation coefficients and interrelations

For the explanatory physiographic-meteorological variables and the parameters of the skew surge distribution locally estimated.

Bibliographie

Aelbrecht, Denis, Michel Benoit et Jean Allilaire (2004). « Renforcement de la protection contre l'inondation du front de Gironde sur le site du Blayais : apports conjoints des modélisations physique et numérique ». In : *La Houille Blanche* 3, p. 37-44. DOI : 10.1051/lhb:200403004.

Ahn, Kuk-Hyun et Richard Palmer (2016). « Regional flood frequency analysis using spatial proximity and basin characteristics : Quantile regression vs. parameter regression technique ». In : *Journal of Hydrology* 540, p. 515-526. DOI : 10.1016/j.jhydrol.2016.06.047.

Ahn, Kuk-Hyun, Richard Palmer et Scott Steinschneider (2017). « A hierarchical Bayesian model for regionalized seasonal forecasts : Application to low flows in the northeastern United States : SEASONAL FORECASTS OF LOW FLOW ». In : *Water Resources Research* 53.1, p. 503-521. DOI : 10.1002/2016WR019605.

Andreevsky, Marc et al. (2020). « Regional frequency analysis of extreme storm surges using the extremogram approach ». In : *Natural Hazards and Earth System Sciences* 20.6, p. 1705-1717. DOI : 10.5194/nhess-20-1705-2020.

Andreewsky, Marc et al. (2014). « Comparaison de différentes méthodes d'estimation des niveaux extrêmes en site à fort et à faible marnage ». In : *La Houille Blanche* 4, p. 26-36. DOI : 10.1051/lhb/2014035.

Arns, A. et al. (2013). « Estimating extreme water level probabilities : A comparison of the direct methods and recommendations for best practise ». In : *Coastal Engineering* 81, p. 51-66. DOI : 10.1016/j.coastaleng.2013.07.003.

Arns, Arne et al. (2015). « Determining return water levels at ungauged coastal sites : a case study for northern Germany ». In : *Ocean Dynamics* 65.4, p. 539-554. DOI : 10.1007/s10236-015-0814-1.

Arns, Arne et al. (2020). « Non-linear interaction modulates global extreme sea levels, coastal flood exposure, and impacts ». In : *Nature Communications* 11.1, p. 1918. DOI : 10.1038/s41467-020-15752-5.

Banerjee, Sudipto, Bradley P. Carlin et Alan E. Gelfand (2015). *Hierarchical modeling and analysis for spatial data*. Second edition. Monographs on statistics and applied probability 135. Boca Raton : CRC Press, Taylor & Francis Group. 562 p. ISBN : 978-1-4398-1917-3.

Bardet, Lise et al. (2011). « Regional frequency analysis of extreme storm surges along the French coast ». In : *Natural Hazards and Earth System Sciences* 11.6, p. 1627-1639. DOI : 10.5194/nhess-11-1627-2011.

Batstone, Crispian et al. (2013). « A UK best-practice approach for extreme sea-level analysis along complex topographic coastlines ». In : *Ocean Engineering*. Sea Level Rise and Impacts on Engineering Practice 71, p. 28-39. DOI : 10.1016/j.oceaneng.2013.02.003.

Bellier, Joseph (2018). « Prévisions hydrologiques probabilistes dans un cadre multivarié : quels outils pour assurer fiabilité et cohérence spatio-temporelle ? » Thèse de doct.

Ben Daoued, Amine et al. (2020). « Modeling dependence and coincidence of storm surges and high tide : methodology, discussion and recommendations based on a simplified case study in Le Havre (France) ». In : *Natural Hazards and Earth System Sciences* 20.12. Publisher : Copernicus GmbH, p. 3387-3398. DOI : 10.5194/nhess-20-3387-2020.

Benito, Gerardo et al. (2004). « Use of Systematic, Palaeoflood and Historical Data for the Improvement of Flood Risk Estimation. Review of Scientific Methods ». In : *Natural Hazards* 31.3, p. 623-643. DOI : 10.1023/B:NHAZ.0000024895.48463.eb.

Bernardara, Pietro, Marc Andreewsky et Michel Benoit (2011). « Application of regional frequency analysis to the estimation of extreme storm surges ». In : *Journal of Geophysical Research : Oceans* 116 (C2). DOI : 10.1029/2010JC006229.

Breilh, Jean-François et al. (2014). « How frequent is storm-induced flooding in the central part of the Bay of Biscay ? » In : *Global and Planetary Change* 122, p. 161-175. DOI : 10.1016/j.gloplacha.2014.08.013.

Bulteau, T. et al. (2015). « How historical information can improve estimation and prediction of extreme coastal water levels : application to the Xynthia event at La Rochelle (France) ». In : *Natural Hazards and Earth System Sciences* 15.6, p. 1135-1147. DOI : 10.5194/nhess-15-1135-2015.

Burn, Donald H. (1989). « Cluster Analysis as Applied to Regional Flood Frequency ». In : *Journal of Water Resources Planning and Management* 115.5, p. 567-582. DOI : 10.1061/(ASCE)0733-9496(1989)115:5(567).

– (1990a). « An appraisal of the "region of influence" approach to flood frequency analysis ». In : *Hydrological Sciences Journal* 35.2, p. 149-165. DOI : 10.1080/02626669009492415.

– (1990b). « Evaluation of regional flood frequency analysis with a region of influence approach ». In : *Water Resources Research* 26.10, p. 2257-2265. DOI : 10.1029/WR026i010p02257.

Calafat, Francisco M. et Marta Marcos (2020). « Probabilistic reanalysis of storm surge extremes in Europe ». In : *Proceedings of the National Academy of Sciences* 117.4, p. 1877-1883.

Chebana, Fateh et Taha B. M. J. Ouarda (2009). « Index flood–based multivariate regional frequency analysis ». In : *Water Resources Research* 45.10. DOI : 10.1029/2008WR007490.

Chokmani, Karem et Taha B. M. J. Ouarda (2004). « Physiographical space-based kriging for regional flood frequency estimation at ungauged sites ». In : *Water Resources Research* 40.12. DOI : 10.1029/2003WR002983.

Clancy, Colm et al. (2016). « Spatial Bayesian hierarchical modelling of extreme sea states ». In : *Ocean Modelling* 107, p. 1-13. DOI : 10.1016/j.ocemod.2016.09.015.

Coles, Stuart (2001). *An Introduction to Statistical Modeling of Extreme Values*. Berlin : Springer Science & Business Media. ISBN : 978-1-85233-459-8.

Cooley, Daniel, Douglas Nychka et Philippe Naveau (2007). « Bayesian Spatial Modeling of Extreme Precipitation Return Levels ». In : *Journal of the American Statistical Association* 102.479, p. 824-840. DOI : 10.1198/016214506000000780.

Cunnane, Conleth (1988). « Methods and merits of regional flood frequency analysis ». In : *Journal of Hydrology* 100.1, p. 269-290. DOI : 10.1016/0022-1694(88)90188-6.

Dalrymple, Tate (1960). *Flood frequency analysis*. U.S. Geological Survey Water Supply Paper, p. 11-51.

D'Arcy, Eleanor et al. (20 juill. 2022). *Accounting for Seasonality in Extreme Sea Level Estimation*. DOI : 10.48550/arXiv.2207.09870. arXiv : 2207.09870[stat]. URL : http://arxiv.org/abs/2207.09870 (visité le 22/07/2022).

Das, Samiran, Dehua Zhu et Yixing Yin (2020). « Comparison of mapping approaches for estimating extreme precipitation of any return period at ungauged locations ». In : *Stochastic Environmental Research and Risk Assessment* 34.8, p. 1175-1196. DOI : 10.1007/s00477-020-01828-7.

De Zolt, S. et al. (2006). « The disastrous storm of 4 November 1966 on Italy ». In : *Natural Hazards and Earth System Sciences* 6.5, p. 861-879. DOI : 10.5194/nhess-6-861-2006.

Desai, Shitanshu et Taha B. M. J. Ouarda (2021). « Regional hydrological frequency analysis at ungauged sites with random forest regression ». In : *Journal of Hydrology* 594, p. 125861. DOI : 10.1016/j.jhydrol.2020.125861.

Dixon, Mark J. et Jonathan A. Tawn (1994). « Extreme sea-levels at the UK A-class sites : site-by-site analyses ». In.

– (1999). « The Effect of Non-Stationarity on Extreme Sea-Level Estimation ». In : *Journal of the Royal Statistical Society : Series C (Applied Statistics)* 48.2, p. 135-151. DOI : 10.1111/1467-9876.00145.

Enríquez, Alejandra R. et al. (2020). « Spatial Footprints of Storm Surges Along the Global Coastlines ». In : *Journal of Geophysical Research : Oceans* 125.9. DOI : 10.1029/2020JC016367.

Frau, Roberto, Marc Andreewsky et Pietro Bernardara (2018). « The use of historical information for regional frequency analysis of extreme skew surge ». In : *Natural Hazards and Earth System Sciences* 18.3, p. 949-962. DOI : 10.5194/nhess-18-949-2018.

Fu, Ying et al. (2017). « Analysis and Prediction of Changes in Coastline Morphology in the Bohai Sea, China, Using Remote Sensing ». In : *Sustainability* 9.6, p. 900. DOI : 10.3390/su9060900.

Gaume, Eric (2018). « Flood frequency analysis : The Bayesian choice ». In : *Wiley Interdisciplinary Reviews : Water* 5.4. DOI : 10.1002/wat2.1290.

Gaume, Eric et al. (2010). « Bayesian MCMC approach to regional flood frequency analyses involving extraordinary flood events at ungauged sites ». In : *Journal of Hydrology* 394, p. 101-117. DOI : 10.1016/j.jhydrol.2010.01.008.

Gaál, Ladislav et al. (2010). « Inclusion of historical information in flood frequency analysis using a Bayesian MCMC technique : a case study for the power dam Orlík, Czech Republic ». In : *Contributions to Geophysics and Geodesy* 40, p. 121-147. DOI : 10.2478/v10126-010-0005-5.

GELMAN, Andrew et al. (2014). *Bayesian Data Analysis, Third edition*. Chapman and Hall/CRC 397 Press. Boca Raton.

GERRITSEN, Herman (2005). « What happened in 1953 ? The Big Flood in the Netherlands in retrospect ». In : *Philosophical Transactions of the Royal Society A : Mathematical, Physical and Engineering Sciences* 363.1831, p. 1271-1291. DOI : 10.1098/rsta.2005.1568.

GILOY, Nathalie et al. (2018). « La base de données TEMPETES : un support pour une expertise collégiale et interdisciplinaire des informations historiques de tempêtes et de submersions ». In : XVèmes Journées Nationales Génie Côtier – Génie Civil. DOI : 10.5150/jngcgc.2018.093.

GILOY, Nathalie et al. (2019). « Quantifying historic skew surges : an example for the Dunkirk Area, France ». In : *Natural Hazards* 98.3, p. 869-893. DOI : 10.1007/s11069-018-3527-1.

GIRARD, Claude, Taha B. M. J. OUARDA et Bernard BOBÉE (2004). « Étude du biais dans le modèle log-linéaire d'estimation régionale ». In : *Canadian Journal of Civil Engineering* 31.2, p. 361-368. DOI : 10.1139/l03-099.

GREHYS (1996a). « Inter-comparison of regional flood frequency procedures for Canadian rivers ». In : *Journal of Hydrology* 186.1, p. 85-103. DOI : 10.1016/S0022-1694(96)03043-0.

– (1996b). « Presentation and review of some methods for regional flood frequency analysis ». In : *Journal of Hydrology* 186.1, p. 63-84. DOI : 10.1016/S0022-1694(96)03042-9.

GROVER, Patrick L., Donald H. BURN et Juraj M. CUNDERLIK (2002). « A comparison of index flood estimation procedures for ungauged catchments ». In : *Canadian Journal of Civil Engineering* 29.5, p. 734-741. DOI : 10.1139/l02-065.

HADDAD, Khaled et Ataur RAHMAN (2012). « Regional flood frequency analysis in eastern Australia : Bayesian GLS regression-based methods within fixed region and ROI framework – Quantile Regression vs. Parameter Regression Technique ». In : *Journal of Hydrology* 430-431, p. 142-161. DOI : 10.1016/j.jhydrol.2012.02.012.

HAIGH, Ivan D., Robert NICHOLLS et Neil WELLS (2010). « A comparison of the main methods for estimating probabilities of extreme still water levels ». In : *Coastal Engineering* 57.9, p. 838-849. DOI : 10.1016/j.coastaleng.2010.04.002.

HAIGH, Ivan D. et al. (2016). « Spatial and temporal analysis of extreme sea level and storm surge events around the coastline of the UK ». In : *Scientific Data* 3.1, p. 160107. DOI : 10.1038/sdata.2016.107.

HAIGH, Ivan David et al. (2017). *An improved database of coastal flooding in the United Kingdom from 1915 to 2016*.

HALBERT, K. et al. (2016). « Reducing uncertainty in flood frequency analyses : A comparison of local and regional approaches involving information on extreme historical floods ». In : *Journal of Hydrology*. Flash floods, hydro-geomorphic response and risk management 541, p. 90-98. DOI : 10.1016/j.jhydrol.2016.01.017.

HAMDI, Y. et al. (2016). « Use of the spatial extremogram to form a homogeneous region centered on a target site for the regional frequency analysis of extreme storm surges ». In : *International Journal of Safety and Security Engineering* 6.4, p. 777-781. DOI : 10.2495/SAFE-V6-N4-777-781.

Hamdi, Yasser (2019). *Estimation des niveaux marins extrêmes - Utilisation de l'information régionale et historique*. IRSN 00325.

Hamdi, Yasser et al. (2014). « Extreme storm surges : a comparative study of frequency analysis approaches ». In : *Natural Hazards and Earth System Sciences* 14.8, p. 2053-2067. doi : 10.5194/nhess-14-2053-2014.

– (2015). « Use of historical information in extreme-surge frequency estimation : the case of marine flooding on the La Rochelle site in France ». In : *Natural Hazards and Earth System Sciences* 15.7, p. 1515-1531. doi : 10.5194/nhess-15-1515-2015.

Hamdi, Yasser et al. (2018). « Analysis of the risk associated with coastal flooding hazards : a new historical extreme storm surges dataset for Dunkirk, France ». In : *Natural Hazards and Earth System Sciences* 18.12, p. 3383-3402. doi : 10.5194/nhess-18-3383-2018.

Hamdi, Yasser et al. (2019). « Development of a target-site-based regional frequency model using historical information ». In : *Natural Hazards* 98.3, p. 895-913. doi : 10.1007/s11069-018-3237-8.

Han, Xudong et al. (2020). « A Network Approach for Delineating Homogeneous Regions in Regional Flood Frequency Analysis ». In : *Water Resources Research* 56.3. doi : 10.1029/2019WR025910.

Hastie, Trevor et Robert Tibshirani (1986). « Generalized Additive Models ». In : *Statistical Science* 1.3, p. 297-310. doi : 10.1214/ss/1177013604.

Hinkel, Jochen et al. (2014). « Coastal flood damage and adaptation costs under 21st century sea-level rise ». In : *Proceedings of the National Academy of Sciences* 111.9. Publisher : Proceedings of the National Academy of Sciences, p. 3292-3297. doi : 10.1073/pnas.1222469111.

Holmes, M. G. R. et al. (2002). « A region of influence approach to predicting flow duration curves within ungauged catchments ». In : *Hydrology and Earth System Sciences* 6.4, p. 721-731. doi : 10.5194/hess-6-721-2002.

Holmes, M. G. R. et al. (2005). « A catchment-based water resource decision-support tool for the United Kingdom ». In : *Environmental Modelling & Software*. Policies and Tools for Sustainable Water Management in the European Union 20.2, p. 197-202. doi : 10.1016/j.envsoft.2003.04.001.

Hosking, J. R. M. et J. R. Wallis (1988). « The effect of intersite dependence on regional flood frequency analysis ». In : *Water Resources Research* 24.4, p. 588-600. doi : 10.1029/WR024i004p00588.

Hosking, J. R. M. et J.R. Wallis (1997). *Regional Frequency Analysis. An approach based on L-moments*. Cambridge University Press.

Hosking, J. R.M. et J. R. Wallis (1987). « Parameter and Quantile Estimation for the Generalized Pareto Distribution ». In : *Technometrics* 29.3, p. 339-349. doi : 10.1080/00401706.1987.10488243.

Idier, Deborah, Franck Dumas et Heloise Muller (2012). « Tide-surge interaction in the English Channel ». In : *Natural Hazards And Earth System Sciences* 12.12, p. 3709-3718. doi : 10.5194/nhess-12-3709-2012.

Kergadallan, Xavier et al. (2014). « Improving the estimation of extreme sea levels by a characterization of the dependence of skew surges on high tidal levels ». In : *Coastal Engineering Proceedings* 1, p. 48. DOI : 10.9753/icce.v34.management.48.

Kjeldsen, T. R, J. C Smithers et R. E Schulze (2002). « Regional flood frequency analysis in the KwaZulu-Natal province, South Africa, using the index-flood method ». In : *Journal of Hydrology* 255.1, p. 194-211. DOI : 10.1016/S0022-1694(01)00520-0.

Kolen, B., R. Slomp et S. N. Jonkman (2013). « The impacts of storm Xynthia February 27–28, 2010 in France : lessons for flood risk management ». In : *Journal of Flood Risk Management* 6.3, p. 261-278. DOI : doi.org/10.1111/jfr3.12011.

Kuswanto, Heri et al. (2021). « Drought Analysis in East Nusa Tenggara (Indonesia) Using Regional Frequency Analysis ». In : *The Scientific World Journal* 2021. Publisher : Hindawi, e6626102. DOI : 10.1155/2021/6626102.

Lima, Carlos H. R. et al. (2016). « A hierarchical Bayesian GEV model for improving local and regional flood quantile estimates ». In : *Journal of Hydrology* 541, p. 816-823. ISSN : 0022-1694. DOI : 10.1016/j.jhydrol.2016.07.042.

Liu, Joan C., Barbara J. Lence et Michael Isaacson (2010). « Direct Joint Probability Method for Estimating Extreme Sea Levels ». In : *Journal of Waterway, Port, Coastal, and Ocean Engineering* 136.1, p. 66-76. DOI : 10.1061/(ASCE)0733-950X(2010)136:1(66).

Love, Charlotte A. et al. (2020). « Integrating Climatic and Physical Information in a Bayesian Hierarchical Model of Extreme Daily Precipitation ». In : *Water* 12.8. Number : 8 Publisher : Multidisciplinary Digital Publishing Institute, p. 2211. DOI : 10.3390/w12082211.

Lucas, C., G. Muraleedharan et C. Guedes Soares (2017). « Regional frequency analysis of extreme waves in a coastal area ». In : *Coastal Engineering* 126, p. 81-95. DOI : 10.1016/j.coastaleng.2017.06.002.

Lumbroso, Darren M. et al. (2019). « The challenges of including historical events using Bayesian methods to improve flood flow estimates in the United Kingdom : A practitioner's point of view ». In : *Journal of Flood Risk Management* 12 (S1), e12525. ISSN : 1753-318X. DOI : 10.1111/jfr3.12525.

Madsen, Henrik et Dan Rosbjerg (1997). « The partial duration series method in regional index-flood modeling ». In : *Water Resources Research* 33.4, p. 737-746. DOI : 10.1029/96WR03847.

Mai Van, Cong, Pieter Van Gelder et Han Vrijling (2007). « Statistical methods to estimate extreme quantile values of the sea data ». In.

Marra, Giampiero et Simon N. Wood (2011). « Practical variable selection for generalized additive models ». In : *Computational Statistics & Data Analysis* 55.7, p. 2372-2387. DOI : 10.1016/j.csda.2011.02.004.

Mazas, Franck et al. (2014). « Applying POT methods to the Revised Joint Probability Method for determining extreme sea levels ». In : *Coastal Engineering* 91, p. 140-150. DOI : 10.1016/j.coastaleng.2014.05.006.

Mediero, Luis et Thomas R. Kjeldsen (2014). « Regional flood hydrology in a semi-arid catchment using a GLS regression model ». In : *Journal of Hydrology* 514, p. 158-171. DOI : 10.1016/j.jhydrol.2014.04.007.

Merz, Ralf et Günter Blöschl (2008a). « Flood frequency hydrology : 1. Temporal, spatial, and causal expansion of information : FLOOD FREQUENCY HYDROLOGY, 1 ». In : *Water Resources Research* 44.8. doi : 10.1029/2007WR006744.

– (2008b). « Flood frequency hydrology : 2. Combining data evidence ». In : *Water Resources Research* 44.8. doi : 10.1029/2007WR006745.

Mo, H. M., W. Ye et H. P. Hong (2022). « Estimating and mapping snow hazard based on at-site analysis and regional approaches ». In : *Natural Hazards* 111.3, p. 2459-2485. issn : 1573-0840. doi : 10.1007/s11069-021-05144-3.

Mojena, R. (1977). « Hierarchical grouping methods and stopping rules : an evaluation ». In : *The Computer Journal* 20.4, p. 359-363. doi : 10.1093/comjnl/20.4.359.

Msilini, Amina, Taha B. M. J. Ouarda et Pierre Masselot (2022). « Evaluation of additional physiographical variables characterising drainage network systems in regional frequency analysis, a Quebec watersheds case-study ». In : *Stochastic Environmental Research and Risk Assessment* 36.2, p. 331-351. doi : 10.1007/s00477-021-02109-7.

Muirhead, Robb J., éd. (1982). *Aspects of Multivariate Statistical Theory*. Wiley Series in Probability and Statistics. Hoboken, NJ, USA : John Wiley & Sons, Inc. isbn : 978-0-470-31655-9 978-0-471-09442-5. doi : 10.1002/9780470316559.

Muis, Sanne et al. (2016). « A global reanalysis of storm surges and extreme sea levels ». In : *Nature Communications* 7.1, p. 11969. issn : 2041-1723. doi : 10.1038/ncomms11969.

Naulet, Robin et al. (2005). « Flood frequency analysis on the Ardèche river using French documentary sources from the last two centuries ». In : *Journal of Hydrology*. Palaeofloods, hystorical data & climate variability : Applications in flood risk assessment 313.1, p. 58-78. doi : 10.1016/j.jhydrol.2005.02.011.

Neppel, Luc et al. (2010). « Flood frequency analysis using historical data : accounting for random and systematic errors ». In : *Hydrological Sciences Journal* 55.2, p. 192-208. doi : 10.1080/02626660903546092.

Nezhad, M. Kamali et al. (2010). « Regional flood frequency analysis using residual kriging in physiographical space ». In : *Hydrological Processes*. doi : 10.1002/hyp.7631.

Nguyen, C.C., E. Gaume et O. Payrastre (2014). « Regional flood frequency analyses involving extraordinary flood events at ungauged sites : further developments and validations ». In : *Journal of Hydrology* 508, p. 385-396. doi : 10.1016/j.jhydrol.2013.09.058.

Nguyen, Chi Cong, Olivier Payrastre et Eric Gaume (2013). « Inventories of extreme floods at ungauged sites and regional flood frequency analyses : methodological reflections and evaluation of performances ». In : *La Houille Blanche* 99.2, p. 16-23. doi : 10.1051/lhb/2013011.

– (2015). « Reducing uncertainties on low-probability flood peak discharge quantile estimates : comparison of historical and/or regional approaches ». In : *La Houille Blanche* 101.3, p. 64-71. doi : 10.1051/lhb/20150035.

O'Connell, Daniel R. H. et al. (2002). « Bayesian flood frequency analysis with paleohydrologic bound data ». In : *Water Resources Research* 38.5, p. 16-1-16-13. issn : 1944-7973. doi : 10.1029/2000WR000028.

Odry, Jean et Patrick Arnaud (2017). « Comparison of Flood Frequency Analysis Methods for Ungauged Catchments in France ». In : *Geosciences* 7.3, p. 88. doi : 10.3390/geosciences7030088.

Ouali, Dhouha, Fateh Chebana et Taha B. M. J. Ouarda (2016). « Non-linear canonical correlation analysis in regional frequency analysis ». In : *Stochastic Environmental Research and Risk Assessment* 30.2, p. 449-462. doi : 10.1007/s00477-015-1092-7.

– (2017). « Fully nonlinear statistical and machine-learning approaches for hydrological frequency estimation at ungauged sites ». In : *Journal of Advances in Modeling Earth Systems* 9.2, p. 1292-1306. doi : 10.1002/2016MS000830.

Ouarda, Taha B. M. J. (2016). « Regional Flood Frequency Modeling ». In : *Handbook of Applied Hydrology*.

Ouarda, Taha B. M. J. et Fahim Ashkar (1998a). « Effect of Trimming on LP III Flood Quantile Estimates ». In : *Journal of Hydrologic Engineering* 3.1, p. 33-42. doi : 10.1061/(ASCE)1084-0699(1998)3:1(33).

Ouarda, Taha B. M. J. et al. (1998b). « Utilisation de l'information historique en analyse hydrologique fréquentielle ». In : *Revue des sciences de l'eau* 11, p. 41. doi : 10.7202/705328ar.

Ouarda, Taha B. M. J. et al. (2000). « Regional Flood Peak and Volume Estimation in Northern Canadian Basin ». In : *Journal of Cold Regions Engineering* 14.4, p. 176-191. doi : 10.1061/(ASCE)0887-381X(2000)14:4(176).

Ouarda, Taha B. M. J. et al. (2001). « Regional Flood Frequency Estimation With Canonial Correlation Analysis ». In : *Journal of Hydrology* 254, p. 157-173. doi : 10.1016/S0022-1694(01)00488-7.

Ouarda, Taha B. M. J. et al. (2006). « Data-based comparison of seasonality-based regional flood frequency methods ». In : *Journal of Hydrology* 1-2.330, p. 329-339. doi : 10.1016/j.jhydrol.2006.03.023.

Ouarda, Taha B. M. J. et al. (2008). « Intercomparison of regional flood frequency estimation methods at ungauged sites for a Mexican case study ». In : *Journal of Hydrology* 348.1, p. 40-58. issn : 0022-1694. doi : 10.1016/j.jhydrol.2007.09.031. url : https://www.sciencedirect.com/science/article/pii/S0022169407005331 (visité le 10/05/2022).

Ouarda, Taha B. M. J. et al. (2018). « Introduction of the GAM model for regional low-flow frequency analysis at ungauged basins and comparison with commonly used approaches ». In : *Environmental Modelling & Software* 109, p. 256-271. doi : 10.1016/j.envsoft.2018.08.031.

Outten, Stephen et al. (2020). *Re-assessing extreme sea level events through interplay of tides and storm surges*.

Pante, Eric et Benoit Simon-Bouhet (2013). « marmap : A Package for Importing, Plotting and Analyzing Bathymetric and Topographic Data in R ». In : *PLoS ONE* 8.9. Sous la dir. de Guy J.-P. Schumann. doi : 10.1371/journal.pone.0073051.

Parent, Eric et Jacques Bernier (2003). « Bayesian POT modeling for historical data ». In : *Journal of Hydrology* 274.1, p. 95-108. doi : 10.1016/S0022-1694(02)00396-7.

Payrastre, O., Eric Gaume et Herve Andrieu (2011). « Usefulness of historical information for flood frequency analyses : Developments based on a case study ». In : *Water Resources Research* 47. doi : 10.1029/2010WR009812.

– (2013). « Historical information and flood frequency analyses : which optimal features for historical floods inventories ? » In : *La Houille Blanche*, p. 5-11. doi : 10.1051/lhb/2013019.

Peterson A., Ryan (2021). « Finding Optimal Normalizing Transformations via bestNormalize ». In : *The R Journal* 13.1, p. 310. issn : 2073-4859. doi : 10.32614/RJ-2021-041.

Peterson, Ryan A. et Joseph E. Cavanaugh (2020). « Ordered quantile normalization : a semiparametric transformation built for the cross-validation era ». In : *Journal of Applied Statistics* 47.13, p. 2312-2327. issn : 0266-4763, 1360-0532. doi : 10.1080/02664763.2019.1630372.

Potter, Kenneth W. et Dennis P. Lettenmaier (1990). « A Comparison of regional flood frequency estimation methods using a resampling method ». In : *Water Resources Research* 26.3, 415_424.

Pugh, David (1987). *Tides, surges, and mean sea-level*. Chichester ; New York : J. Wiley. 472 p. isbn : 978-0-471-91505-8.

Pugh, D.T. et J.M. Vassie (1978). « Extreme sea levels from tide and surge probability ». In : *Coastal Engineering Proceedings* 1.16, p. 52. doi : 10.9753/icce.v16.52.

Pugh, Dt et Jm Vassie (1980). « Applications of the joint probability method for extreme sea level computations ». In : *Proceedings of the Institution of Civil Engineers* 69.4, p. 959-975. doi : 10.1680/iicep.1980.2179.

Rao, A. Ramachandra et Khaled H. Hamed (2019). *Flood Frequency Analysis*. Boca Raton : CRC Press. 376 p. isbn : 978-0-429-12881-3.

Reich, Brian J. et Benjamin A. Shaby (2012). « A hierarchical max-stable spatial model for extreme precipitation ». In : *The Annals of Applied Statistics* 6.4, p. 1430-1451. doi : 10.1214/12-AOAS591.

Reis, Dirceu et Jery Stedinger (2005). « Bayesian MCMC Flood Frequency Analysis With Historical Information ». In : *Journal of Hydrology* 313, p. 97-116. doi : 10.1016/j.jhydrol.2005.02.028.

Renard, B. (2011). « A Bayesian hierarchical approach to regional frequency analysis ». In : *Water Resources Research* 47.11. doi : 10.1029/2010WR010089.

Rencher, Alvin C. et William F. Christensen (2012). *Methods of multivariate analysis*. Third Edition. Wiley series in probability and statistics. Hoboken, New Jersey : Wiley. 758 p. isbn : 978-0-470-17896-6.

Reza Najafi, Mohammad et Hamid Moradkhani (2013). « Analysis of runoff extremes using spatial hierarchical Bayesian modeling : Hierarchical Bayesian Model of Flood ». In : *Water Resources Research* 49.10, p. 6656-6670. doi : 10.1002/wrcr.20381.

Ribatet, M.A. (2006). *A User's Guide to the POT Package (Version 1.0)*.

Ribatet, Mathieu et al. (2007). « A regional Bayesian POT model for flood frequency analysis ». In : *Stochastic Environmental Research and Risk Assessment* 21.4, p. 327-339. doi : 10.1007/s00477-006-0068-z. arXiv : 0802.0433[stat].

Ribeiro-Corréa, J. et al. (1995). « Identification of hydrological neighborhoods using canonical correlation analysis ». In : *Journal of Hydrology* 173.1, p. 71-89. DOI : 10.1016/0022-1694(95)02719-6.

Sabourin, Anne et Benjamin Renard (2015). « Combining regional estimation and historical floods : A multivariate semiparametric peaks-over-threshold model with censored data ». In : *Water Resources Research* 51.12, p. 9646-9664. DOI : 10.1002/2015WR017320.

Saint Criq, Laurie et al. (2022a). « Extreme Sea Level Estimation Combining Systematic Observed Skew Surges and Historical Record Sea Levels ». In : *Water Resources Research* 58.3. DOI : 10.1029/2021WR030873.

Saint Criq, Laurie et al. (2022b). « Extreme skew surge estimation combining systematic skew surges and historical record sea levels on the English Channel and North Sea coasts ». In : *Journal of Flood Risk Management* (Flood risk and resilience in coastal zones and tropical islands). In press.

Saint Criq, Laurie et al. (2022c). « Regional frequency analysis of extreme skew surges at ungauged locations ». In : On the review.

Schendel, Thomas et Rossukon Thongwichian (2017). « Considering historical flood events in flood frequency analysis : Is it worth the effort ? » In : *Advances in Water Resources* 105, p. 144-153. DOI : 10.1016/j.advwatres.2017.05.002.

Seidou, O. et al. (2006). « A parametric Bayesian combination of local and regional information in flood frequency analysis ». In : *Water Resources Research* 42.11. DOI : 10.1029/2005WR004397.

Shao, Kan (2012). « A comparison of three methods for integrating historical information for Bayesian model averaged benchmark dose estimation ». In : *Environmental Toxicology and Pharmacology* 34.2, p. 288-296. DOI : 10.1016/j.etap.2012.05.002.

Sharkey, Paul et Hugo C. Winter (2019). « A Bayesian spatial hierarchical model for extreme precipitation in Great Britain : A Bayesian hierarchical model for extreme precipitation ». In : *Environmetrics* 30.1, e2529. DOI : 10.1002/env.2529.

Shu, Chang et Donald H. Burn (2004). « Artificial neural network ensembles and their application in pooled flood frequency analysis ». In : *Water Resources Research*.

Shu, Chang et Taha B. M. J. Ouarda (2007). « Flood frequency analysis at ungauged sites using artificial neural networks in canonical correlation analysis physiographic space ». In : *Water Resources Research* 43.7. DOI : 10.1029/2006WR005142.

Shu, Chang et Taha B.M.J. Ouarda (2008). « Regional flood frequency analysis at ungauged sites using the adaptive neuro-fuzzy inference system ». In : *Journal of Hydrology* 349.1, p. 31-43. DOI : 10.1016/j.jhydrol.2007.10.050.

Stedinger, Jery R. (1983). « Estimating a regional flood frequency distribution ». In : *Water Resources Research* 19.2, p. 503-510. DOI : 10.1029/WR019i002p00503.

Stephens, Scott A., Robert G. Bell et Ivan Haigh (2019). « Spatial and temporal analysis of extreme sea level and skew surge events around the coastline of New Zealand ». In : DOI : 10.5194/nhess-2019-353.

Stephenson (2015). *TideHarmonics : harmonic analysis of tides*.

Sterl, A. et al. (2009). « An ensemble study of extreme storm surge related water levels in the North Sea in a changing climate ». In : *Ocean Science* 5.3, p. 369-378. doi : 10.5194/os-5-369-2009.

Strupczewski, W. G., K. Kochanek et E. Bogdanowicz (2014). « Flood frequency analysis supported by the largest historical flood ». In : *Natural Hazards and Earth System Sciences* 14.6, p. 1543-1551. doi : 10.5194/nhess-14-1543-2014.

Sweet, William V. et al. (2020). « A Regional Frequency Analysis of Tide Gauges to Assess Pacific Coast Flood Risk ». In : *Frontiers in Marine Science* 7. doi : 10.3389/fmars.2020.581769.

Tawn, Ja, Jm Vassie et Ej Gumbel (1989). « Extreme sea levels ; the joint probabilities method revisited and revised ». In : *Proceedings of the Institution of Civil Engineers* 87.3, p. 429-442. doi : 10.1680/iicep.1989.2975.

Tawn, Jonathan A. (1992). « Estimating Probabilities of Extreme Sea-Levels ». In : *Applied Statistics* 41.1, p. 77. doi : 10.2307/2347619.

Tomasin, Alberto et Paolo Antonio Pirazzoli (2008). « Extreme Sea Levels in the English Channel : Calibration of the Joint Probability Method ». In : *Journal of Coastal Research* 4, p. 1-13. doi : 10.2112/07-0826.1.

Tramblay, Yves et al. (2010). « Regional estimation of extreme suspended sediment concentrations using watershed characteristics ». In : *Journal of Hydrology* 380.3, p. 305-317. doi : 10.1016/j.jhydrol.2009.11.006.

Van Gelder, Pieter et Neyko M. Neykov (1998). « Regional frequency analysis of extreme water along the Dutch coast using L-moments : a preliminary study ». In.

Viglione, Alberto et al. (2013). « Flood frequency hydrology : 3. A Bayesian analysis ». In : *Water Resources Research* 49.2, p. 675-692. doi : 10.1029/2011WR010782.

Vries, Hans de et al. (1995). « A comparison of 2D storm surge models applied to three shallow European seas ». In : *Environmental Software* 10.1, p. 23-42. doi : 10.1016/0266-9838(95)00003-4.

Wahl, Thomas et Don P. Chambers (2015). « Evidence for multidecadal variability in US extreme sea level records ». In : *Journal of Geophysical Research : Oceans* 120.3, p. 1527-1544. doi : 10.1002/2014JC010443.

Ward, Joe H. (1963). « Hierarchical Grouping to Optimize an Objective Function ». In : *Journal of the American Statistical Association* 58.301, p. 236-244. doi : 10.1080/01621459.1963.10500845.

Wazneh, Hussein, Fateh Chebana et Taha B. M. J. Ouarda (2013). « Optimal depth-based regional frequency analysis ». In : *Hydrology and Earth System Sciences* 17.6, p. 2281-2296. doi : 10.5194/hess-17-2281-2013.

Weiss, Jérôme (2014). « Analyse régionale des aléas maritimes extrêmes ». Thèse de doct. Paris Est.

Weiss, Jérôme et Pietro Bernardara (2013a). « Comparison of local indices for regional frequency analysis with an application to extreme skew surges ». In : *Water Resources Research* 49.5, p. 2940-2951. doi : 10.1002/wrcr.20225.

Weiss, Jérôme, Pietro Bernardara et Michel Benoit (2012). « Assessment of the regional frequency analysis to the estimation of extreme storm surges ». In : *Coastal Engineering Proceedings* 33, p. 27-27. doi : 10.9753/icce.v33.management.27.

– (2013b). « A method to identify and form homogeneous regions for regional frequency analysis of extreme skew storm surges ». In.

– (2014a). « Formation of homogeneous regions for regional frequency analysis of extreme significant wave heights ». In : *Journal of Geophysical Research : Oceans* 119.5, p. 2906-2922. doi : 10.1002/2013JC009668.

– (2014b). « Modeling intersite dependence for regional frequency analysis of extreme marine events ». In : *Water Resources Research* 50.7, p. 5926-5940. doi : 10.1002/2014WR015391.

Williams, Joanne et al. (2016). « Tide and skew surge independence : New insights for flood risk ». In : *Geophysical Research Letters* 43.12, p. 6410-6417. doi : 10.1002/2016GL069522.

Wood, Simon N. (2017). *Generalized Additive Models : An Introduction with R*. 2e éd. New York : Chapman et Hall/CRC. 496 p. isbn : 978-1-315-37027-9. doi : 10.1201/9781315370279.

Woodworth, P. L. et al. (2007). « The dependence of UK extreme sea levels and storm surges on the North Atlantic Oscillation ». In : *Continental Shelf Research* 27.7, p. 935-946. doi : 10.1016/j.csr.2006.12.007.

Wu, Yun-biao, Lian-qing Xue et Yuan-hong Liu (2019). « Local and regional flood frequency analysis based on hierarchical Bayesian model in Dongting Lake Basin, China ». In : *Water Science and Engineering* 12.4, p. 253-262. doi : 10.1016/j.wse.2019.12.001.

Yin, Shui-qing et al. (2018). « Using Kriging with a heterogeneous measurement error to improve the accuracy of extreme precipitation return level estimation ». In : *Journal of Hydrology* 562, p. 518-529. doi : 10.1016/j.jhydrol.2018.04.064.

Zrinji, Zolt et Donald H. Burn (1994). « Flood frequency analysis for ungauged sites using a region of influence approach ». In : *Journal of Hydrology* 153.1, p. 1-21.